

UNIVERSITY OF BELGRADE
FACULTY OF TECHNOLOGY AND METALLURGY

Abdul Moneim Mohamed Saed Kazuz

**BIOACTIVE MATERIALS BASED ON
 α -TRICALCIUM PHOSPHATE CEMENTS AND
FLUOROAPATITE: SYNTHESIS, PROPERTIES
AND APPLICATIONS IN DENTISTRY**

Doctoral Dissertation

Belgrade, 2022

УНИВЕРЗИТЕТ У БЕОГРАДУ
ТЕХНОЛОШКО-МЕТАЛУРШКИ ФАКУЛТЕТ

Абдул Монеим Мохамед Саед Казуз

**BIOAKTIVNI MATERIJALI NA BAZI
 α -TRIKALCIJUM-FOSFATNIH CEMENATA I
FLUOROAPATITA: SINTEZA, SVOJSTVA I
PRIMENA U STOMATOLOGIJI**

докторска дисертација

Београд, 2022

Supervisor:

Dr. Đorđe Janačković, Full Professor,
University of Belgrade, Faculty of Technology and Metallurgy

Committee Members:

Dr. Željko Radovanović, Research Associate,
University of Belgrade, Innovation Centre of the Faculty of Technology and Metallurgy

Dr. Đorđe Veljović, Associate Professor,
University of Belgrade, Faculty of Technology and Metallurgy

Dr. Rada Petrović, Full Professor,
University of Belgrade, Faculty of Technology and Metallurgy

Dr. Vesna Miletić, Full Professor,
University of Sydney, School of Dentistry, Sydney, Australia

Date of Defence _____

Acknowledgement

In the name of Allah, The Beneficent, the Merciful...

First of all, I would like to thank God (ALLAH) for giving me the strength and courage throughout the duration of this research project. There are times when words are inadequate. I grant my grateful appreciation and thanks to all those who have contributed to this work.

This thesis is dedicated to the soul of my father may Allah Almighty bless him. I miss him every day, but I am glad to know he saw this process through to its completion, offering the support to make it possible, as well as plenty of friendly encouragement.

Undertaking this PhD has been a truly life-changing experience for me and it would not have been possible to do without the support and guidance that I received from many people.

Firstly, I would like to express my sincere gratitude to my supervisor Dr. Prof. Đorđe Janačković, for the continuous support of my PhD study and related research, for his patience, motivation, and immense knowledge. His guidance helped me in all the time of research and writing of this thesis. I could not have imagined having a better advisor and mentor for my PhD study. I thank him again for the patience on my progress, for his suggestions on shaping the thesis and his countless hours that he spent on reading and editing my thesis.

My sincere and special gratitude to Dr. Prof. Đorđe Veljović, for his guidance, suggestions, continual support and advice throughout my study, without his assistances this dissertation would not be accomplished.

I would like to express the deepest appreciation to Dr. Željko Radovanović, who has attitude and the substance of a genius: he continually and convincingly conveyed a spirit of adventure in regard to research. Without his guidance and persistent help this dissertation would not have been possible.

I cannot begin to express my thanks to thanking the rest of the committee members Dr Rada Petrović and Dr Vesna Miletić my thesis examiners for their interest in my work and for their insightful suggestions and comments on my thesis. They were always willing to help and give me best suggestions.

I would also like to extend my deepest gratitude to Dr. Maja Zebić for her support and help. She has taught me, how good experimental are done. I appreciate all her contributions of time, ideas, and suggestions that helped to make my research skills experience productive and stimulating.

My warm and heartfelt thanks go to my mother for her tremendous support and hope she had given to me. Without that hope, this thesis would not have been possible. Thank you for strength you gave me. I love you.

I would like to thank my wife for her constant love, support and encouragement. Without her none of this would have been possible. I cannot begin to thank her enough, and she will always have my respect and love.

I also extend my appreciation and thanks to my brothers and sisters, for their support, and to all named and unnamed helpers, I again extend my thanks. Finally, I would like to express my thanks to Belgrade University for the delight support.

Abdulmoneim Mohamed Kazuz

Abstract

Calcium phosphates (CaPs) are an important group of ceramic materials widely used in dentistry and medicine as many of them are very similar to the inorganic part of teeth and bones in humans. Among CaPs, hydroxyapatite ($\text{Ca}_{10}(\text{PO}_4)_6(\text{OH})_2$, HAp) is the most attractive and intensely studied biomaterial due to exceptional biocompatibility and bioactivity. However, the main drawback of HAp is its brittleness which makes it difficult to use it as a primary material for implants or fillers. By using CaPs derived from HAp, it is possible to overcome this disadvantage while retaining good properties. α -Tricalcium phosphate ($\alpha\text{-Ca}_3(\text{PO}_4)_2$, α -TCP) can be prepared from calcium deficient HAp by calcination above temperatures ~ 1150 °C, and it can be used as bone cement. The most stable CaPs – fluorapatite ($\text{Ca}_{10}(\text{PO}_4)_6\text{F}_2$, FAp) can be obtained by replacing the OH^- ions in HAp with the F^- ions. FAp can slow down demineralization by releasing F^- ions that strengthen the enamel. These two materials, α -TCP and FAp, form a composite with satisfactory mechanical properties that could fill the cavity after removal of damaged dental tissue and also remineralize the surrounding tissue.

The research work presented in this dissertation focuses on synthesis and characterization of composite cements based on α -TCP and nanostructured FAp, α -TCP/FAp, appropriate for dental usage as root canal filling material. Synthesized α -TCP/FAp composites had improved mechanical properties and biocompatibility in comparison to α -TCP. The α -TCP powder was prepared by calcination of hydrothermally synthesized HAp at 1500 °C for 2 h. The processing conditions for FAp powders synthesis were optimized and the powder with optimal properties was chosen to obtain α -TCP/FAp composite types of cement. The influence of FAp concentration on the composite cement properties was investigated. The FAp powder was mixed with α -TCP to obtain composites with 0, 2.5, 5 and 10 wt% of FAp. The phosphate solution (2.5 wt% Na_2HPO_4) was added to the prepared powder mixtures at a liquid to powder ratio of 0.32 ml g^{-1} to obtain cement paste and then make specimens in the appropriate mold for further testing. Morphology and phase composition of powders were investigated by X-ray diffraction (XRD), Fourier transformed infrared spectroscopy (FTIR), Field emission scanning electron microscopy (FESEM), and energy-dispersive X-ray spectroscopy (EDS). Soaking of α -TCP/FAp specimens in simulated body fluid (SBF) affected the successful transformation of α -TCP into HAp, while the compressive test revealed the influence of this transformation and FAp content on the mechanical properties of the composites. Specimen containing 5% of FAp after 10 days in simulated body fluid (SBF) solution showed the highest compressive strength, 33.8 MPa, which is a 84-fold increase compared to α -TCP/FAp before SBF. *In vitro* MTT and DET biocompatibility tests, performed using cell culture of MRC-5 human fibroblast cells, revealed that α -TCP/FAp had no cytotoxic effect. These findings

showed that α -TCP/FAp composite cements could yield favorable mechanical properties with no adverse effect on biocompatibility.

In the second part of the thesis, cement pastes made from different liquid compositions were investigated and the most suitable one for obtaining rheologically optimal paste was chosen for further analysis. The α -TCP/FAp cements with 0, 5 and 10 wt% of FAp were obtained with new liquid and investigated as dental root canal filling cements. Morphological changes in the cement materials as a result of the formation of HAp after SBF immersion, an influence on the cell viability, and the final success of the fillings were investigated by FESEM. Treatment of α -TCP/FAp mixtures in SBF at 37 °C led to a complete transformation of α -TCP into HAp after 10 days. The exposure of MRC-5 human and L929 animal fibroblast cells to the cement showed a complete absence of cytotoxicity. When the root canal of an extracted tooth was filled with α -TCP/FAp cement containing 5 wt. % of FAp relatively strong adhesion between the cement and dentin was observed after 48 h. The same cement material was immersed during 10 days in SBF and subsequently subjected to *in vitro* MTT testing on human and animal fibroblast cells, during which showed increased cell viability compared to a control sample. These findings lead to a conclusion that α -TCP/FAp based cement with 5 wt% FAp showed the greatest potential for further development towards dental application.

Keywords: Composites, Mechanical properties, Apatite, Biomedical applications

Scientific field: Technical engineering

Major in: Materials engineering

Сажетак

Калцијум-фосфати (КФ) су важна група керамичких материјала који се широко користе у стоматологији и медицини јер су многи од њих веома слични неорганском делу зуба и костију људи. Међу КФ, хидроксиапатит ($\text{Ca}_{10}(\text{PO}_4)_6(\text{OH})_2$, ХАп) је најатрактивнији и најинтензивније проучаван биоматеријал, који се одликује значајном биокомпатибилношћу и биоактивношћу. Међутим, главни недостатак ХАп-а је његова кртост због чега није погодан за употребу као примарни имплантат или пунилац. Коришћењем КФ-а изведених из ХАп-а, могуће је превазићи овај недостатак уз задржавање добрих својстава. α -Трикалцијум фосфат ($\alpha\text{-Ca}_3(\text{PO}_4)_2$, α -ТКФ) се може добити калцинацијом калцијум дефицитарног ХАп-а изнад ~ 1150 °C и може се користити као коштани цемент. Најстабилнији КФ – флуорапатит ($\text{Ca}_{10}(\text{PO}_4)_6\text{F}_2$, ФАп) се добија заменом OH^- јона у структури ХАп-а F^- јонима. ФАп може успорити деминерализацију зуба ослобађањем F^- јона који јачају глеђ. Ова два материјала, α -ТКФ и ФАп, могу створити композит задовољавајућих механичких својстава који би могао попунити шупљину након уклањања оштећеног зубног ткива и такође реминерализовати околно зубно ткиво.

У овој дисертацији представљена је синтеза и карактеризација композитних цемената на бази α -ТКФ и наноструктурног ФАп, α -ТКФ/ФАп, погодних за стоматолошку употребу као материјала за пуњење канала корена зуба. α -ТКФ/ФАп су припремљени са побољшаним механичким својствима и биокомпатибилношћу. α -ТКФ прах је припремљен калцинацијом хидротермално синтетизованог ХАп-а на 1500 °C током 2 сата. Услови синтезе ФАп праха су оптимизовани и прах са најбољим својствима је изабран за добијање α -ТКФ/ФАп композитних цемента. Испитан је утицај концентрације ФАп на својства композитног цемента. ФАп прах је помешан са α -ТКФ у таквом односу да би се добили композити са 0; 2,5; 5 и 10 мас.% ФАп-а. Раствор фосфата (2,5 мас.% Na_2HPO_4) је додат припремљеним мешавинама праха при односу течност: прах од $0,32 \text{ ml g}^{-1}$ да би се добила цементна паста, а затим су направљени узорци у одговарајућем калупу за даља испитивања. Изглед и фазни састав прахова испитивани су рендгенском дифракцијом праха (РДП), инфрацрвеном спектроскопијом са Фуријеовом трансформацијом (ИЦФТ), скенирајућом електронском микроскопијом (СЕМ) и енергетском дисперзивном рендгенском спектроскопијом (ЕДС). Одстојавање α -ТКФ/ФАп узорака у симулираној телесној течности (СТТ) довело је до успешне трансформације α -ТКФ у ХАп, док је испитивање притисне чврстоће показало утицај ове трансформације и садржаја ФАп на механичке својства композита. Узорак са 5 мас.% ФАп-а после 10 дана у СТТ показао је највећу чврстоћу на притисак, 33,8 МПа, што је повећање од 84 пута у поређењу са α -ТКФ/ФАп пре СТТ. *In vitro* тестови

биокомпатибилности МТТ и ДЕТ, спроведени са ћелијском културом МРЦ-5 хуманих фибробласта, открили су да α -ТКФ/ФАп нема цитотоксични ефекат. Ови налази су показали да α -ТКФ/ФАп композитни цементи могу обезбедити повољна механичка својства без штетног утицаја на биокомпатибилност.

У другом делу дисертације испитане су различите течности за добијање цементне пасте и за даљу анализу изабрана је течност најпогоднија за добијање реолошки најбољих пасте. α -ТКФ/ФАп цементи са 0, 5 и 10 мас.% ФАп-а, умешани са новом течношћу испитивани су као цементи за пуњење зубних канала. Морфолошке промене у цементним материјалима као последица формирања ХАп-а након држања у СТТ, утицај на вијабилност ћелија и ефикасност пуњења испитивани су СЕМ-ом. Третман композитних α -ТКФ/ФАп цемената у СТТ на 37 °С резултирао је потпуном трансформацијом α -ТКФ у ХАп после 10 дана. Излагање МРЦ-5 хуманих и Л929 животињских фибробластних ћелија цементу показало је потпуно одсуство цитотоксичности. Канал корена екстрахованог зуба испуњен је α -ТКФ/ФАп цементом са 5 мас.% ФАп и релативно јака адхезија између цемента и дентина примећена је након 48 сати. Исти цементни материјал је уроњен током 10 дана у СТТ и након тога подвргнут *in vitro* МТТ тестовима са хуманим и животињским фибробластним ћелијама које су показале већу вијабилност у поређењу са контролним узорком. Ови налази доводе до закључка да цемент на бази α -ТКФ/ФАп са 5 мас.% ФАп показује највећи потенцијал за даљи развој у правцу стоматолошке примене.

Кључне речи: композити, механичка својства, апатит, примена у биомедицини

Научна област: Технолошко инжењерство

Ужа научна област: Инжењерство материјала

CONTENTS

LIST OF FIGURES	iv
LIST OF TABLES	vi
1. INTRODUCTION	1
2. THE STRUCTURE, DECAY AND TREATMENT OF TOOTH.....	4
2.1 Tooth structure	4
2.2 Tooth decay	6
2.2.1 Tooth treatment	7
3. DEFINITION, TYPES AND PROPERTIES OF BIOMATERIALS.....	8
3.1. Polymers	8
3.2 Metals	9
3.3 Ceramics	10
3.3.1. Bioinert ceramics	11
3.3.2. Bioactive ceramics	12
3.3.2.1. Bioactive glasses	12
3.3.2.2. Calcium phosphates	14
3.4 Composite materials	16
4. HYDROXYAPATITE	18
4.1 Composition, structure and properties of HAp	18
4.2 Synthesis of HAp	19
4.3 Chemical modifications of HAp	24
4.4 Application of HAp and its composites	26
4.4.1. HAp based commercial products	26
4.4.2. HAp application for bone and tooth replacement and reconstruction	27
4.4.2.1. HAp coatings	27
4.4.2.2. HAp scaffolds and drug delivery	28
5. α - AND β - TRICALCIUM PHOSPHATES	30

6. CALCIUM PHOSPHATE CEMENTS	32
7. CURRENT TRENDS IN DENTAL MATERIALS DEVELOPMENT	34
8. EXPERIMENTAL PART	37
8.1. Materials and methods	37
8.2. Sample preparation	38
8.2.1. Synthesis of FAp and HAp powders	38
8.2.2. Synthesis of α -TCP	39
8.2.3. Preparation of α -TCP/FAp composites	39
8.2.4. Tooth filling cement preparation	40
8.2.5. Preparation of simulated body fluid (SBF)	40
8.3. The tooth filling procedure	41
8.4. Characterization of starting constituents, composites and pastes.....	43
8.4.1. Field emission scanning electron microscopy (FESEM).....	43
8.4.2. Energy dispersive X-ray spectroscopy (EDS)	43
8.4.3. Fourier transformed infrared spectroscopy (FTIR)	43
8.4.4. X-ray powder diffraction analysis (XRPD)	43
8.4.5. Ion release test	44
8.4.6. Compressive test	44
8.4.7. In vitro biocompatibility tests	45
8.4.7.1. Cell lines	45
8.4.7.2. Colorimetric assays with tetrazolium salts (MTT test)	46
8.4.7.3. Trypan Blue dye exclusion test (DET test)	46
8.4.7.4. Cells preparation for staining	47
8.4.8. Physical properties of tooth filling pastes	47
8.4.8.1. Solubility test	48
8.4.8.2. Flow test	48
8.4.8.3. Working time	48
8.4.8.4. Setting time	48
9. RESULTS AND DISCUSSION	49
9.1. Characterization of HAp and FAp powders	49
9.1.1. XRPD analysis	49
9.1.2. FTIR analysis	50

9.1.3. FESEM and EDS analysis	51
9.1.3.1. FESEM	51
9.1.3.2. EDS	52
9.1.4. Bioactivity of composite cement specimens	55
9.1.5. Mechanical properties of composite cements	57
9.1.6. Ion release	58
9.1.7. MTT and DET assay for composites α -TCP/FAp	59
9.2. Characterization of cement pastes	60
9.2.1. Physical properties of cement samples: setting and working time, flow and solubility	60
9.2.2. FESEM analysis of composite cements bioactivity	61
9.2.3. XRPD analysis of composite cements bioactivity	62
9.2.4. FESEM analysis of composite cements biocompatibility	63
9.2.5. <i>In vitro</i> MTT and DET assay of composite cements biocompatibility	65
9.2.6. Analysis of dental cement adhesion to the tooth	68
10. CONCLUSION	70
11. References	72
Biography	94

LIST OF FIGURES

Figure 1.	Tooth structure [26].....	4
Figure 2.	Transmission electron microscopy image of enamel structure in a mature tooth [1].....	5
Figure 3.	Schematic presentation of the cariogenic biofilm formation. 1A) Cariogenic dental plaque biofilm, 1B) Cariogenic biofilm; 1C) Acidic attack and 1D) The net mineral loss for enamel and dentine [33].....	7
Figure 4.	Schematic representation of different polymer structures [37].....	9
Figure 5.	Application of ceramic biomaterials in human body [52].....	11
Figure 6.	SiO ₂ -CaO-Na ₂ O phase diagram with composition of 45S5 bioactive glass [61]..	13
Figure 7.	Surface modifications of bioactive glass due to interaction with simulated body fluid [61].....	13
Figure 8.	Different CaP structures obtained with various synthesis conditions [85].....	16
Figure 9.	Structural formula of HAp.....	18
Figure 10.	Crystal structure of HAp [100].....	19
Figure 11.	Techniques for HAp synthesis.....	20
Figure 12.	Hydrothermal synthesis of rod-shaped HAp nanoparticles [106].....	22
Figure 13.	Influence of hydrothermal synthesis parameters on the formation of HAp particles [85].....	23
Figure 14.	Projection of the crystal structure of FAp on the (001) crystallographic plane [147]. Ca - purple, F - green, O - red, P - yellow.....	25
Figure 15.	Protection from demineralization of enamel by FAp deposition [13].....	26
Figure 16.	Dental implants coated with CaP by a plasma-spray process at magnification of 10x (bar = 1 mm) (a) and 1kx (bar = 1 μm) (b) [6].....	28
Figure 17.	3D image of HAp scaffold [11].....	29
Figure 18.	Projection of α-TCP unit cell on the <i>ab</i> - (left) and <i>bc</i> -plane (middle). Tetrahedra represent PO ₄ groups, and light balls denote Ca atoms; Projection of β-TCP unit cell on the <i>ac</i> -plane (right). Tetrahedra represent PO ₄ groups, small balls designate Ca atoms, and big balls are for the Ca atoms with half occupancy [196].....	31
Figure 19.	Microstructure of porous α-TCP [152].....	31
Figure 20.	CPCs common constituents, setting reaction and structure of formed apatite and brushite [268].....	32

Figure 21.	Furnace for thermal treatment (calcination) of HAp and the obtained α -TCP powder.....	39
Figure 22.	Teeth prepared for filling.....	41
Figure 23.	Teeth after filling.....	41
Figure 24.	Fixed tooth to gypsum (left) and a slice of cut tooth for XRPD (right).....	42
Figure 25.	Precision cutter with the fixed tooth.....	42
Figure 26.	Ion Selective Electrode (ISE).....	44
Figure 27.	Shimadzu universal testing machine [263].....	45
Figure 28.	XRPD patterns of FAp and HAp powders [19].....	38
Figure 29.	FTIR spectra of FAp and HAp powders [19].....	50
Figure 30.	FESEM images of synthesized series of FAp and HAp powders.....	51
Figure 31.	Rietveld refinement (up) and crystal packing diagram in <i>ab</i> plane (down) of FAp.....	53
Figure 32.	Rietveld refinement (up) and crystal packing diagram in <i>ab</i> plane (down) of nHAp.....	54
Figure 33.	FESEM images of specimen surface: 5-3 (a), 5-10 (b), and 5-30 (c).....	56
Figure 34.	FESEM images of fracture surfaces: 5-3 (a), 5-10 (b), and 5-30.....	56
Figure 35.	FESEM images of surfaces at magnification of 10kx: 5-3 (a), 5-10 (b), and 5-30 (c).....	56
Figure 36.	FESEM images: 0-30 surface (a) and 0-30 fracture surface (b).....	57
Figure 37.	FESEM images: 10-30 surface (a) and 10-30 fracture surface (b).....	57
Figure 38.	MTT assay of cytotoxic effects of α -TCP/FAp composites on MRC-5 cells.....	59
Figure 39.	DET assay of cytotoxic effects of α -TCP/FAp composites on MRC-5 cells.....	60
Figure 40.	FESEM images of the surface of samples after 10 days in SBF: α -TCP/FAp(0) (a), α -TCP/FAp(5) (b), and α -TCP/FAp(10) (c) and α -TCP/FAp(0) without staying in SBF (d).....	62
Figure 41.	XRPD patterns of samples: α -TCP/FAp(0) (a), α -TCP/FAp(5) (b) and α -TCP/FAp(10) (c), and the same samples (1, 2 and 3, respectively) after 10 days in SBF. * HAp-PDF#74-0556, ** α -TCP-PDF#29-0359 and *** FAp-PDF#83-0556.....	63
Figure 42.	FESEM images of L929 (a) on: α -TCP/FAp(0) (b), α -TCP/FAp(5) (c), and α -TCP/FAp(10) (d).....	64

Figure 43.	FESEM images of MRC-5 (a) on: α -TCP/FAp(0) (b), α -TCP/FAp(5) (c), and α -TCP/FAp(10) (d).....	65
Figure 44.	Appearance of MRC-5 cells before MTT and DET tests.....	66
Figure 45.	Appearance of L929 cells before MTT and DET tests.....	66
Figure 46.	The results of <i>in vitro</i> MTT assay on samples: α -TCP/FAp(0) (a), α -TCP/FAp(5) (b), and α -TCP/FAp(10) (c).....	67
Figure 47.	The results of <i>in vitro</i> DET assay on samples: α -TCP/FAp(0) (a), α -TCP/FAp(5) (b), and α -TCP/FAp(10) (c).....	68
Figure 48.	FESEM images of tooth canal filling with α -TCP/FAp(5) without (a–c) and with gutta-percha (d–f).....	69

LIST OF TABLES

Table 1.	Advantages and disadvantages of using amalgam tooth filling [48].....	10
Table 2.	Ca/P ratio for different CaPs [11].....	14
Table 3.	Structural parameters for various CaPs [64].....	15
Table 4.	Phase analysis, Ca/P ratio and carbonate replacement of the synthesized CaP powders [85].....	16
Table 5.	Chemical composition of enamel, bone, dentin and HAp [61].....	19
Table 6.	Mechanical properties of HAp.....	19
Table 7.	Wet synthesis of HAp [105].....	24
Table 8.	Mass (g) and volume (mL) of reaction ingredients and pH value in the synthesis of FAp powders.....	38
Table 9.	The composition of different water-based liquids for cement pastes and best LPR values.....	40
Table 10.	Labels for α -TCP/FAp composite samples.....	47
Table 11.	The unit cell parameters and $\langle D \rangle$ of FAp and HAp powders (JADE software)...	50
Table 12.	EDS results of FAp and HAp powders (at. %)......	52
Table 13.	Crystallographic and Rietveld refinement parameters of nHAp and FAp.....	54
Table 14.	Selected bond lengths (\AA) for nHAp and FAp.....	55
Table 15.	Compressive test results for composite cements after immersing in SBF.....	57
Table 16.	F ⁻ ion release (in ppm) for control (FAp) and composite specimens.....	58
Table 17.	Physical properties of α -TCP and α -TCP/FAp composite cement.....	62

1. INTRODUCTION

Teeth have unique, mineral-rich structure that and consist of crown and root. Crowns' outer layer, enamel, underneath which lies dentin and pulp cavity are tissues made of organic and inorganic components. The inorganic part of enamel mostly consists of biological calcium phosphate – hydroxyapatite (about 96 wt.%) while the dentin contains a mixture of hydroxyapatite, organic substance - collagen, water, and salts [1]. Lowering of pH value in the mouth, caused by the action of bacteria that break down food rich in carbohydrates (starches and sugars) creating an acidic environment, induce dissolving of calcium phosphates in dentine and enamel (the process of demineralization of dentine and enamel), until they reach the pulp [2]. This leads to the creation of tooth cavities and decay, known as caries. Since the tooth structure cannot be repaired spontaneously by the body, once cavitation occurs dental treatment that includes use of various types of materials (called biomaterials) must be applied to fill or to reconstruct the tooth.

Biomaterials are a class of materials that, according to the European Society for Biomaterials Consensus, are defined as components anticipated to be interfacing in biological systems, in order to augment, treat or replace any tissue, organ or the body functioning [3,4]. The biomaterials could be natural or have artificial origin and their main roles are to replace the damaged tissue or organ and thus improve the quality or even prolong human life. Depending on the properties and chemistry, biomaterials could be classified as polymers, metal alloys, ceramics, and composites.

Biocompatibility is the most important biomaterials property i.e., the absence of toxic effect on the surrounding tissue and host body environment. Another important property of biomaterials is their ability to be resorbed in the body – bioresorbability, crucial when body needs to heal and to replace bioresorbable material. Also, valuable property of biomaterials is bioactivity - an ability to interact with the host tissue, supporting its growth. Biomaterials should have appropriate mechanical and chemical properties to withstand pressure and wear that body is exposed to, and to avoid any undesirable reaction with body environment. Many applications of biomaterials include cardiovascular surgery (heart valves, vascular grafts), dentistry (tooth fillings, dental crowns and bridges), dermatology (artificial skin), orthopedics, etc [5–9]. Biocompatible ceramic materials (bioceramics) are materials that are used for reparation, reconstruction, or a replacement of damaged teeth, joints, or bones [10]. Calcium phosphates (CaPs) represent a class of bioceramics with excellent biological, physical and chemical properties due to their compositional similarity to teeth and bones, ensuring excellent biocompatibility in a host body. Further, due to the ability to release Ca and P ions that lead to the remineralization of tooth, CaPs represent a valuable group of materials for application in dentistry. They could be used as cement, crowns, implants, and dental bridges material, as well as

coatings on titanium and titanium alloy implants, and in that way combining the bioactivity and superior mechanical properties of metals [11].

Hydroxyapatite (HAp), is the dominant dentine and bone constituent, ensuring the high biocompatibility of built implants. With excellent osteoconductive and bioactive properties, HAp is favored as the biomaterial used in both dentistry and orthopedics. Another CaP that has been recognized as a potential dental material is α -tricalcium phosphate (α -TCP) [12]. The possibility of α -TCP to be transformed spontaneously into HAp in reaction with body fluids after the application in the mouth, allows its usage as the material for the cavity filling after removal of damaged dental tissue, and also to initiate remineralization of the surrounding tissue. Fluorine represents an essential element that contributes to teeth mineralization by substituting OH⁻ in HAp, making fluorapatite (FAp), constitutive material of enamel with higher wear and acid resistance and lower solubility compared to HAp [13–15]. FAp represents a very useful component of ceramic-based dental composite materials, increasing the biocompatibility and mechanical strength of the matrix [16–18]. It can be used for modification of calcium phosphate cements (CPCs), obtaining materials for the root canal filling with the possibility of tailoring mechanical properties, biocompatibility and bioactivity. These properties could be controlled for the cement pastes based on α -TCP and FAp by varying the FAp/ α -TCP ratio [19].

CPCs based on HAp are usually combined with natural (collagen, chitosan, cellulose) or synthetic (polyethylene glycol, polycaprolactone) polymers, with the aim of controlling porosity, rheological and mechanical properties [20]. Although composites built with polymers offer advantages in processing, price and chemical diversity, major drawbacks in their application lie in lower biocompatibility compared to HAp or α -TCP. Composites HAp/titanium dioxide obtained using the sol-gel procedure, as well as high-temperature sintered HAp/zirconia are also attractive due to their improved mechanical and thermal properties, as well as high biocompatibility [21].

The research efforts presented in this dissertation are focused on the synthesis, characterization and processing of cement constituents based on α -TCP and FAp, as well as the processing of α -TCP-FAp composites with different FAp content. Further, the influence of FAp on biocompatibility, bioactivity and mechanical properties of α -TCP-FAp composites was also investigated. Tooth filling pastes were also prepared and optimized and tested using standards for dental materials (standard ISO6876 - Dental root canal sealing materials) in order to obtain the cement filling paste with desired rheological and chemical properties (values of solubility, flow, working and setting time). For this purpose, the influence of different liquid components on the rheology of dental root canal filling paste was also investigated, as well as the overall success of the tooth filling (root canal sealer). The influence of the FAp on the bioactivity of obtained α -TCP/FAp based cement after ex-

posure to the simulated body fluid (SBF) was also determined by *in vitro* MTT and DET tests performed on MRC-5 and L929 cells [22–25].

The research goals of this thesis are:

- Investigation of the influence of hydrothermal synthesis parameters on the size and morphology of FAp particles;
- Synthesis of dental materials for filling of tooth roots based on α -TCP and different proportions of nanoparticle powder FAp synthesized by hydrothermal method;
- Investigation of the influence of the FAp/ α -TCP ratio on the mechanical properties, bioactivity and biocompatibility of the obtained composite materials;
- Examination of the influence of additional of citric acid, polyethylene glycol, hydroxypropyl-methyl cellulose on the setting time, solubility, working time of dental cements based on α -TCP and FAp and the microstructure of the root canal filling.
- Examination of biocompatibility of starting powders and dental cements with different FAp content by performing colorimetric tests with tetrazolium salts (MTT) and color exclusion test (DET) *in vitro* in contact with MRC-5 human fibroblast cells and L929 mouse fibroblast cells.

2. THE STRUCTURE, DECAY AND TREATMENT OF TOOTH

2.1 Tooth structure

Teeth represent the hardest tissue in the human body and are partly made of organic and partly of inorganic material [1]. The inorganic component mainly consists of hydroxyapatite, which will be discussed in detail (Chapter 4). Crown and root are the two main parts of the tooth, while the main tooth constituents are: enamel, dentin, pulp and periodontium (Figure 1).

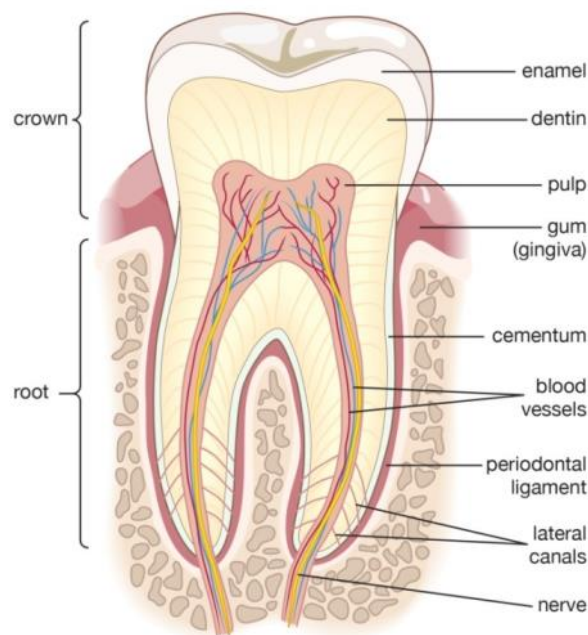


Figure 1. Tooth structure [26].

Enamel is a material that mainly (approximately 96%) consists of long, ribbon-shaped hydroxyapatite crystals, forming the outer layer of the tooth through the complex process called *amelogenesis*. It is also the hardest material in the human body that is responsible for the tooth mechanical performance. In a fully mature tooth, enamel crystals are stacked into irregular shapes and grouped as rod and interrod enamel, as presented in Figure 2 [1,14].

The organic part of the enamel contains residual proteins that are secreted by ameloblasts in order to create an appropriate environment for the deposition of minerals, and mostly removed during the tooth maturation. Main enamel proteins are enamelin, ameloblastin and amelogenin. Low amounts of some types of collagens can also be found in the organic part of the enamel. Beneath the enamel, the bulk of a tooth is made of dentin, which represents a mixture of inorganic minerals, organic compounds, water and salts. The process of dentin formation is called *dentinogenesis*, re-

sulting in tubular structures connected to the enamel *via* dentinoenamel junction [27]. Around 70% of dentine is constituted of minerals, 20% is organic fraction, and water fills remaining 10% [2].



Figure 2. Transmission electron microscopy image of enamel structure in a mature tooth [1].

Organic part contains three different types of collagen (I, III and V) and phosphoprotein. Among them, collagen I is the dominant component of the organic part that carries inorganic components in the hollow parts of the fibriles [28]. Inorganic fraction mostly consists of biological hydroxyapatite. The pulp represents the central soft tissue part of the tooth that contains blood vessels and nerves. It is connected to dentin as a part of dentin-pulp complex filling the pulp chamber and root canals of the tooth [1]. Fibroblasts are dominant cells contained in the pulp, especially in the pulp chamber of the crown. Odontoblasts occupy the edge of the pulp, along the entire tooth surface. Both fibroblast and odontoblast cells are responsible for the production of collagen and noncollagenous tooth proteins. Cementum, periodontal ligament and tooth sockets (alveolus) are the main parts of periodontium, tissue group that gives tooth mechanical support through the connection with a jaw. Root of each tooth is covered with cementum, connective tissue similar in composition to the bone [2]. All listed constituents and biochemical processes associated to them are equally important for the tooth forming, maturation and functioning, thus requiring thorough knowledge of their structure from the cellular level, with the aim of finding the proper treatment for each problem that occurs during the tooth lifecycle.

2.2 Tooth decay

Dental plaque is a naturally occurring microflora rich biofilm that covers the teeth surface in the oral cavity [29]. It contains numerous strains of bacteria that are kept in homeostasis by biochemical interactions. However, oral cavity can become very favorable environment for microorganisms, depending on dietary habits and overall immune state of the organism. Teeth are subjected to greater temperature variations than most of the other body parts and therefore can cope with exposure to cold or hot beverages. Tooth decay (caries and mechanical damage) mostly occurs when teeth are frequently exposed to foods containing carbohydrates (starches and sugars). Dental biofilm contains acidogenic bacteria, mostly lactic acid bacteria, such as *Lactobacillus* or *Streptococcus* (mutans and sobrinus) species, which metabolize sugars, producing acids [30,31]. As a consequence of this process, pH value can be significantly decreased, causing the apatite dissolving from the enamel (demineralization) and dentine, until they reach the pulp, forming a cavity [32]. Saliva and biofilm fluid pH dictates migration of Ca^{2+} and PO_4^{3-} ions from and into the tooth. If pH value falls below 5.5, ions will diffuse from the enamel, while dentine releases ions below 6.5 [33]. The acidic attack from cariogenic bacteria that causes demineralization of enamel and dentine resulting in dental cavity is schematically presented in Figure 3. Unlike the rest of the skeleton, body cannot spontaneously repair teeth, therefore, they need tending in the form of dental filling. Tooth decay is a worldwide problem in people of all ages, which is the reason for constant research expansion in the field of dental materials.

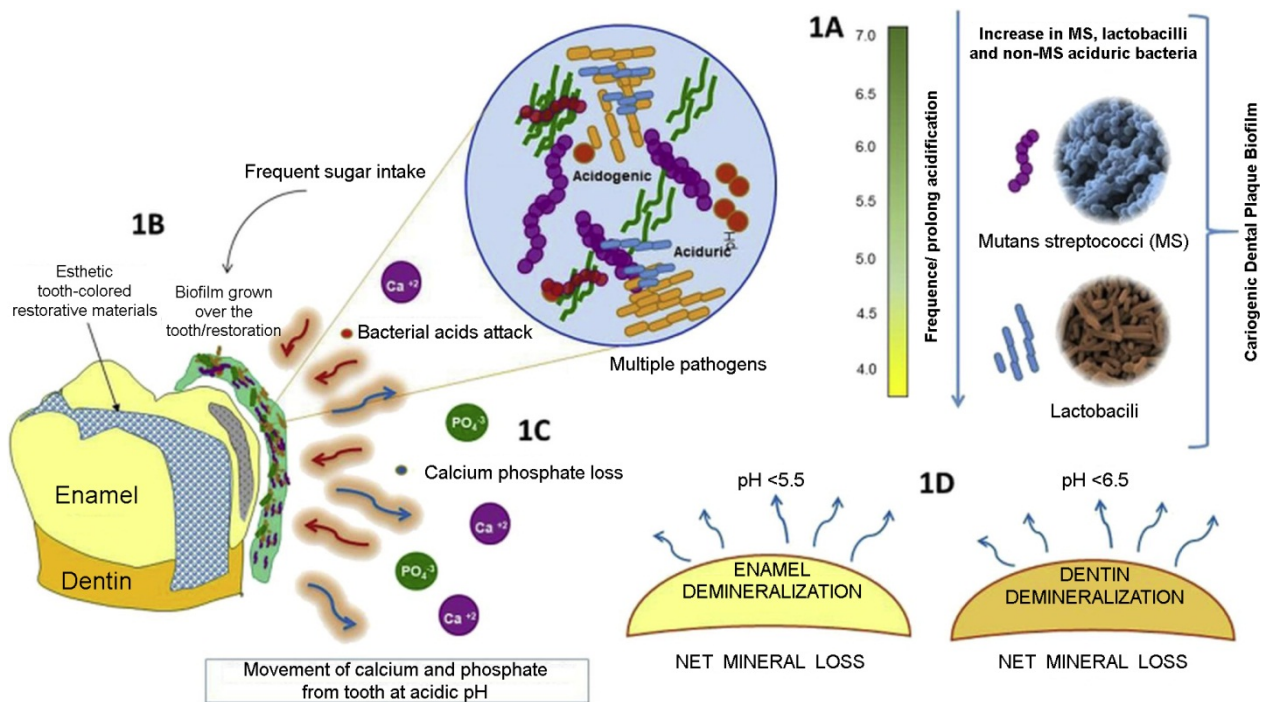


Figure 3. Schematic presentation of the cariogenic biofilm formation. 1A) Cariogenic dental plaque biofilm, 1B) Cariogenic biofilm; 1C) Acidic attack and 1D) The net mineral loss for enamel and dentine [33].

2.2.1 Tooth treatment

Decay due to apatite dissolution induced by the everyday dietary habits of humans, and mechanical damage caused by the impact on the teeth, represent problems that have to be approached very seriously, in regards to mechanical and aesthetic demands. Various materials for tooth remineralization and cavity treatment have already been proposed and implemented in dentistry, with the focus on their compatibility to the surrounding tissue and non-toxicity [8,34,35]. Tooth treatments that are primarily discussed in this dissertation, are based on bioceramic materials, a class of materials that will be presented in the subsection 3.3. Among them, enamel and dentin treatment and repair using materials based on calcium phosphates and fluorine have shown to be very promising due to the tooth composition and structure similarity.

3. DEFINITION, TYPES AND PROPERTIES OF BIOMATERIALS

Among different definitions of biomaterials the most well-versed is the one given by the European Society for Biomaterials Consensus Conference-II: "biomaterial as the material anticipated interfacing in biological systems, in order to estimate the augment, treat or replace any tissue, organ or the functioning of the body" [3,4]. The most important feature of biomaterials is their biocompatibility, ability to be incorporated into a living organism without toxic effect on the host body. In accordance to their interaction with the living tissue, biomaterials can be:

- inactive,
- biomimetic and
- bioactive.

Another property of biomaterials is their ability to be resorbed in the body – bioresorbability. This ability is crucial since host body needs to heal and to replace bioresorbable material [36]. Biomaterials should have good mechanical and chemical properties, to withstand pressure and wear that they are exposed to in the body, and to avoid any undesirable reaction with the environment. They found applications in cardio-vascular surgery (heart valves, vascular grafts), dentistry (tooth filling, dental crowns, and bridges), dermatology (artificial skin), etc [5–10]. Considering that the use of biomaterials improves the quality, prolongs, and saves human lives, a lot of research efforts were made to synthesize better materials throughout the years. Based on the properties, biomaterials belong to one of the following large groups of the materials:

- polymers,
- metals,
- ceramics and
- composites [37,38].

3.1. Polymers

Polymers are macromolecules with chain-like structure, with the backbone composed of many repeating subunits. Small organic molecules called *monomers* are bonded during the polymerization reaction. Linear polymers consist of a long chain and side groups while branched have multiple sidechains. Cross-linked polymers have bonds between chains, which build a 3D network. Figure 4 shows linear, branched and cross-linked polymer structures.

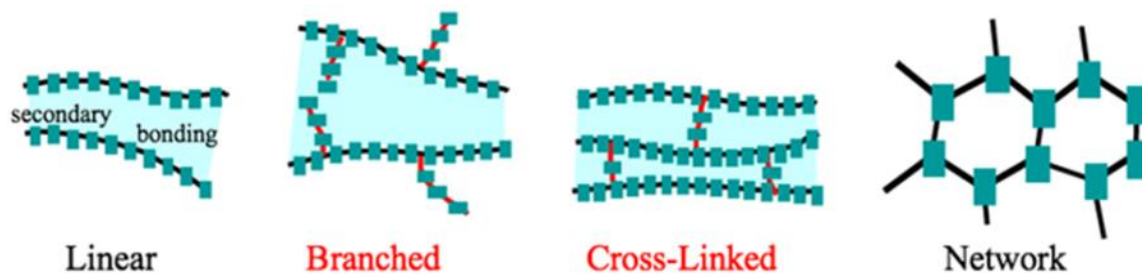


Figure 4. Schematic representation of different polymer structures [37].

Unlike metals that melt at a fixed temperature, polymers show a range of temperatures at which phase transitions occur. There are two major classes of polymers used as biomaterials: thermosetting and thermoplastic [39]. Thermosetting polymers solidify when a low-viscosity resin, monomer, cures into cross-linked structure during processing, with the addition of a curing agent, or application of heat or UV light that initiate the reaction. Once the material is cross-linked, it cannot be reshaped or melted. Thermoplastic polymers are a high-viscosity resins that can be processed by heating above its melting temperature. Low density, corrosion and chemical resistance, thermal insulating properties along with the low-cost processing are some of the advantages that make polymer materials attractive as dental restorative materials combined with ceramics and metals. A thermoplastic polymer, polymethyl methacrylate (PMMA) is often applied as acrylic cement for implants [40]. Polymers that are used for filling of bone voids are degradable in biological surrounding, i.e. *biodegradable*. In an ideal case, they should degrade as the new bone generates. Most commonly used polymers for this purpose are poly(lactide), polyglycolide and their copolymers [41].

3.2 Metals

Advantages of metals are superior mechanical properties (modulus of elasticity, impact and wear resistance) [42]. Metallic materials have been studied and applied as biomaterials for a long time, as pure metals and alloys [43,44]. One of the most frequently used metals as a biomaterial is titanium [45]. Due to its high hardness value, titanium alloys are used for hip replacement and other load bearing structures in human body [46]. However, titanium is inert and cannot bond to a bone; therefore, it requires coating composed of materials similar to the bone [47]. Mixture of mercury, silver, tin and copper, called *amalgam*, was used in dentistry as tooth fillings for a very long time. Although it has many advantages, certain toxicological and environmental concerns have been brought into the spotlight, along with the change of aesthetic requirements in society over the years. Table 1 presents some important advantages and disadvantages of amalgam, which can explain why

it was abandoned as a biomaterial [48]. Due to their high biocompatibility and bioactivity, dentistry has turned towards composite materials for tooth fillings.

Table 1. Advantages and disadvantages of using amalgam tooth filling [48].

Advantages	Disadvantages
<ul style="list-style-type: none"> • Reasonably priced and cost effective • Strong, resistant to wear and durable • Dependable • Least time-consuming kind of filling for a dentist to perform • Average lifetime of amalgam fillings is about 15 years • Used for more than a century with good results 	<ul style="list-style-type: none"> • Silver color is no longer considered aesthetically acceptable • Does not stick to the tooth • Conducts heat too well, which results in people experiencing pain when they eat hot or cold foods • Contains mercury (mercury compounds are poisonous) • Getting rid of millions of potentially environmentally hazardous old fillings

3.3 Ceramics

Ceramics represent materials of high hardness, compression strength and wear resistance, as well as great thermal insulation capability and chemical resistance [49]. For the application in dentistry, the main advantages of ceramic materials are biocompatibility and bioactivity. However, they are prone to failure due to brittleness, which limits use of ceramics without modification. Among the most important properties that characterize ceramics is thermal shock (sudden temperature change) resistance, a property that defines the environment in which the material could be used [50]. Ceramic materials have high values of Young's modulus, compared to metals and polymers. Also, their constituent atoms are light (oxygen, carbon, calcium, phosphorus) and not packed tightly, making them low density materials and causing exceptionally high specific modulus values. Due to the resistance of the lattice to the dislocation movement, ceramics are considered extremely hard materials. These properties make ceramic materials great candidates for reinforcement of polymers, which will be further addressed in the subsection of composite materials. With the technological development, quality improvement of lives increased, leading to a further search for stronger and lighter materials that would satisfy various societal needs. Among different research directions, synthesis and studying of biomaterials gained attention in the mid-20th century.

Biocompatible ceramic materials, bioceramics, serve as repair or replacement materials for damaged teeth, joints, or bones [51]. Over decades, bioceramics were developed in numerous forms and compositions, and they can be classified as bioinert and bioactive ceramics.

Figure 5 depicts the use of bioceramic materials in the human body [52]. As presented, bioceramics found wide application in tissue repair and replacement, as well as drug delivery agents, which are not presented in the figure.

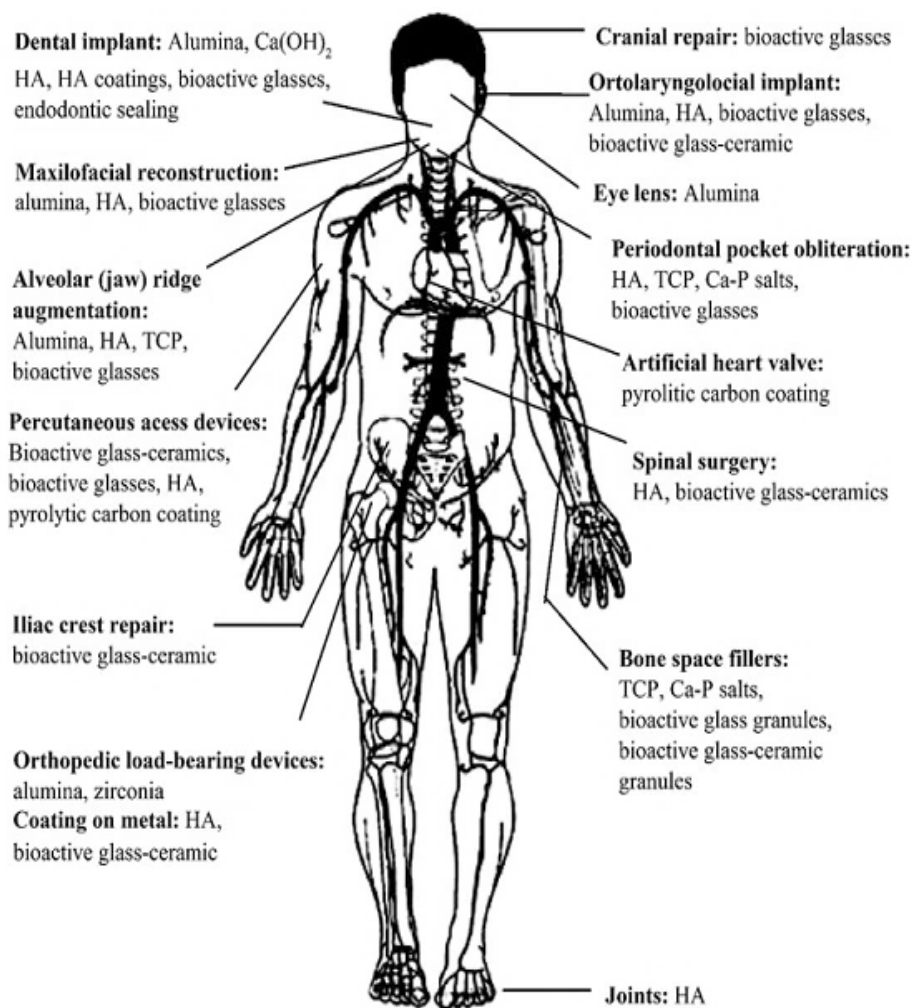


Figure 5. Application of ceramic biomaterials in human body [52].

3.3.1. Bioinert ceramics

Aluminum oxide (alumina, Al_2O_3) and zirconium oxide (zirconia, ZrO_2) are widely used in dentistry and orthopedics, replacing metal due to their chemical inertness and higher wear and corrosion resistance [53,54]. Polycrystalline alumina is the most used ceramics material for the production of hip implants. Zirconia has higher mechanical strength and toughness than alumina, as well

as lower Young's modulus of elasticity; therefore, it is used as a replacement of alumina in hip, knee and teeth prostheses fabrication [55,56]. However, in order to prevent mechanical failure of zirconia based implants, it has to be doped with yttrium or magnesium oxide. Synergistic effect of both alumina and zirconia could yield implants with improved mechanical properties and therefore wider their applications [54]. Major drawback for the use of alumina and zirconia lies in their inertness, which causes inability to interact with the surrounding tissue.

3.3.2. Bioactive ceramics

Unlike bioinert, the main purpose of bioactive ceramics is to interact chemically/biochemically (bond and support bone growth) with the host bone, which is why these materials need reactive surfaces [57]. Chemical and biological processes take place at the surface, once bioceramic material is incorporated, which results in temporary and permanent changes at their contact interface. Bioactive ceramics should replace damaged hard tissue and ensure structural integrity while it recovers through various biological processes. Sometimes, an implant is placed as a permanent replacement for the bone or tooth, and it should withstand harsh conditions in human or animal biological systems over the years [58]. Furthermore, along with the successful interaction with the host surroundings, bioactive materials should not enhance bacterial activity and multiplication that would lead to an infection [59]. The greatest challenge for researchers designing ceramic biomaterials represents improving their mechanical performance and endurance. Unlike metallic materials, ceramics are brittle, which could result in failure when load is applied [56]. There are many reports and proposals dealing with the modification of bioactive ceramics, focusing on improved antimicrobial activity, biocompatibility, and mechanical properties. Bioceramics can be divided into glasses and calcium phosphates (CaP).

3.3.2.1. Bioactive glasses

Bioactive glasses represent a group of glasses that interact with body fluids, and in physiological reaction forming carbonated hydroxyapatite (cHAp), allowing an attachment of the implant to a host bone [60]. Weight fraction of SiO_2 is crucial for bioactivity of glasses. Bioglass[®] (45S5) contains 45% of SiO_2 and represents the most used bioactive glass. It is mainly composed of SiO_2 , CaO , Na_2O and P_2O_5 , but various compounds (such as MgO , Al_2O_3 , CaF_2 , etc.) have been added for modification, in order to improve 45S5 mechanical properties [61–63]. Phase diagram presenting composition of 45S5 is shown in Figure 6.

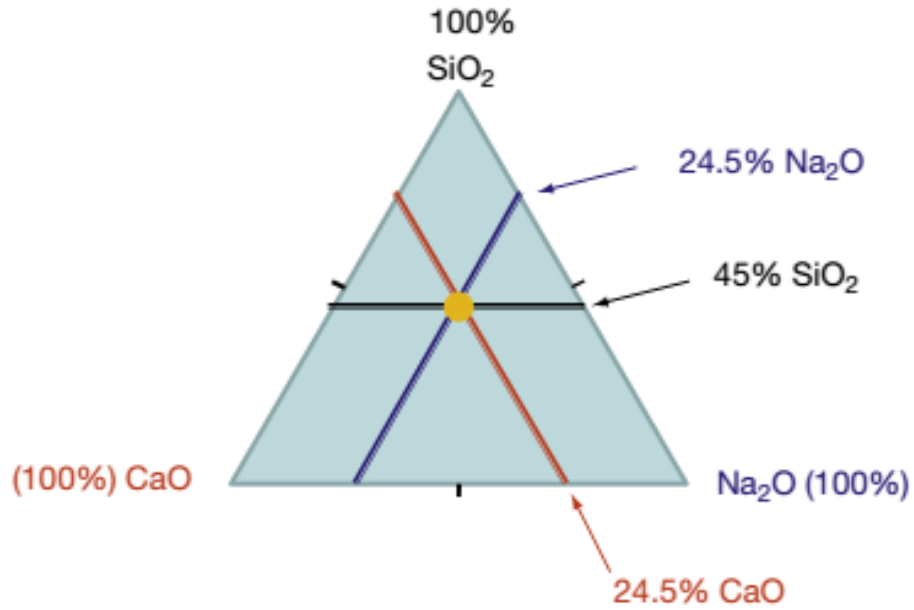


Figure 6. $\text{SiO}_2\text{-CaO-Na}_2\text{O}$ phase diagram with composition of 45S5 bioactive glass [61].

In vitro tests in the simulated body fluid (SBF) showed generation of a cHAp at the interface of bioactive glasses. Figure 7 shows scheme of glass dissolution at the interface and precipitation of calcium phosphate that transforms into cHAp [61]. These chemical reactions enable interaction with a surrounding host bone tissue, making bioactive glasses valuable biomaterials with high biocompatibility. However, their poor mechanical properties require further modifications of glasses, through structural changes and by introducing reinforcements to build composites, which will be further explained in the subsection 3.4.

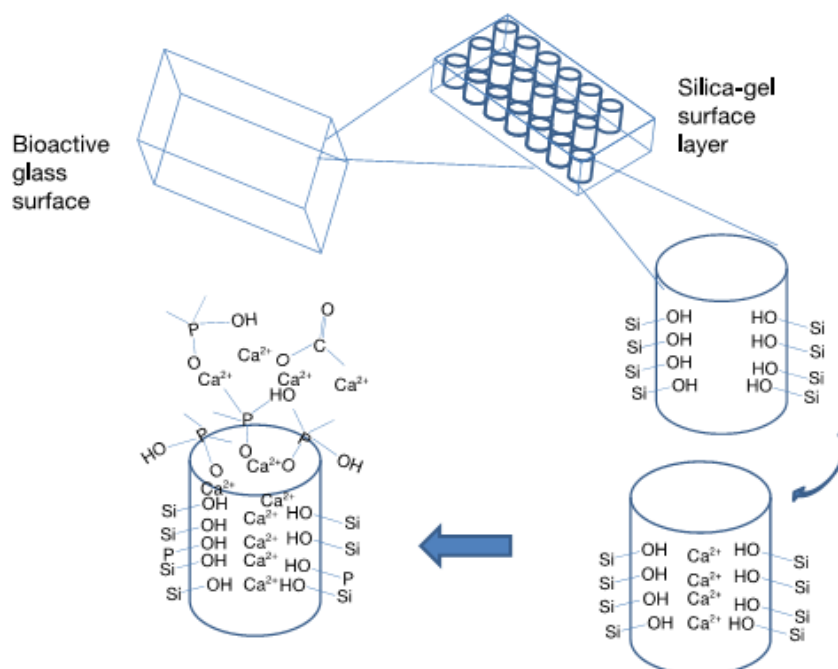


Figure 7. Surface modifications of bioactive glass due to interaction with simulated body fluid [61].

3.3.2.2. Calcium phosphates

Calcium phosphates are considered excellent biomaterials due to their compositional resemblance to teeth and bones, which ensures high biocompatibility, opening the route for their synthesis, investigation, and modification, in order to achieve good adaptability in the host body [64–74]. Osteoconductivity is another valuable property of CaPs, making them ideal candidates for scaffolds, discussed in detail in subsection 4.4.2.2. The first use of CaPs started in the early 20th century, with the constant development and expanding through various applications. They are used for the repair of alveolar bone, teeth, sinus lifts and bones caught by cancer, osteoporosis, and other illnesses. Because of the ability to release Ca and P ions that lead to remineralization of tooth, CaPs have become valuable group of materials for the application in dentistry [13, 75–79]. They are also utilized as cements or coatings on titanium and titanium alloy implants, combining the ceramics bioactivity and superior mechanical properties of metals [58]. Along with biocompatibility, porosity and mechanical properties are considered incredibly important for the application of CaPs. Higher porosity enables vascularization and bone tissue cells migration into the structure, creating stronger bonding to the natural bone [80]. In addition, porosity influences bioresorbability. Structures can be divided into microporous (pore dimensions less than 5 mm) and macroporous (pore dimensions bigger than 100 mm). Pore size and volume fraction influence mechanism and efficiency of bone growth into the ceramic structure. Table 2 presents calcium phosphates with various Ca/P ratios [11]. Phosphates, with the ratio higher than 1, are suitable for the production of implants. Due to their high porosity, CaPs can also be used as drug carriers [81–84].

Table 2. Ca/P ratio for different CaPs [11].

Ca/P	Name	Symbol	Formula	pK _s at 25 °C
0.5	Monocalcium phosphate monohydrate	MCPM	Ca(H ₂ PO ₄) ₂ H ₂ O	1.14
0.5	Monocalcium phosphate anhydrous	MCPA	Ca(H ₂ PO ₄) ₂	1.14
1.0	Dicalcium phosphate dehydrate (brushite)	DCPD	CaHPO ₄ ·2H ₂ O	6.59
1.0	Dicalcium phosphate anhydrous (monetite)	DCPA	CaHPO ₄	6.90
1.33	Octacalcium phosphate	OCP	Ca ₈ (HPO ₄) ₂ (PO ₄) ₄ ·5H ₂ O	96.6
1.5	α-Tricalcium phosphate	(α-TCP)	Ca ₃ (PO ₄) ₂	25.5
1.5	β-Tricalcium phosphate	(β-TCP)	Ca ₃ (PO ₄) ₂	28.9
1.2–2.2	Amorphous calcium phosphate	ACP	Ca _x (PO ₄) _y ·nH ₂ O	–
1.67	Hydroxyapatite	HAp	Ca ₁₀ (PO ₄) ₆ ·nH ₂ O	116.8

Crystallographic parameters of CaPs are presented in Table 3, reprinted [64]. Different lattice parameters dictate the ion doping ability, solubility, and density.

Sadat-Shojai et al. have shown how different CaPs could be obtained from the same starting ingredients depending on the synthesis conditions [85]. By changing reaction temperature, time, or

pressure all the CaPs can be produced from the same batch due to induced phase transformations. An overview of the formed phases and Ca/P ratios that they obtained is presented on Figure 8 and in Table 4, where denotations of images are described.

Table 3. Structural parameters for various CaPs [64].

Compound	Crystal system	Space group	Unit cell parameters	Z^a	Density (g cm ⁻³)
MCPM	Triclinic	$P\bar{1}$	$a = 5.6261(5)$, $b = 11.889(2)$, $c = 6.4731(8)$ Å $\alpha = 98.633(6)$, $\beta = 118.262(6)$, $\gamma = 83.344(6)^\circ$	2	2.23
MCPA	Triclinic	$P\bar{1}$	$a = 7.5577(5)$, $b = 8.2531(6)$, $c = 5.5504(3)$ Å $\alpha = 109.87(1)$, $\beta = 93.68(1)$, $\gamma = 109.15(1)^\circ$	2	2.58
DCPD	Monoclinic	Ia	$a = 5.812(2)$, $b = 15.180(3)$, $c = 6.239(2)$ Å $\beta = 116.42(3)^\circ$	4	2.32
DCPA	Triclinic	$P\bar{1}$	$a = 6.910(1)$, $b = 6.627(2)$, $c = 6.998(2)$ Å $\alpha = 96.34(2)$, $\beta = 103.82(2)$, $\gamma = 88.33(2)^\circ$	4	2.89
OCP	Triclinic	$P\bar{1}$	$a = 19.692(4)$, $b = 9.523(2)$, $c = 6.835(2)$ Å $\alpha = 90.15(2)$, $\beta = 92.54(2)$, $\gamma = 108.65(1)^\circ$	1	2.61
α -TCP	Monoclinic	$P2_1/a$	$a = 12.887(2)$, $b = 27.280(4)$, $c = 15.219(2)$ Å $\beta = 126.20(1)^\circ$	24	2.86
β -TCP	Rhombohedral	$R3cH$	$a = b = 10.4183(5)$, $c = 37.3464(23)$ Å $\gamma = 120^\circ$	21	3.08
HAp	Monoclinic	$P2_1/b$	$a = 9.84214(8)$, $b = 2a$, $c = 6.8814(7)$ Å $\gamma = 120^\circ$	4	3.16
	Hexagonal	$P6_3/m$	$a = b = 9.4302(5)$, $c = 6.8911(2)$ Å $\gamma = 120^\circ$	2	
FAp	Hexagonal	$P6_3/m$	$a = b = 9.367$, $c = 6.884$ Å $\gamma = 120^\circ$	2	3.20
OAp ^b	Hexagonal	$P6$	$a = b = 9.432$, $c = 6.881$ Å $\alpha = 90.3$, $\beta = 90.0$, $\gamma = 119.9^\circ$	1	~3.2
TTCP ^c	Monoclinic	$P2_1$	$a = 7.023(1)$, $b = 11.986(4)$, $c = 9.473(2)$ Å, $\beta = 90.90(1)^\circ$	4	3.05

^aNumber of molecules in the unit cell.

^bOxyapatite

^cTetracalcium phosphate

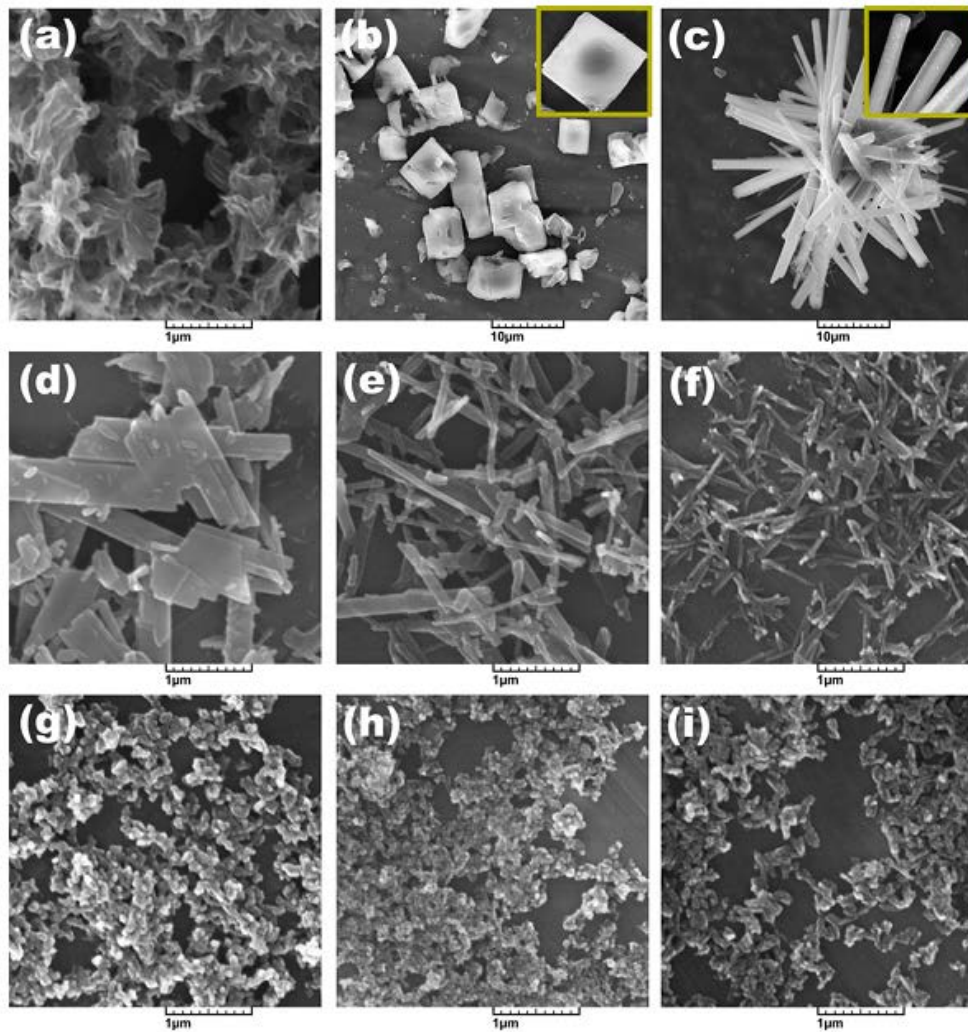


Figure 8. Different CaP structures obtained with various synthesis conditions [85].

Table 4. Phase analysis, Ca/P ratio and carbonate replacement of the synthesized CaP powders [85].

	Phase composition	Ca/P	Carbonate replacement
a	DCPD	1.05	No carbonated
b	DCPA	1.15	No carbonated
c	HAp+DCPA+minor OCP	1.75	No carbonated
d	HAp+DCPA+OCP	1.39	No carbonated
e	HAp+DCPA+minor OCP	1.52	No carbonated
f	HAp+OCP	1.48	No carbonated
g	HAp	1.64	Carbonated (B-type)
h	HAp	1.5	Carbonated (AB-type)
i	HAp	1.71	Carbonated (B-type)

3.4 Composite materials

Composites are defined as multiphase (usually two-phase) materials that combine properties of the constituents [37]. The reason for the composite invention was the need for low density/weight materials that have desired mechanical, chemical, electrical or thermal properties. Namely, all the

properties of composites can be modified by the type and ratio of components. Matrix is a continuous phase in which reinforcing filler particles are dispersed as a discontinuous phase. Unlike metal alloys, chemical and physical properties of the components in composite are not altered. During the last century, research and development in science and industry has led to processing of various composites comprised of metals, polymers and ceramics. Composites can be classified according to the matrix or the shape of the reinforcement [86]. The first classification divides composites into three groups: 1) metal, 2) polymer and 3) ceramic matrix composites. By the shape of the reinforcement, the following are recognized: 1) particle, 2) whisker and 3) fiber reinforced composites.

Reinforcements modify and improve mechanical, chemical, optical, thermal and electrical properties, as well as biocompatibility of the matrix [87]. The most frequently used composites in dentistry are polymer-based, with different kinds of ceramic reinforcements. They can be used for various restorative purpose [33,88–91]. Matrix material is usually bisphenol A-glycidyl dimethacrylate (Bis-GMA) [92]. The inorganic reinforcement can be silica, alumina, titania, etc [93], as they enhance poor mechanical performance of polymeric matrix. Particle and fiber nanosized reinforcements can drastically improve tensile and compressive strength, while reducing polymerization shrinkage, the biggest disadvantage of polymers used in dental application [90]. Ceramic matrix composites are the focus of this thesis and they will be thoroughly presented through the HAp applications in the following section. As mentioned in the section 3.3, ceramics are brittle and have exceptionally low fracture toughness that makes them risky for the use in load-bearing applications. They are reinforced with different ceramics, similar to those for the reinforcement of polymer matrix. Calcium phosphates can be used both as matrix or reinforcement, depending on the demands [16,94].

4. HYDROXYAPATITE

Hydroxyapatite (HAp) is a dominant dentine and bone constituent. Therefore synthetic apatite-based materials and implants have high biocompatibility of. With excellent osteoconductive and bioactive properties, HAp is favored as the biomaterial of choice in both dentistry and orthopedics [95,96].

4.1 Composition, structure, and properties of HAp

Among those listed in the Table 2, hydroxyapatite ($\text{Ca}_{10}(\text{PO}_4)_6(\text{OH})_2$, HAp) is the most attractive and well-studied calcium phosphate [97]. Structural formula of HAp is presented in Figure 9 [98]. It has a theoretical chemical composition of 39.6 wt% of Ca and 18.5 wt% P, with Ca/P weight ratio of 2.151 and molar ratio of 1.667 [61]. Natural and synthetic HAp have different chemical composition; the former one contains additional elements, such as Na, Mg, Zn, K, F, leading to a formation of non-stoichiometric crystal structure where cations replace calcium, while anions replace hydroxyl group [99].

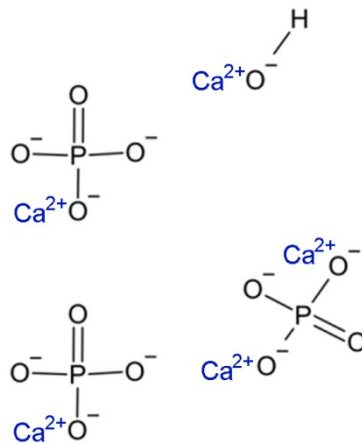


Figure 9. Structural formula of HAp.

The crystal structure of HAp is usually hexagonal, with space group $P6_3/m$, which is presented in Figure 10; while lattice parameters are presented in Table 3 [99,100]. Synthetic HAp with Ca/P ratio of 1.67 has a great stability, but the HAp in the body is non-stoichiometric and shows higher level of natural degradability due to osteoclast action/remodeling of the bone. Similarity of HAp to bone, dentin and enamel is depicted in Table 5.

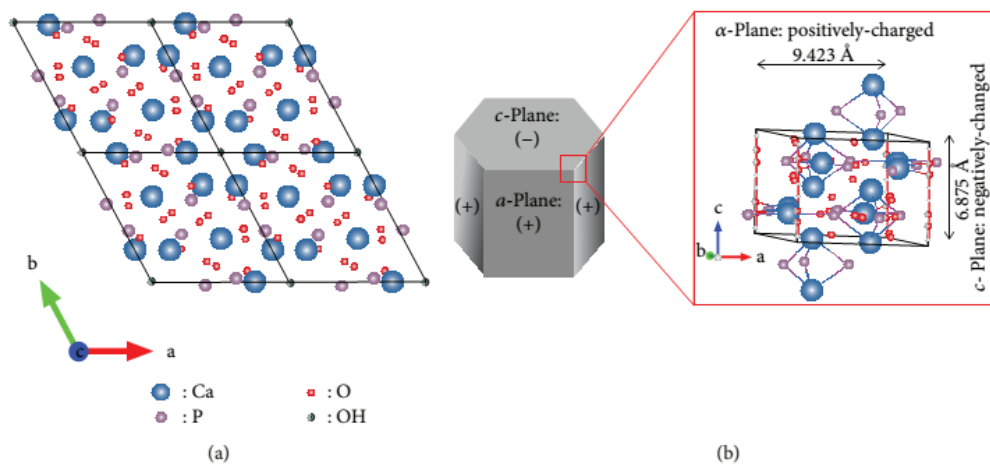


Figure 10. Crystal structure of HAp [100].

Table 5. Chemical composition of enamel, bone, dentin and HAp [61].

Composition (wt. %)	Enamel	Dentin	Bone	HAp
Calcium	36.5	35.1	34.8	39.6
Phosphorus	17.7	16.9	15.2	18.5
Ca/P	1.63	1.61	1.71	1.67
Sodium	0.50	0.60	0.9	-
Magnesium	0.44	1.23	0.72	-
Potassium	0.08	0.05	0.03	-
Carbonate (as CO_3^{2-})	3.5	5.6	7.4	-
Fluoride	0.01	0.06	0.03	-
Chloride	0.30	0.01	0.13	-

Another disadvantage of HAp, as of all ceramic materials, represents their relatively poor mechanical performance under load [101–103]. Mechanical properties of HAp are listed in Table 6 [65,104]. The values of modulus of elasticity are comparable to those of bones and teeth, but the overall strength of porous HAp is lower. Dense HAp has much higher values, but porosity is necessary for good bioactivity, as well as cell and tissue proliferation. The challenge is to build a material that can withstand load and retain bioactivity, to ensure healthy tissue growth.

Table 6. Mechanical properties of HAp.

HAp	Tensile strength, MPa	Compressive strength, MPa	Bending strength, MPa
Dense	38–300	120–900	38–250
Porous	~3	2–100	2–11

4.2 Synthesis of HAp

As registered in the Table 2, depending on the molar ratio of Ca and P, different phases could be formed during synthesis, altering the bioactivity of the resulting material. HAp synthesis tech-

niques can be divided into three groups [105,106]: high temperature, dry and wet synthesis. Classification of synthesis techniques is schematically presented in Figure 11.

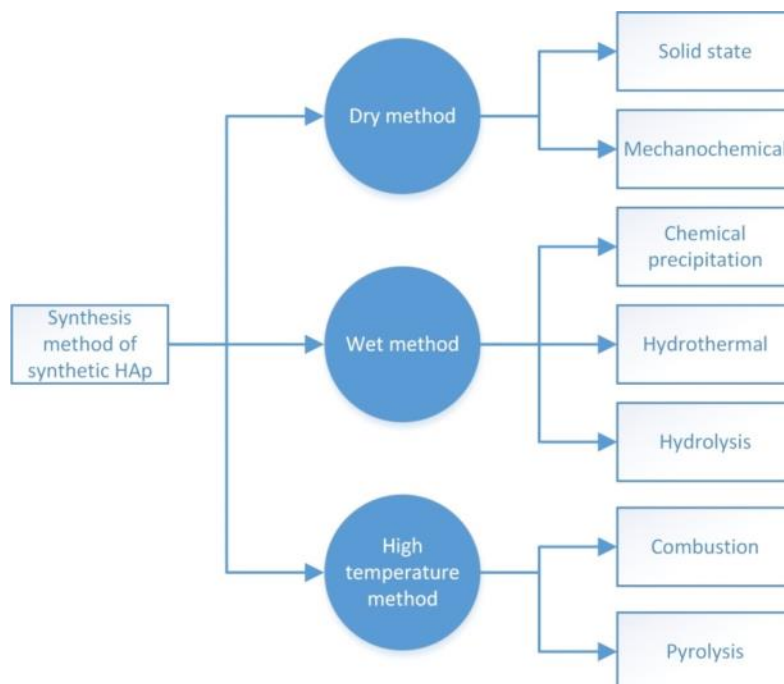


Figure 11. Techniques for HAp synthesis.

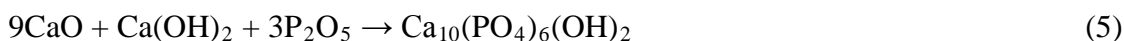
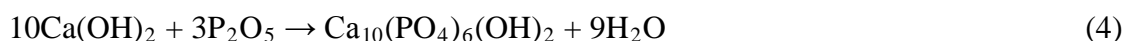
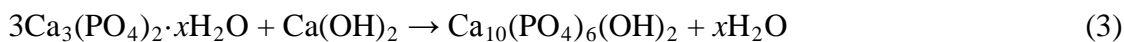
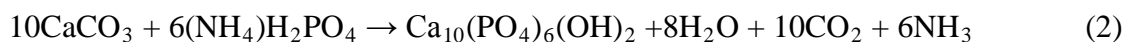
High temperature synthesis

Combustion and pyrolysis represent high temperature synthesis techniques that include thermal decomposition of reagents and the reaction in gas phase with the formation of the powder. The difference between the two techniques is that combustion starts at lower temperatures with sudden heating, while in pyrolysis reagents are sprayed into a heated furnace [105]. Pyrolysis is a preferred technique because it results in HAp with high degree of crystal phase homogeneity [107–109].

Dry synthesis

As can be seen in Figure 11, dry synthesis can be performed via solid-state or mechanochemical reactions. Solid-state process is the simplest, requiring only calcium and phosphate-based powders that are calcined at high temperatures. HAp obtained using this procedure shows high degree of crystallinity. However, formation of different phases and large grains represent drawbacks for the application of solid-state synthesis [105]. Mechanochemical technique employs different mechani-

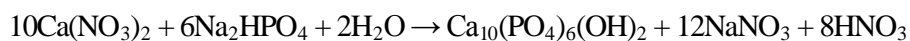
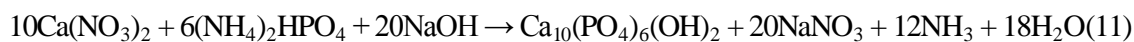
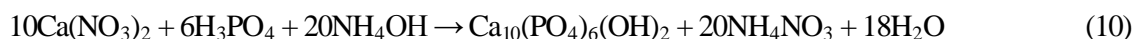
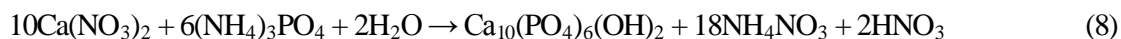
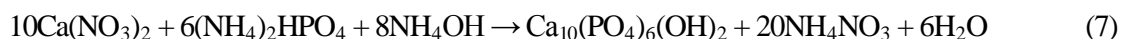
cal forces to induce chemical reaction between reactants [110]. With the control of several parameters, fine, regularly shaped nanocrystals of HAp could be synthesized [111,112]. Relevant reactions that occur in dry synthesis route are as follows [106]:



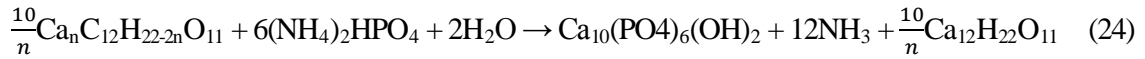
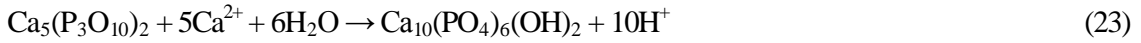
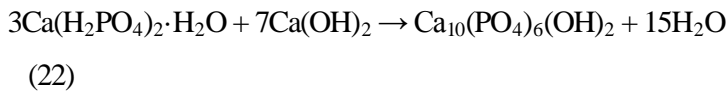
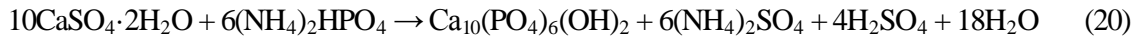
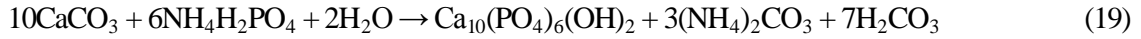
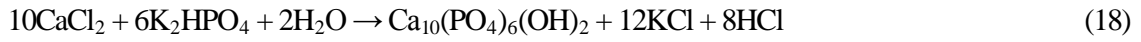
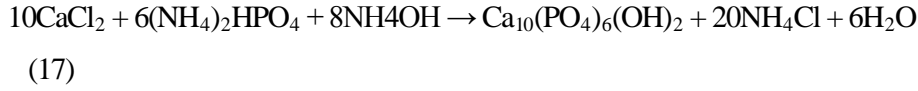
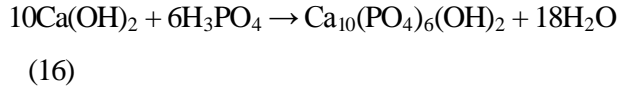
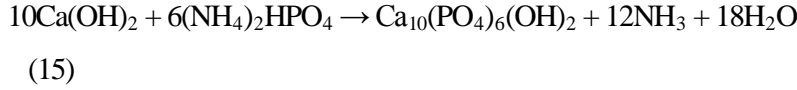
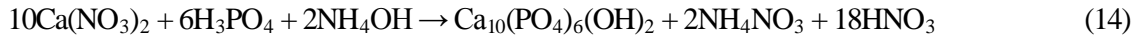
(6)

Wet synthesis

Synthesis in aqueous medium, called wet synthesis, can be separated into chemical precipitation, hydrolysis, and hydrothermal technique. They offer the ability to control size and morphology of the synthesized powder by the addition of different amounts of reagents, as well as adjusting the reaction temperature and time [113]. Chemical precipitation is frequently applied technique, offering the possibility of synthesizing large amounts of powder for a short time. Various chemicals containing Ca^{2+} and PO_4^{3-} ions were proposed and explored as reactants [114,115]. However, although synthesized HAp is in the form of fine nanopowder, it has low crystallinity, irregular crystal shape and impurities. Through many research efforts, it was established that pH value, temperature and solution maturing time play the key roles for the control of HAp powder morphology and stoichiometric Ca/P ratio. [104]. Very high temperatures and pH ensure obtaining pure crystalline HAp nanopowder. Typical chemical reactions included in wet synthesis are [106]:



(13)



Synthesis of HAp via hydrolysis of TCP or some other calcium phosphate is rarely used technique due to a poor control of purity and morphology, along with long reaction time [116,117]. Hydrothermal synthesis is performed at higher temperature and pressure, where precipitation of HAp occurs as a result of induced chemical reaction in the solution [118]. It is often applied for the synthesis of rod shaped, stoichiometric, pure crystalline HAp nanopowder [119–122]. Figure 12 depicts synthesis of rod-shaped HAp nanoparticles via hydrothermal method [106].

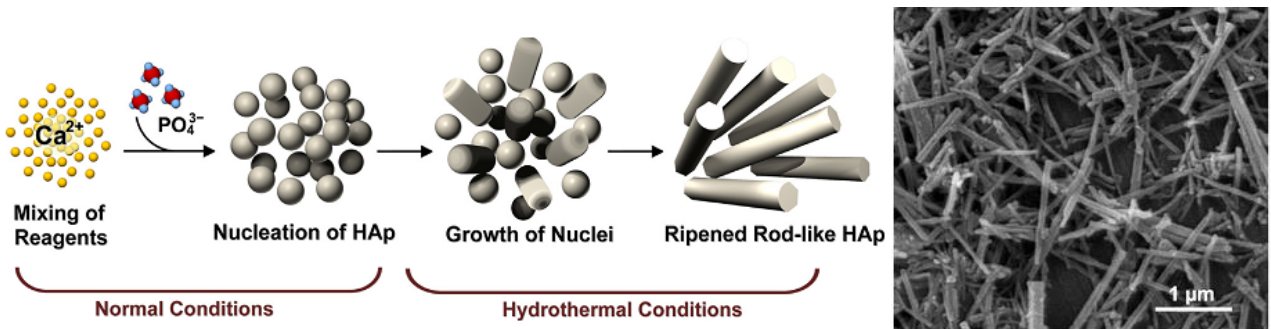


Figure 12. Hydrothermal synthesis of rod-shaped HAp nanoparticles [106].

Same as in the case of conventional chemical precipitation, hydrothermal synthesis requires careful control of parameters. Lower pH values lead to formation of different phases and shapes (Figure 13).

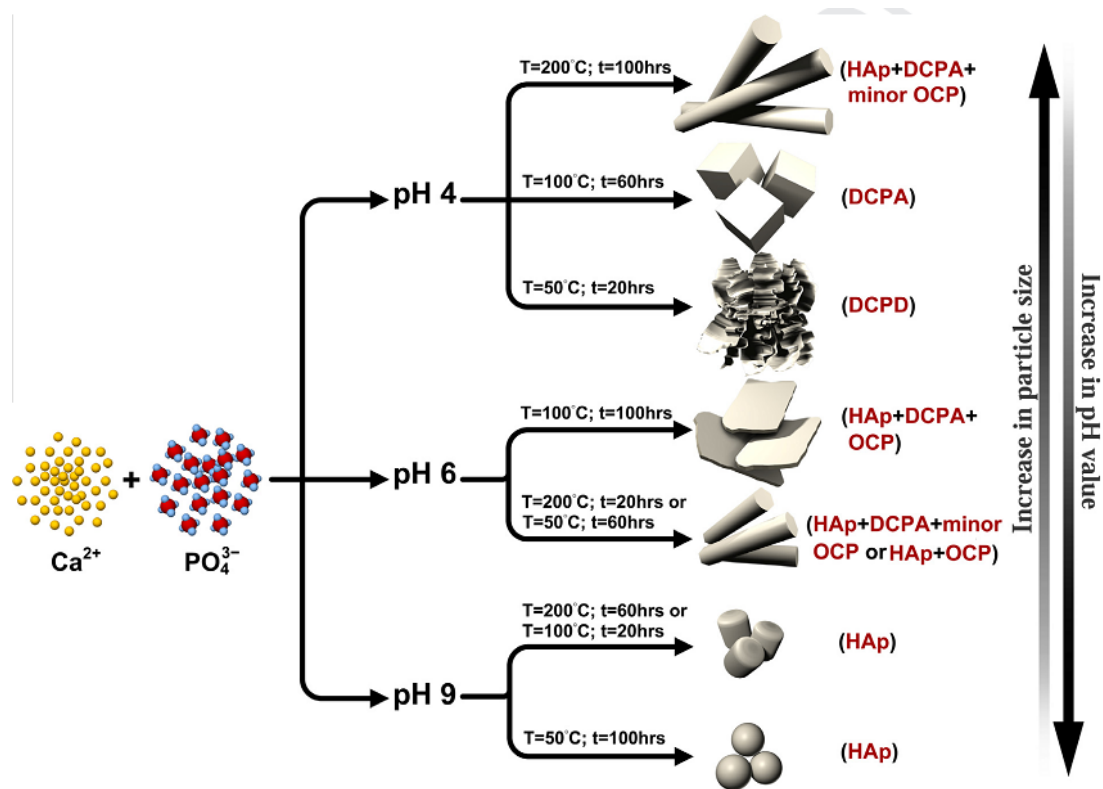


Figure 13. Influence of hydrothermal synthesis parameters on the formation of HAp particles [85].

In order to obtain fine, controlled morphology, organic modifiers and surfactants are used [123–125]. Surfactants can be synthetic (cetyltrimethylammonium bromide (CTAB)) or natural (vitamin C). Ethylene diamine tetraacetic acid (EDTA) is used to trap free Ca^{2+} ions by chelating, resulting in smaller HAp particles. Poly(ethylene glycol) (PEG) is also used for the synthesis of longer, fiber-like rods of HAp nanopowder. Various studies reported use of organic modifiers, with a high success rate in achieving uniform size and shape [126–128]. Table 7 shows different procedures for wet synthesis techniques.

After the synthesis, obtained HAp powder needs to be further processed, in order to adjust morphology and handling [11]. Particle agglomerates are grinded and milled to produce fine deagglomerated particles. Powders can be compacted using pressure (die or isostatic) or solid-state sintered, in order to reduce porosity and increase density, which greatly influences mechanical properties of synthesized ceramics. Synthesis and post-processing conditions influence porosity and consequently, compressive strength [129–131]. Higher sintering temperatures ($\sim 1250^\circ\text{C}$) result in HAp with higher density and grain size, which leads to an increased modulus of elasticity and compressive strength [132–134]. Above 1300°C , HAp decomposes unless high pressure and water are supplied, which could cause uncontrolled grain growth that decreases hardness of bioceramic material [135–137].

Table 7. Wet synthesis of HAp [105].

Method	Ca/P source	Temperature (°C)	Result
Precipitation	Ca(OH) ₂ , H ₃ PO ₄	r. t. ^a	• Spherical particles with the size in the range of 0.2–1.6 μm
	Ca(OH) ₂ , H ₃ PO ₄	r. t.	• Rod-like particles, with about 200 nm in length and 50 nm diameter.
	Ca(NO ₃) ₂ ·4H ₂ O, (NH ₄) ₂ HPO ₄	r. t.	• Almost spherical particles with diameter in the range of 8–20 nm
	Ca(NO ₃) ₂ ·4H ₂ O, Na ₃ PO ₄	r. t.	• Short nano-rod particles, with diameter in the range of 1.9–14.2 nm and length in the range of 4.0–36.9 nm
Hydrothermal	CaCl ₂ , H ₃ PO ₄	100	• Rod-like particles (80 nm length and 15 nm width)
	Ca(OH) ₂ , (NH ₄) ₃ PO ₄	200	• Irregular agglomerates of cHAp (5–40 nm), Ca/P ratio: 1.86–2.08
	CaCl ₂ , K ₂ HPO ₄	60–150	• Rod-like particles at 120 °C (diameter in the range of 15–20 nm and length in the range of 60–75 nm length)
	Ca(NO ₃) ₂ ·4H ₂ O, (NH ₄) ₂ HPO ₄	25–180	• HAp (pH = 10) with granule-like shape (30, 50 and 75 nm)

^a room temperature

4.3 Chemical modifications of HAp

Ion doping

HAp ion doping has drawn attention of researchers due to the possibility of including different ions in the crystal lattice of HAp, without the disruption of its integrity. In order to increase antimicrobial activity and to avoid a possibility of infection upon dental implant introduction in the bone, HAp was doped with Ag⁺ and Cu²⁺ [22]. Several research reports reported incorporating Sr²⁺, Co²⁺, Mg²⁺, Mn²⁺ and Fe³⁺ ions to elevate similarity to the bone composition [138–143]. It was shown that metal cations are not harmful for the organism when included in the reasonable concentrations. Low concentrations can influence morphological and chemical properties [144,145]. According to the studies, the addition of Zn²⁺ leads to the higher antibacterial activity [139]. Doping with more than one element was also reported, reducing the particle size, while increasing crystallinity at the same time [138,141]. Overall, this type of HAp modification is very attractive due to many advantages and improvements ions could bring to increase bioactive properties of HAp.

Hydroxyl group substitution with fluorine

Fluorine represents essential element that contributes to bone mineralization, which makes it an excellent candidate for substitution of OH⁻ in HAp. As a result of this substitution, fluorapatite (FAp), with chemical formula Ca₁₀(PO₄)₆F₂ is formed. Structure of FAp is presented in Figure 14,

with lattice parameters: $a = 9.368$ and $c = 6.875$ Å [146]; unit cell along a -axis is smaller compared to HAp due to the difference in size between F^- and OH^- ions.

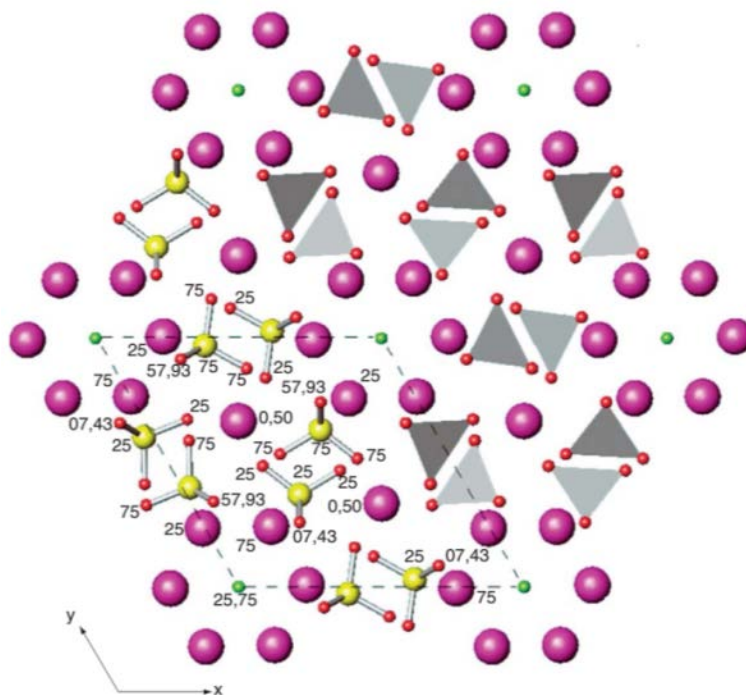


Figure 14. Projection of the crystal structure of FAp on the (001) crystallographic plane [147]. Ca - purple, F - green, O - red, P - yellow.

FAp shows higher thermal stability and lower solubility compared to HAp, being more suitable for processing near HAp decomposition temperatures [148]. FAp is more resistant to acidic environment and therefore used for protection from demineralization; HAp dissolves when pH drops below 5.5, while FAp starts dissolving below 4.5. In saliva, presence of fluorine slows down demineralization by substituting hydroxyl group from dissolved HAp and depositing on the enamel (Figure 15) [6,13–15,149]. Synthetic FAp is obtained by similar techniques to those used for the synthesis of HAp. Along with better chemical and thermal properties, compared to HAp, FAp has more superior mechanical properties as well. Higher hardness values, modulus of elasticity and fatigue resistance are some of the FAp ceramics features that gave this material advantage over other apatites. However, fluorine is highly toxic element and thus careful studies have to be performed in order to find the best concentration of FAp that is safe for use in the human body [147].

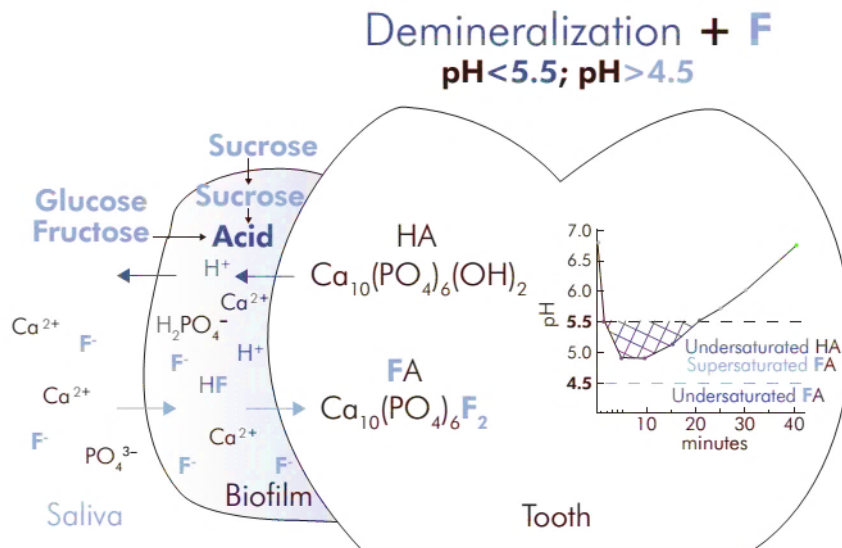


Figure 15. Protection from demineralization of enamel by FAp deposition [13].

4.4 Application of HAp and its composites

HAp powder found applications as a biomaterial in various parts of the human body. Some of them are bones and teeth fillings, toothpastes, titanium implant coatings and reinforcements in polymer-based materials [150–157]. Applications of HAp can be divided into commercial products, tissue engineering and drug delivery systems.

4.4.1. HAp based commercial products

Toothpastes and mouth washing products containing HAp have become very attractive over the past few years [158]. Demineralization of teeth is a common phenomenon, caused by the enamel exposure to wear, pressure and pH changes in saliva. Although fluorine is a common ingredient in oral care products due to the ability to slow down demineralization, its toxicity and the need for treating dental hypersensitivity on a daily basis with enamel remineralization, brought attention to incorporation of HAp in toothpastes [159–161]. Efforts were made to use biomimetic approach for dentin tubules sealing and protection by depositing synthetic HAp nanoparticles [162]. They are small enough to penetrate open tubules and create protection from oral environment. In this manner, pain caused by dental hypersensitivity could be reduced, as well as expanding the tooth lifecycle [158,163–165].

4.4.2. HAp applications for bone and tooth replacement and reconstruction

4.4.2.1. HAp coatings

The replacement of a lost tooth can be performed using dental implant, usually metallic, titanium-based alloys, as mentioned in section 3.2. [45,46]. Although they offer excellent mechanical properties, much higher wear and fracture resistance compared to ceramics, their inability to bond to a host surrounding tissue requires coating with bioactive and biocompatible material, such as HAp [166]. Beside structure similarity to teeth, low solubility of HAp gives it advantage over other CaPs [167–169]. Coating performance depends on the layer thickness, porosity/density, phase crystallinity and purity. For avoiding mechanical damage during implementation, adhesion between HAp coating and metallic implant must be strong. Coating with HAp increases osteointegration and osteoconductivity [170]. Furthermore, research has shown that coated implants last longer compared to the uncoated [64,171,172]. The most frequently employed method for metallic implant coating is plasma spraying (Figure 16) [6,173,174]. Melted or softened HAp particles are sprayed on a metallic implant in the presence of plasma (He, Ar, N₂ and H₂ or the mixture are used for plasma gas; Ar is used as a base gas). Radio frequency and direct current are the most used plasmas for the coating with HAp, where a gas temperature can reach over 9000 °C. The main disadvantage of this procedure is in thick, non-uniform layer deposited on the metal surface, making the implant prone to mechanical damage during handling and in the host body. Nonetheless, this method is overall better compared to the rest that include pulsed laser deposition, ion beam-assisted deposition, hot isostatic pressing, dip coating and biomimetic process [167].

HAp is known for the ability to create bonds with proteins due to the highly reactive interface [100]. Having nanoscale diameters, HAp particles can cross cell barrier and deliver the drug to the low accessible sites. Composites and implant coatings containing nano-HAp were used for different drug release [21,175].

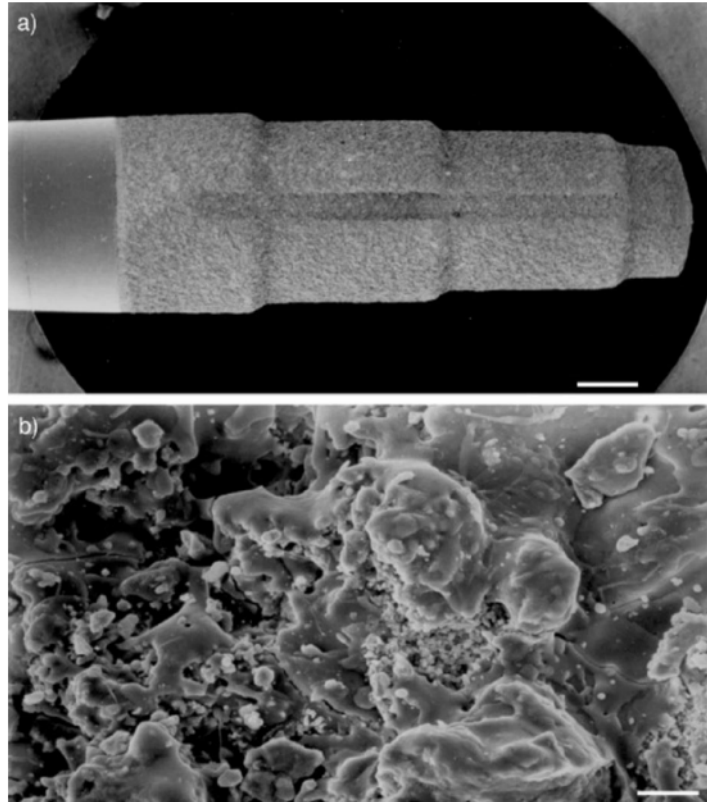


Figure 16. Dental implants coated with CaP by a plasma-spray process at magnification of 10x (bar = 1 mm) (a) and 1kx (bar = 1 μ m) (b) [6].

4.4.2.2. HAp scaffolds and drug delivery

As mentioned before, HAp is not suitable for load-bearing applications due to the poor mechanical properties. However, it is appropriate for the production of scaffolds, to enhance cell proliferation and integration in the structure [176]. X-ray microtomography 3D image of porous HAp based scaffold is presented in Figure 17 [11]. HAp scaffolds with pores up to 300 μ m were produced using replication technique for the application in bone tissue regeneration [177]. Saso-2 cells were able to proliferate and migrate through scaffolds that achieved similar compressive strength as a bone.

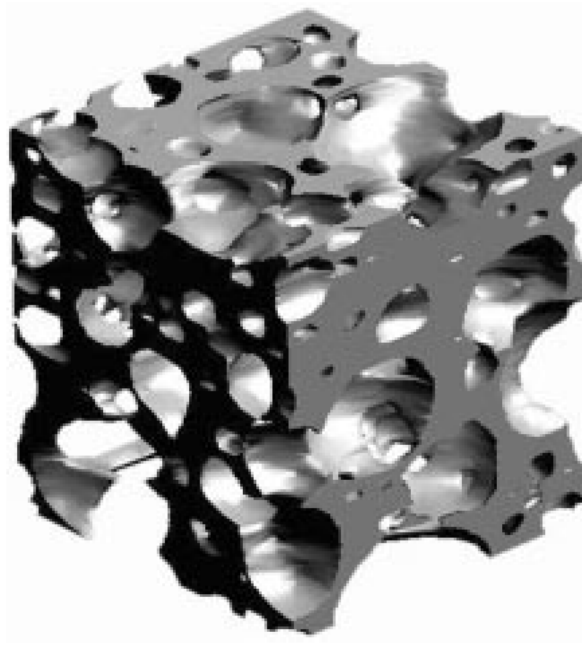


Figure 17. 3D image of HAp scaffold [11].

3D printing technique proved to be a valuable tool for the preparation of HAp based scaffolds with interconnected channels that showed high capacity for MC3T3-E1 cells proliferation, which makes these materials potential candidates for bone tissue engineering [178]. Composite scaffolds containing HAp and natural or synthetic polymers have also been the subject of extensive research. Scaffolds based on nano-HAp and collagen were successfully applied for stem cells delivery, helping effective bone regeneration treatment [179,180]. Nano HAp was also combined with gelatin and chitosan to build composite porous scaffolds with high MC3T3-E1 cell proliferation and growth, suitable for tissue engineering application [181]. HAp obtained from biological sources was used for the preparation of gelatine/chitosan/fibrin/bone ash/HAp composite scaffold that showed high biocompatibility on MG-63 cells and can be safely used as a bone replacement [182]. Electrospun nanofiber composite scaffolds of insulin-modified HAp/PLGA (poly (lactic acid-co-glycolic acid)) showed high osteogenesis potential, making it a promising material for artificial bone production [82]. Scaffold based on HAp doped with Ag^+ ions, modified with sodium alginate and chitosan, was reported as an efficient local drug delivery system for the release of lidocaine [183]. Chitosan/HAp scaffold was proven effective for the loading of gentamicin sulfate, to treat and prevent infections during regeneration [184]. Recently, nano-HAp/graphene oxide nanocomposite was reported as a promising material for the delivery of anticancer therapy doxorubicin [185].

5. α - AND β - TRICALCIUM PHOSPHATES

Tricalcium phosphates ($\text{Ca}_3(\text{PO}_4)_2$, TCP) represent biodegradable ceramic material that occurs as four allotropes, among which α - and β -TCP are the most common ones. Since TCP is soluble in aqueous environment, there is a great potential for its use in bone tissue regeneration. However, depending on the numerous factors, such as Ca/P ratio, porosity and purity, resorption rate of TCP could vary significantly [9,52,186,187]. If a rate is too high, tissue will not be able to regenerate, thus making this material unsuitable as a scaffold. Compared to HAp, TCP with molar ratio Ca/P of 1.5 resorbs faster, making it more challenging to control, but still a good candidate for mixing with HAp [188]. In this manner, by adjusting the amounts of the two compounds, desired bioactivity could be achieved.

Allotrope β -TCP has been thoroughly studied and incorporated as a replacement for bones [16,24,189–191]. Similar to HAp, β -TCP does not occur in the nature, but it can be successfully synthesized using high-temperature techniques [192]. It shows higher thermal stability than HAp and faster resorption rate due to its solubility. However, bioresorbability of the β -TCP is strongly influenced by porosity and surface roughness; therefore, there are different reports about its low bioactivity due to the high density [152]. With a proper morphology control, bioactivity can be significantly increased, resulting in a material well-suited for bone replacement [193–195]. In addition, β -TCP can be used in commercial toothpastes for better teeth polishing [64].

The other important calcium phosphate polymorph, α -TCP, was also recognized as a material for bone cement and bioceramics [12,186]. Allotrope α -TCP has the same chemical formula as β -TCP, but their crystal structures are different, as presented in Table 3 and in Figure 18a; β -TCP has more ordered structure (Figure 18b), which causes lower solubility compared to α -TCP.

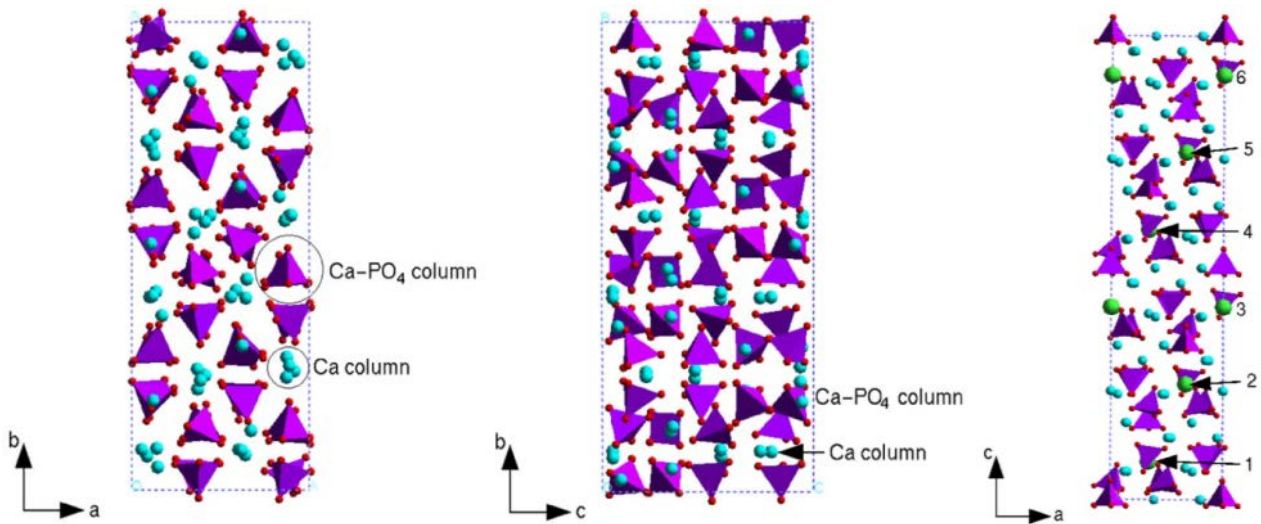


Figure 18. Projection of α -TCP unit cell on the ab - (left) and bc -plane (middle). Tetrahedra represent PO_4 groups, and light balls denote Ca atoms; Projection of β -TCP unit cell on the ac -plane (right). Tetrahedra represent PO_4 groups, small balls designate Ca atoms, and big balls are for the Ca atoms with half occupancy [196].

Being thermally stable, α -TCP is also obtained by high-temperature synthesis, higher than $1200\text{ }^\circ\text{C}$, and cannot be found in biological systems. Porous morphology could be obtained by sintering process; microstructure of porous α -TCP found in literature is presented in Figure 19. As discussed, α -TCP is more soluble than β -TCP, which makes it more suitable candidate for scaffolds [197–200]. Possibility of α -TCP to transform spontaneously into HAp after the application in the mouth placed it in the spotlight for research as the material that would fill the cavity after removal of damaged dental tissue and also remineralize the surrounding tissue. Major drawback in TCPs use lies in their brittleness, which could be overcome by combination with more ductile materials [24].

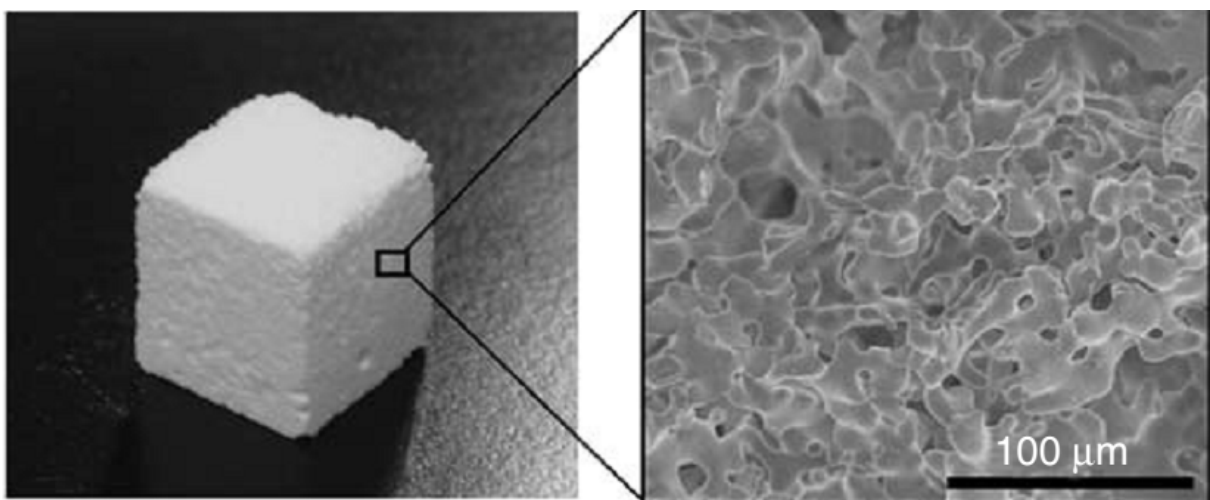


Figure 19. Microstructure of porous α -TCP [152].

6. CALCIUM PHOSPHATE CEMENTS

Calcium phosphate cements (CPCs) consist of solid and liquid components. The solid part contains calcium compounds, such as DCPD, TTCP, TCP, calcium carbonate, calcium silicate, calcium sulfate, etc. The liquid part can be inorganic or organic solution in water or other appropriate solvent. CaP dissolves in liquid, HAp precipitates, which crystals entanglements cause stiffening of the paste [201]. CPCs biodegradability, nontoxicity and injectability make them attractive bio-materials for bone grafts and substitutes [52,202–204].

Based on the end product, CPCs are divided into apatite and brushite (DCPD) cements. For the first group, the end product is HAp, while brushite is for the latter [205]. Figure 20 presents examples of CPCs constituents, setting reaction and structure of formed HAp and brushite.

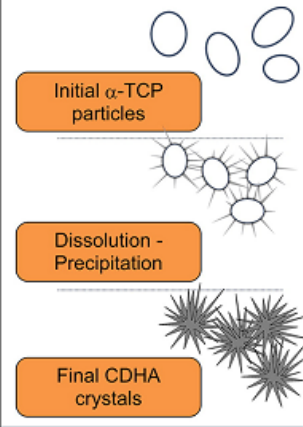
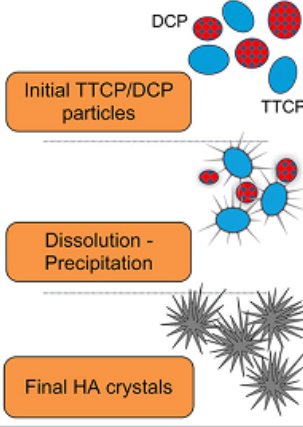
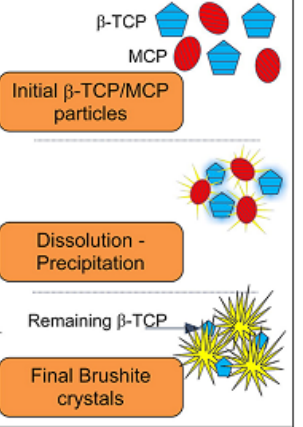

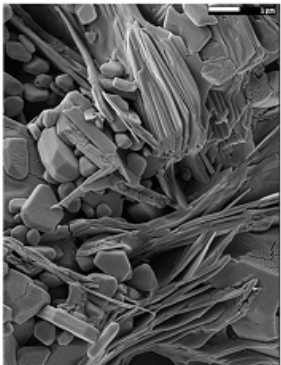
	Apatitic Cement		Brushitic Cement
	Single Component	Multiple Components	
Reactives	α -TCP	TTCP + DCPA/DCPD	β -TCP + MCPM/MCPA
Reaction	$3\alpha\text{-Ca}_3(\text{PO}_4)_2 + \text{H}_2\text{O} \rightarrow \text{Ca}_9(\text{HPO}_4)_4(\text{PO}_4)_5(\text{OH})$	$2\text{Ca}_4(\text{PO}_4)_2\text{O} + 2\text{CaHPO}_4 \rightarrow \text{Ca}_{10}(\text{PO}_4)_6(\text{OH})_2$	$\beta\text{-Ca}_3(\text{PO}_4)_2 + \text{Ca}(\text{H}_2\text{PO}_4)_2 \cdot \text{H}_2\text{O} + 7\text{H}_2\text{O} \rightarrow 4\text{CaHPO}_4 \cdot 2\text{H}_2\text{O}$
Type of Reaction	Hydrolysis	Acid-Base	Acid-Base
Setting mechanism and crystal morphology			
SEM		<p style="text-align: center;">← APATITE</p> <p style="text-align: center;">BRUSHITE →</p>	

Figure 20. CPCs common constituents, setting reaction and structure of formed apatite and brushite [268].

Cements are characterized for their:

- physical properties, such as solubility, flow, setting, working time, mechanical properties,
- biocompatibility and
- bioactivity.

Desired paste properties could be achieved by controlling the powder and liquid content and liquid-to-powder ratio (LPR).

HAp has been known to have higher biocompatibility and osteoconductivity compared to other CaPs [206]. Allotrope α -TCP has high solubility and in saliva transforms into HAp, making it a good material for root canal filling cements, which are the focus of this thesis. HAp based cements are already used for post-surgery facial bone regeneration [207–209]. In addition, various composite cements including glass ionomers or polymer resins have been reinforced with HAp for the application in dental surgery [210–212]. The focus of this thesis is on root canal filling CPCs-based composites and the most commonly used formulations for solid and liquid phase.

Liquid phase is usually comprised of water and phosphates, especially sodium dihydrogen phosphate (NaH_2PO_4) [213,214]. Cements used in dental applications must require suitable setting time, to ensure that dentist/surgeon has enough time to finish the procedure [215]. Citric acid is often added to the solution because it was reported as setting accelerator and calcium ion chelating agent that improves mechanical properties [66,216,217]. Polysaccharides are added to increase viscosity and affect setting time as well [67,218,219]. For cohesion and flow control, polymer agents are mixed with the ingredients of the liquid phase [220,221]. Another ingredient added to the solution for rheology modification is hydroxypropyl methylcellulose (HPMC) [214,222–224]. In addition, HPMC reduces washability, which prolongs the lifetime of cements. Polyethylene glycol (PEG) is often used for phase stability i.e., to prevent segregation [221,225]. All the ingredients added to the starting solution should ensure better cement paste handling and mechanical properties. Biocompatibility and bioactivity can also be controlled by the HAp and α -TCP fraction in the cement pastes [19]. Biocompatibility is evaluated using different tests of cement influence on cell cultures, with the aim of determining cell viability after the exposure to the cement (cytotoxicity) [22,226]. Bioactivity is investigated by following the formation of apatite after *in vitro* cement immersion in a simulated body fluid [19,227–229].

CPCs are promising materials for root canal fillings due to the possibility of tailoring mechanical properties without decreasing biocompatibility, which is their major advantage over polymer-based cements that are not similar to tooth structure.

7. CURRENT TRENDS IN DENTAL MATERIALS DEVELOPMENT

Over the last two decades, great efforts were employed to produce more efficient, aesthetically acceptable and durable dental materials, some of which will be presented in this chapter. In order to produce bone-like materials for orthopedic use, HAp was successfully modified with fluorine and chlorine [34].

Borkowski et al. [230] used sol-gel method and calcination for the synthesis of FAp with the goal of achieving higher bioactivity compared to HAp. They varied calcination temperature in order to find FAp sample with optimal porosity and highest F^- ions release ability. *In vitro* tests proved the absence of toxic effect on the cells, while the best FAp sample showed high cell-proliferation potential, which makes this material safe for the use in orthopedic applications.

For the increase of corrosion resistance, Mansoorianfar et al. introduced fluorine into the HAp [231]. Along with the corrosion protective coating, obtained fluorhydroxyapatite showed good biocompatibility when tested on MG-63 osteoblast cells.

Khan et al. [8] synthesized FAp nanoparticles, using them as fillers for polyurethane (PU) matrix, in order to build nanocomposite for root canal filling. Investigations showed efficient F^- ion release from the composite, as well as homogenous structure and good adhesion to the surrounding tissue. In some research reports, FAp and HAp nanoparticles were investigated as scaffolds for orthopedic and dental application [6,232,233].

Altaie et al. prepared an acrylate-based composite scaffold containing silanised barium aluminium silicate glass particles and FAp as reinforcement [15]. The results showed that the addition of FAp increased fracture toughness and enabled F^- ion release in the acid environment, suggesting that this composite could find application as a smart dental material.

Montazeri et al. used sol-gel method to synthesize nano-FAp with the aim of investigating biocompatibility [35]. *In vitro* tests on animal fibroblast cells showed the absence of cytotoxicity, making this material suitable for the potential application as a bone scaffold. As a mechanical reinforcement to the restorative material, FAp and HAp nanoparticles were embedded in a glass-ionomer cement [146,234].

Barandehfard et al. synthesized nano-FAp and HAp using wet-chemical precipitation method, with the aim of reinforcing glass-ionomer cement [17]. Performed compressive, tensile and microhardness tests on the obtained composites showed an improvement of all the investigated mechanical properties before and after the immersion in distilled water.

Elghazel and associates presented a study of FAp addition to β -TCP on the mechanical performance of the obtained composite [16]. The results showed that FAp concentration increases wear resistance, which is important for the use in dental applications.

Wei et al. prepared FAp-based cement for the restoration of enamel [235]. The cement showed good mechanical and adhesive properties, as well as high biocompatibility when tested on L929 fibroblast cells, which opened a pathway for the investigations of this FAp-based material as a direct enamel repair.

Azami et al. investigated composite containing calcium fluoride and co-substituted HAp with FAp for the treatment of osteoporosis [236]. The composite showed high bioactivity, which was tested in simulated body fluid (SBF).

In the recent research published by Anastasiou et al., doping of FAp with Sr^+ and Ce^{3+} ions was reported, with the aim of modifying chitosan-based scaffolds efficient against bacteria appearing at the implantation site [237]. The results suggested that Ce^{3+} doped FAp could be applied in reconstructive surgery, due to a high osteoconductivity and antimicrobial activity. With the emerging development of nanotechnology, biocompatibility and bioactivity of calcium phosphate based dental materials could be enhanced and controlled using various synthesis routes [24,33].

Stojanović et al. presented synthesis of α -TCP implants to evaluate biocompatibility and potential for the use in dentistry [238]. The histological analysis of the animal tissue after different number of days with the implanted α -TCP, revealed high biocompatibility similar to commonly used ceramics. Along with being non-toxic, this material provided efficient production of collagen fibers.

Nanoparticles of HAp were used in toothpastes and oral rinses, to slow demineralization and induce remineralization of teeth [160,163,239–242]. Taha et al. prepared fluorhydroxyapatite-containing toothpaste with high efficiency in the treatment of dentin hypersensitivity [243].

Tredwin et al. compared HAp, FAp and F^- substituted HAp with different substitution levels, as materials for implant coatings, concluding that the increase in F^- ion presence in HAp leads to lower solubility and higher biocompatibility [244].

Radovanović et al. doped HAp/ α -TCP composite with Ag^+ and Cu^{2+} ions, in order to increase antibacterial activity against various types of bacteria that commonly occur during and after bone surgery [22]. Along with antimicrobial activity, the results showed high biocompatibility, using MTT and DET *in vitro* tests on fibroblast cells. The same team successfully doped HAp and HAp/ α -TCP composite with Zn^{2+} ions, showing high antibacterial activity and biocompatibility when evaluated on MRC-5 fibroblast cells [245].

Cements are a subject of different literature reports, with the aim of improving setting time, flow, mechanical properties, along with biocompatibility and bioactivity [246-248]. Modification of magnesium CPC based on calcium dihydrogen phosphate ($\text{Ca}(\text{H}_2\text{PO}_4)_2$) with citric acid resulted in higher mechanical strength and biocompatibility [216].

Recent study by Toledano et al. presented sealing potential of several cements, among which zinc oxide-modified HAp cement showed the best mechanical properties for root canal sealing application [249].

Researchers investigated the influence of addition of PEG to the paste, proving that it can increase stability of injectable CPC [221]. Cellulose ethers were added to control paste flow with the change of ether molecular weight [215]. Novel cements based on tricalcium silicate have proved to be efficient for bone healing, as well as cements based on HAp nanoparticles and bioactive glass [250–252].

In order to improve bioactivity of CPC, Davaie et al. successfully used bioactive glass for modification [253]. Samples were soaked in SBF for a different number of days, after which visual and structural characterization revealed more efficient HAp formation compared to the control sample.

Ebrahimi et al. added bioactive glass to HAp cement, in order to increase setting time with the concentration of bioactive glass [254]. Compressive strength and bioactivity investigated after the soaking of cements in SBF showed a significant increase, making this composite suitable for scaffold application.

Fathi et al. mixed α -TCP, HAp and DCPD powders with varying LPR for the preparation of pastes, in order to achieve the optimal setting time. The cement showed high bioactivity and great potential for the use in tooth filling application [255].

The research published by Imataki et al. presented glass-ionomer cement modified with HAp, which improved mechanical and F^- ion releasing properties [256]. Calcium-aluminate cements were successfully modified with chitosan, reducing porosity, and increasing the bond strength [257].

Sharma et al. introduced a novel tooth filling material, composed of nano-HAp, gelatin and acrylic acid [258]. Prepared dental material proved to be non-toxic and durable during pH and temperature changes, which indicates that it could be applied in restorative dentistry.

Fillers based on α -TCP obtained by solid-state technique and afterwards modified with triazole were presented by Moraveji et al. for the possible application as bone substitutes [259]. After 7 days in SBF, triazole-modified α -TCP transformed into plate-like HAp, structure more similar to the bone compared to morphology of HAp obtained from pure α -TCP, showing the potential of this novel material for orthopedic and dental applications.

8. EXPERIMENTAL PART

8.1. Materials and methods

The following reactants of p.a. grade were used for the HAp and FAp synthesis:

- Calcium nitrate tetrahydrate, $\text{Ca}(\text{NO}_3)_2 \cdot 4\text{H}_2\text{O}$, $\geq 98\%$ (Carl Roth, Germany),
- Disodium ethylenediaminetetraacetate dihydrate, $\text{Na}_2\text{H}_2\text{EDTA} \cdot 2\text{H}_2\text{O}$ (CIII) (Sigma-Aldrich, USA),
- Sodium dihydrogen phosphate dihydrate, $\text{NaH}_2\text{PO}_4 \cdot 2\text{H}_2\text{O}$, 99.8 % (VWR, USA),
- Ammonium hydroxide, NH_4OH , p.a. (Zorka Pharma, Serbia),
- Sodium fluoride, NaF , 99 % (Riedel-de Haën, Seelze-Hannover, Germany) and
- Urea, $\text{CH}_4\text{N}_2\text{O}$ (Zorka Pharma, Serbia).

The following ingredients were used for the preparation of tooth filling paste:

- Citric acid (CA), $\text{HOC}(\text{CH}_2\text{CO}_2\text{H})_2$, p.a. (Zorka Pharma, Serbia),
- Polyethyleneglycole (PEG), $\text{C}_{2n}\text{H}_{4n+2}\text{O}_{n+1}$, (Sigma-Aldrich, USA),
- Disodium hydrogen phosphate, Na_2HPO_4 , p.a. (Merck, Germany) and
- Hydroxypropylmethylcellulose (HPMC), $\text{C}_{56}\text{H}_{108}\text{O}_{30}$ (Sigma-Aldrich, USA).

For the preparation of SBF the following reagents were used:

- Sodium chloride, NaCl , (NRK inženjering, Serbia),
- Sodium bicarbonate, NaHCO_3 , (Centrohem, Serbia),
- Potassium chloride, KCl , (Lach:ner, Czech Republic),
- di-Potassium phosphate trihydrate, K_2HPO_4 , (Fisher chemical, USA),
- Magnesium chloride hexahydrate, $\text{MgCl}_2 \cdot 6\text{H}_2\text{O}$, (Lach:ner, Czech Republic),
- Calcium chloride, CaCl_2 , (Lach:ner, Czech Republic),
- Sodium sulfate, Na_2SO_4 , (Centrohem, Serbia) and
- Tris(hydroxymethyl)aminomethan, $(\text{CH}_2\text{OH})_3\text{CNH}_2$, (Centrohem, Serbia).

8.2. Sample preparation

8.2.1. Synthesis of FAp and HAp powders

The HAp powder was synthesized according to the already published method, where hydrothermal technique was used [238]. The following masses of ingredients were used for the HAp synthesis:

- $m(\text{Ca}(\text{NO}_3)_2 \cdot 4\text{H}_2\text{O}) = 27.40 \text{ g}$
- $m(\text{CIII}) = 14.80 \text{ g}$
- $m(\text{NaH}_2\text{PO}_4 \cdot 2\text{H}_2\text{O}) = 12.00 \text{ g}$
- $m(\text{Urea}) = 12.00 \text{ g}$

The ingredients were dissolved in 2 L of distilled water and the solution was heated for 2 h at 160 °C in the sealed tube. The obtained particles were washed with distilled water and dried for 2 h at 105°C. Molar ratio Ca/P was 1.50.

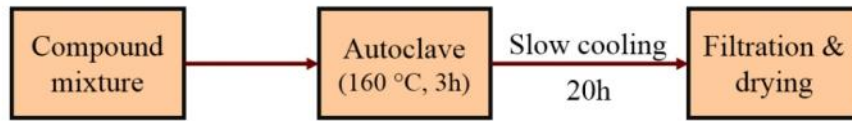
In order to find the best candidate for the preparation of dental composite material, three series of fluorapatite (FAp) samples were prepared. Samples of FAp are denoted as FAp-1, FAp-2 and FAp-3.

The synthesis of FAp-1 was similar to the synthesis of HAp, but NaF was used to obtain FAp and Ca/P ratio and the amount of CIII was different as presented in Table 8. Further, FAp-2 and FAp-3 powders were synthesized by changing pH values of the reaction solutions in comparison to FAp-1. $\text{Ca}(\text{NO}_3)_2 \cdot 4\text{H}_2\text{O}$, CIII, $\text{NaH}_2\text{PO}_4 \cdot 2\text{H}_2\text{O}$, and urea, whose masses are presented in Table 8, were dissolved in 2 L of distilled water. The values of pH for FAp-2 and FAp-3 (Table 8) were controlled by the addition of NH_3 . The final pH values for the syntheses are presented in the last column of Table 8. Compounds were mixed until the solution was homogenized and placed in the autoclave for 3 h at 160 °C. After slow cooling during 20 h, the mixture was filtered out and dried.

Table 8. Mass (g) and volume (mL) of reaction ingredients and pH value in the synthesis of FAp powders.

Sample	Reaction ingredients						pH
	$\text{Ca}(\text{NO}_3)_2 \cdot 4\text{H}_2\text{O}$, g	CIII, g	$\text{NaH}_2\text{PO}_4 \cdot 2\text{H}_2\text{O}$, g	NaF, g	Urea, g	NH_4OH , mL	
FAp-1	35	17.12	13.85	1.26	12.00	–	9.21
FAp-2	35	17.12	13.85	1.26	–	80	9.75
FAp-3	35	0	13.85	1.26	–	50	10.10

The simplified synthesis pathway method is presented in Scheme 1.



Scheme 1. Synthesis of FAp powders.

Sample with the most suitable morphology and the highest content of F^- ions was chosen for further investigations.

8.2.2. Synthesis of α -TCP

For the synthesis of α -TCP, hydroxyapatite was calcined at 1500 °C for 2 h [238]. Figure 21 presents powder of α -TCP obtained after the calcination of pure HAp.



Figure 21. Furnace for thermal treatment (calcination) of HAp and the obtained α -TCP powder.

8.2.3. Preparation of α -TCP/FAp composites

In order to obtain ceramic composites, synthesized FAp-3 powder was added in different amounts (0, 2.5, 5 and 10 wt.%) to the α -TCP powder. To prepared powder mixtures, phosphate

solution (2.5 wt.% Na₂HPO₄) was added at a liquid to powder ratio of 0.32 mL g⁻¹ and the tablets were formed. The formulation of solutions for composites was:

- 0 wt.% FAp 6 g α -TCP + 2 mL phosphate solution
- 2.5 wt.% FAp 6 g α -TCP + 0.15 g FAp + 2 mL phosphate solution
- 5 wt.% FAp 6 g α -TCP + 0.32 g FAp + 2 mL phosphate solution
- 10 wt.% FAp 6 g α -TCP + 0.64 g FAp + 2.3 mL phosphate solution

Composite tablets were made in accordance with ISO 6876 standard for root canal sealing materials [260].

8.2.4. Tooth filling cement preparation

Composite cement pastes were made using α -TCP/FAp composite powder with the addition of different liquids and 5 wt.% of FAp in order to obtain pastes with the best rheological properties.

CA, Na₂HPO₄, PEG and HPMC were selected for the preparation of the water-based liquid phase based on the literature data [215,216,221,224,261] but they were mixed with water in different wt.% in order to optimize the composition of liquid for the powder mixture. Also, varying the liquid-to-powder ratio (LPR) was varied from 0.3 to 0.5 mL/g, with the step of 0.01, the best LPR ratio was determined. Five series of samples, F1–F5, with different liquid/powder ratio (LPR) and the composition of the water-based liquid phase, were made as presented in Table 9.

Table 9. The composition of different water-based liquids for cement pastes and best LPR values.

Samples series	Composition of the liquid, wt. %	LPR, mL/g
F1	20% CA, 10% PEG	0.32
F2	2.5% Na ₂ HPO ₄	0.32
F3	10% PEG	0.34
F4	10% CA	0.39
F5	0.5% HPMC, 15% CA, 10% PEG	0.45

8.2.5. Preparation of simulated body fluid (SBF)

In order to investigate *in vitro* behavior of composite dental materials, solution that simulates body fluid was prepared according to Kokubo et al [262]. The formulation for SBF was as follows:

- $m(\text{NaCl}) = 15.992 \text{ g}$
- $m(\text{NaHCO}_3) = 0.7 \text{ g}$
- $m(\text{KCl}) = 0.448 \text{ g}$

- $m(\text{K}_2\text{HPO}_4) = 0.348 \text{ g}$
- $m(\text{MgCl}_2 \cdot 6\text{H}_2\text{O}) = 0.945 \text{ g}$
- $m(\text{CaCl}_2) = 0.556 \text{ g}$
- $m(\text{Na}_2\text{SO}_4) = 0.142 \text{ g}$
- $m((\text{CH}_2\text{OH})_3\text{CNH}_2) = 12.114 \text{ g}$

Each chemical was previously dried in the oven, then dissolved in 2 L of distilled water and left at 4 °C in the refrigerator. All the measurements in SBF were performed at 37 °C.

8.3. The tooth filling procedure

Two teeth were used, first molar and premolar, for filling with the paste. After the filling, the teeth were placed in a flask filled with SBF solution, and placed in the water bath at 37 °C for 24 h. Figures 22 and 23 show teeth before and after the filling.



Figure 22. Teeth prepared for filling.



Figure 23. Teeth after filling.

The two teeth were fixed in gypsum and prepared for cutting, in order to study the extent of mixture adhesion to the roots of the teeth by using FESEM analysis. Fixed tooth is presented in Figure 24.

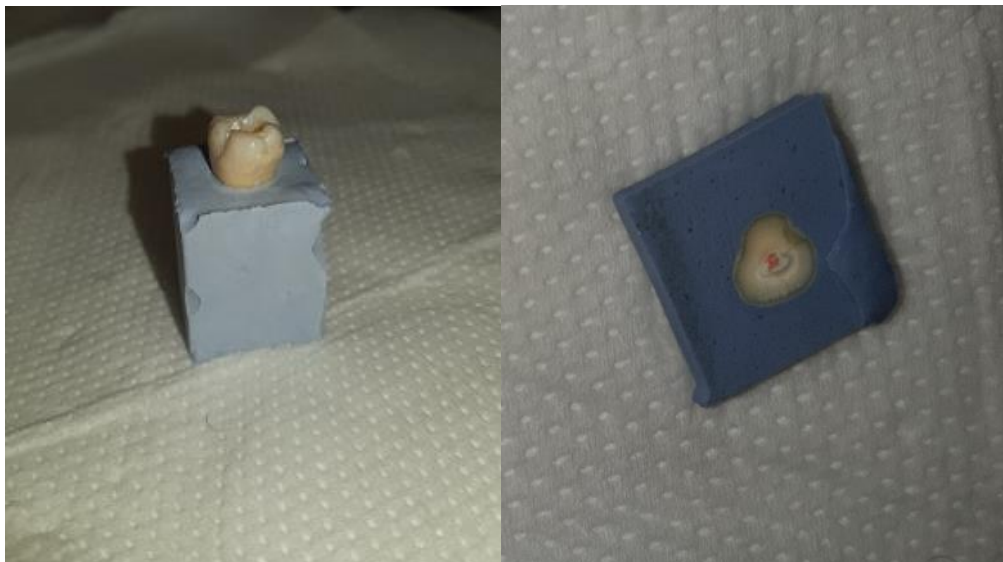


Figure 24. Fixed tooth in gypsum (left) and a slice of cut tooth for XRPD (right).

Precision cutter (Buehler isoMet-4000) used for cutting the teeth at the Faculty of Dental Medicine is presented in Figure 25.



Figure 25. Precision cutter with the fixed tooth.

8.4. Characterization of starting constituents, composites and pastes

8.4.1. Field emission scanning electron microscopy (FESEM)

Morphological changes and bioactivity evaluation of the powders were observed by Tescan Mira 3 XMU field emission scanning electron microscopy (FESEM). Before the analysis, the powders were coated with gold using a Polaron SC502 sputter coater.

8.4.2. Energy dispersive X-ray spectroscopy (EDS)

Energy dispersive X-ray spectroscopy (EDS) of the compacted powders was performed on a Jeol JSM 5800 SEM with a SiLi X-Ray detector (Oxford Link Isis series 300, UK). Measurements for each specimen were performed at five different spots ($N = 5$ group⁻¹).

8.4.3. Fourier transformed infrared spectroscopy (FTIR)

Determination of characteristic chemical groups in synthesized and calcined powders were performed by Fourier transform infrared spectroscopy (FTIR) using a Thermo Scientific Nicolet iS10 spectrometer in the wavenumber range from 4000 to 400 cm⁻¹.

8.4.4. X-ray powder diffraction analysis (XRPD)

X-ray powder diffraction patterns of powders were recorded on ITAL Structures APD 2000 instrument using a copper cathode as the X-ray source ($\lambda = 0.15406$ nm), in the 2θ angle range from 20 to 60 ° with a step size of 0.05 ° s⁻¹. The unit cell parameters and the average crystallite size $\langle D \rangle$ were determined using JADE software. XRPD measurements for Rietveld refinement were performed on a Rigaku SmartLab diffractometer using CuK α radiation, at 40 KV and 30 MA, in Bragg–Brentano geometry. Diffraction data were collected in the range 5 ° < 2θ < 120 ° (scan speed: 1 ° min⁻¹, step width: 0.01 ° 2θ) at room temperature.

8.4.5. Ion release test

For F^- ion release test, α -TCP, FAp and composite pills were placed in glasses that were filled with standard fluoride solution with added Fluoride Ionic Strength Adjustor (ISA). Measurements were done using Ion Selective Electrode (ISE) (Figure 26) in predetermined time intervals 5 min, 1 h, 1, 3 and 7 days, in order to measure the release of F^- ions from pills with 0, 2.5, 5 and 10 % of FAp in α -TCP.



Figure 26. Ion Selective Electrode (ISE).

8.4.6. Compressive test

Mechanical tests of composite tablets were performed on Shimadzu universal testing machine presented in Figure 27. Each tablet was tested after immersing in SBF for 0, 3, 10 and 30 days. Compressive test was performed using steel plate with mass of 0.1535 kg (applied force was 1.51 N), with the speed of 5 mm min^{-1} . Surface of the specimens was $2.5 \cdot 10^{-5} \text{ m}^2$. Measurements of compressive strength and stroke strain for each composite were performed on five samples.



Figure 27. Shimadzu universal testing machine [263].

8.4.7. In vitro biocompatibility tests

Trypan Blue dye exclusion test (DET) and reduction of the tetrazolium salt 3-(4,5-dimethylthazol-2-yl)-2,5-diphenyl tetrazolium bromide (MTT) test were performed after 48 h from seeding of diluted cell cultures in 96-well plates.

8.4.7.1. Cell lines

Tests were performed on the cell line human fibroblasts of lung (MRC-5) and animal L929 that were grown attached to the surface of the flasks (Costar, 25 cm³) in Eagle's medium modified by Dulbecco (DMEM, Gibco BRL, England) with 4.5 g L⁻¹ glucose and 10 % fetal calf serum - FCS (Sigma, USA). The medium contained the antibiotics: penicillin 100 IU mL⁻¹ and streptomycin 100 µg ml. The cell line were maintained under standard conditions at 37 °C in an atmosphere of saturated humidity with 5% CO₂ (Heraeus, Germany). They were transplanted twice weekly, whereas in the experiments the logarithmic phase of growth was used between the third and tenth transplantation. Only viable cells were used in the experiments. The number of cells and their viability were determined by the color test rejection with 0.1 % Trypan Blue. The viability of cells used in the experiment was greater than 90 %.

8.4.7.2. Colorimetric assays with tetrazolium salts (MTT test)

The cells were collected during the logarithmic phase of growth, trypsinized, resuspended and counted in 0.1 % Trypan Blue [264]. Viable cells were sown at the concentration of $2 \cdot 10^5$ cells mL⁻¹ in Petri dishes (50 mm, Center well, Falcon) in which the powders for the analysis were located. Control samples did not contain the investigated powders. Petri dishes with sown cells were thermostated at 37 °C with 5 % CO₂ for 48 h. At the end of the incubation, the cells were re-sown to fresh medium. Viable cells were sown ($5 \cdot 10^3$ cells 100 μL⁻¹) in microtiter 96-well plates. The plates with sown cells were thermostated at 37 °C with 5 % CO₂ for 48 h. The MTT solution, prepared just before addition, was added to all the wells of the plate, in a volume of 10 μL per well and incubation was continued for the next 3 h (in the incubator at 37 °C with 5 % CO₂). Upon expiration of 3 h, 100 μL of HCl in 2-propanol (0.04 mol L⁻¹) was added to each well. The absorbance readings was performed immediately after incubation on a microtiter plate reader (Multiscan, MCC/340) at a wavelength of 540 nm with reference to 690 nm. Wells on a plate that contained only medium and MTT but no cells were used as a blank.

The fraction of surviving cells (% *K*) was expressed as a percentage of the control values according to the equation (25):

$$\% K = 100N_s/N_k \quad (25),$$

where N_k is the number of cells in the control sample and N_s is the number of cells with the tested substance.

8.4.7.3. Trypan Blue dye exclusion test (DET test)

The cells were collected during the logarithmic phase of growth, trypsinized, resuspended and counted in 0.1 % Trypan Blue [265]. Viable cells were sown at a concentration of $2 \cdot 10^5$ cells mL⁻¹ in Petri dishes (50 mm, Center well, Falcon) in which the powders for the analysis were located. Control samples did not contain the investigated powders. The Petri dishes with sown cells were thermostated at 37 °C with 5 % CO₂ for the next 48 h. At the end of incubation, the cells were counted in the counting chambers after 48 h using an inverted microscope. A Neubauer chamber was used for counting the cells in four squares. Each square was divided into 16 smaller squares so the total was 64. 100 μL of cells was taken and added to 100 μL of 0.1 % Trypan Blue. After intensive shaking, a few drops were placed on both counting fields of the chambers. Trypan Blue

stained dead cells while living cells remain unstained. The number of cells in 1 mL of suspension (X) was calculated using formula (26):

$$X = x \cdot 10 \cdot 2 \cdot 1000 \quad (26),$$

where x is the number of cells in 16 squares (the average number of cells in 4 · 16 squares); 10 is the depth of the chamber; 2 is the dilution factor and 1000 is the volumetric coefficient.

8.4.7.4. Cells preparation for staining

All substances were placed in a serum-free medium (DMEM) so that the concentration was 200 mg mL⁻¹. After 72 h, the medium was filtered (for sterility), 10 % serum was added, so that the medium would be used in all the investigated samples except for the control. The cells were collected during the logarithmic phase of growth, trypsinized, resuspended and counted in 0.1 % Trypan Blue. Viable cells were sown in a Petri dish (50 mm, Center well, Falcon) with a medium that has been tested 72 h with powder at a concentration 2 · 10⁵ cells mL⁻¹. The control samples contained no test substance. Petri dishes with sown cells were thermostated at 37 °C with 5 % CO₂ for 48 h. Staining was performed at the end of the incubation. Composite pills were denoted with the concentration of FAp in the α -TCP/FAp composite and the number of days pills were exposed to SBF (Table 10).

Table 10. Labels for α -TCP/FAp composite samples.

	Concentration of FAp, %			
	0	2.5	5	10
Series 0 day in SBF	0	2.5	5	10
Series 3 day in SBF	0–3	2.5–3	5–3	10–3
Series 10 day in SBF	0–10	2.5–10	5–10	10–10
Series 30 day in SBF	0–30	2.5–30	5–30	10–30

8.4.8. Physical properties of tooth filling pastes

Determination of solubility, flow, working and setting time were performed in accordance with standard ISO6876- Dental root canal sealing materials. In all the tests, F5 liquid components were used. All of the physical properties were determined for the samples of pure α -TCP, α -TCP/FAp with 5 and 10 wt% of FAp in F5, that were labeled as α -TCP/FAp(0), α -TCP/FAp(5) and α -TCP/FAp(10), respectively.

8.4.8.1. Solubility test

Pastes α -TCP/FAp(0), α -TCP/FAp(5) and α -TCP/FAp(10) were placed in a metal ring on a glass slide with another glass and metal ballast on the top for 7 min. After that, the metal ring with the paste was placed in SBF and kept in water bath on 37 °C for 24 h. The water uptake was determined by the change in the weight of the samples before and after the immersion in distilled water for 24 h.

8.4.8.2. Flow test

Pastes α -TCP/FAp(0), α -TCP/FAp(5) and α -TCP/FAp(10) were placed at the center of the glass plate (40 mm x 40 mm), mixed for 180 s, then pressed by the identical glass plate and the additional metal ballast for 7 min and placed in SBF for 24 h [260]. The minimum and maximum diameters of the produced discs were measured.

8.4.8.3. Working time

The same steps were followed as in flow test, but with longer mixing times before the addition of the load [260]:

- α -TCP/FAp(0): 180 s + 30 s = 210 s
- α -TCP/FAp(5): 180 s + 90 s = 270 s
- α -TCP/FAp(10): 180 s + 180 s = 360 s

8.4.8.4. Setting time

Pastes α -TCP/FAp(0), α -TCP/FAp(5) and α -TCP/FAp(10) were poured into the stainless steel ring mold (10mm diameter and 2mm height) placed on the glass plate and kept in SBF for 24 h. After that, they were placed on glass plates and let for 15–30 min to set, then tested by the Gilmore-type indenter until the indentation stopped being visible, and measuring the time since the end of the mixing [260].

9. RESULTS AND DISCUSSION

9.1. Characterization of HAp and FAp powders

9.1.1. XRPD analysis

Diffraction patterns for FAp and HAp powders are presented in Figure 28. XRPD patterns verified the formation of pure FAp and HAp powders, which crystallize in the hexagonal space group $P6_3/c$. The unit cell parameters and the values of the average crystallite size ($\langle D \rangle$) are presented in Table 11. Compared to the HAp pattern, a slight shift towards higher values of 2θ angles has been observed for FAp powders. This is the consequence of the smaller unit cell of FAp powders, due to the presence of F^- ions, instead of OH^- ions. Besides, the crystallites of FAp-1 are slightly elongated along the c axis with the highest value of $\langle D \rangle$ (Table 11).

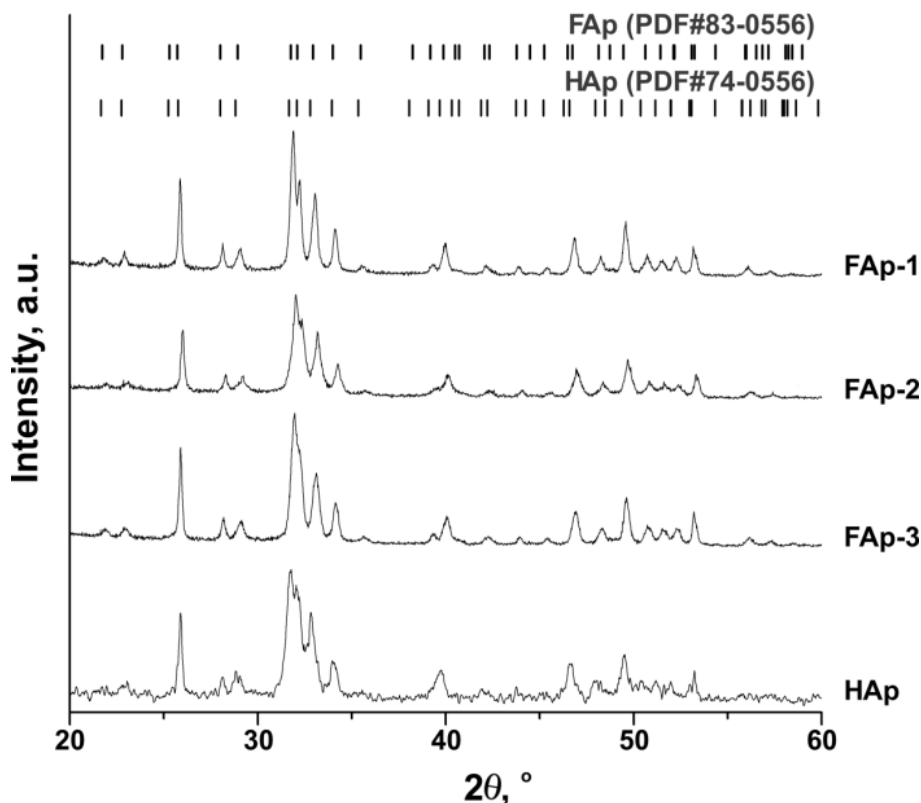


Figure 28. XRPD patterns of FAp and HAp powders [19].

Table 11. The unit cell parameters and $\langle D \rangle$ of FAp and HAp powders (JADE Software).

	a (Å)	c (Å)	V (Å ³)	$\langle D \rangle$ (nm)
FAp-1	9.37251(3)	6.88511(6)	523.7(9)	40.7(8)
FAp-2	9.36961(9)	6.87045(9)	522.3(5)	31.3(4)
FAp-3	9.37434(7)	6.88147(4)	523.7(1)	31.4(3)
HAp	9.44074(5)	6.87913(6)	530.9(8)	31.9(4)

9.1.2. FTIR analysis

For the identification of crucial bonds within synthesized FAp and HAp powders, FTIR analysis was used and resulted spectra are presented in Figure 29. In all spectra, the sharp bands around 1093 and 1019 cm^{-1} were found and ascribed to asymmetric stretching of the P–O bond [266]. Symmetric stretching of P–O was observed at around 965 cm^{-1} , while bending of O–P–O appeared at 600 and 560 cm^{-1} [267]. Low intensity peak appeared at 875 cm^{-1} , indicating the presence of HPO_4^{2-} . The main difference between the spectra of FAp powders and HAp was in the appearance of the band at 632 cm^{-1} , and at 3570 cm^{-1} , originating from –OH bending and stretching vibration in HAp, which did not occur in FAp [266]. The FTIR spectra of all FAp powders are very similar.

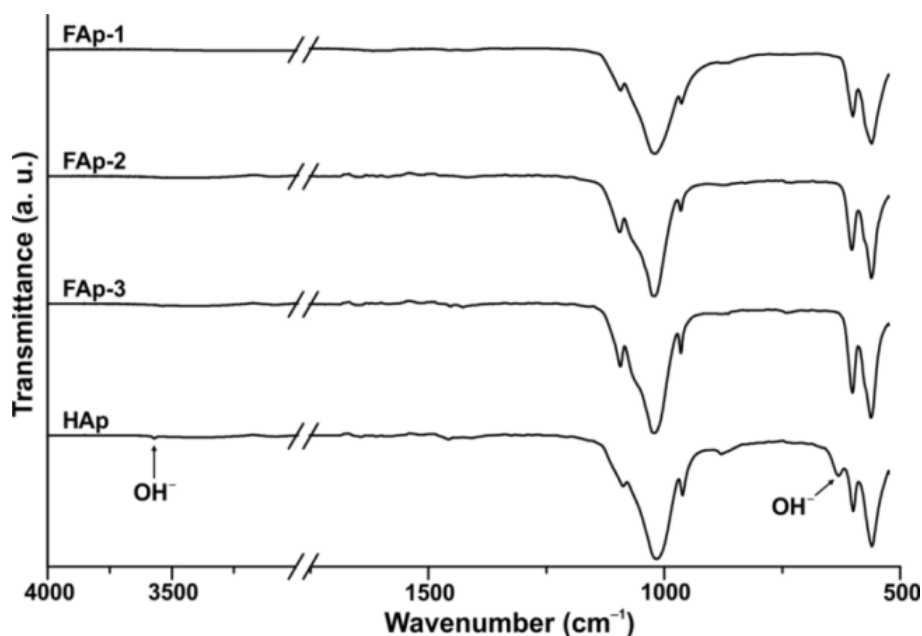


Figure 29. FTIR spectra of FAp and HAp powders [19].

9.1.3. FESEM and EDS analysis

9.1.3.1. FESEM

The results of the FESEM analysis of FAp and HAp powders at different magnification are presented in Figure 30. The rod-like particles with hexagonal cross-section were observed for FAp-1, which further formed aggregates of spherical shape, with an average size of about 5 μm . Due to agglomeration, it was not possible to measure the length of the particles. The morphology of HAp powder was similar but with much smaller particles that agglomerated into spheres with an average diameter of about 1–2 μm . The size difference of the rod-like particles, as well as the agglomerates in FAp-1 and HAp powders occurred most likely due to different concentrations of CIII in their respective syntheses.

The particles of FAp-2 can be described as vascular and rod-like with a wide particle size distribution ranging from about 70 nm to about 10 μm . The most consistent filler morphology was observed in the case of FAp-3, which consisted of uniform rod-like nanoparticles with an average size of about 90 nm. These nanoparticles also formed agglomerates, but unlike FAp-2 powder, these agglomerates are of irregular shape and soft. The difference in particle size and agglomeration of FAp-2 and FAp-3 powders appeared probably due to the change in synthesis conditions.

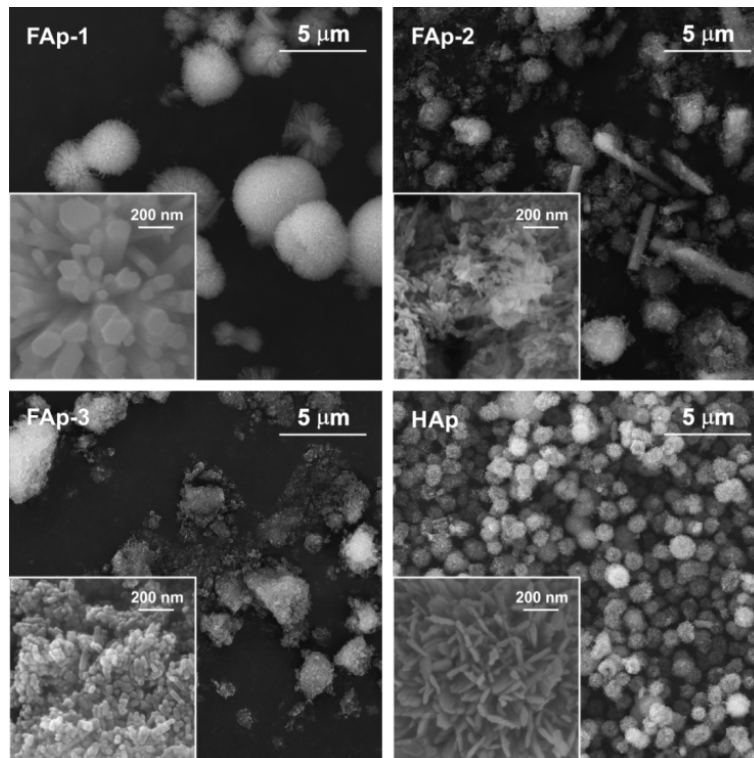


Figure 30. FESEM images of synthesized series of FAp and HAp powders.

9.1.3.2. EDS

EDS analysis revealed the atomic % of Ca, P, F, and O (Table 12). This analysis showed the presence of non-stoichiometric HAp and FAp powders with molar ratio $\text{Ca/P} < 1.67$, which means that in all cases Ca-deficient apatite was synthesized. The content of F^- ions in all FAp powders was close to the theoretical content, indicating the successful synthesis of pure FAp in all cases, which was in agreement with the obtained XRD and FTIR results.

Table 12. EDS results of FAp and HAp powders (at. %).

	FAp-1	FAp-2	FAp-3	HAp
O	66.13 ± 0.38	66.90 ± 0.40	66.16 ± 1.06	72.71 ± 0.23
F	4.78 ± 0.52	4.59 ± 0.62	5.00 ± 0.58	–
P	11.38 ± 0.24	11.70 ± 0.13	11.58 ± 0.27	11.53 ± 0.05
Ca	17.71 ± 0.27	16.82 ± 0.28	17.26 ± 0.69	15.75 ± 0.20
Ca/P	1.56	1.44	1.49	1.37

Based on the characterization results of prepared FAp powders, FAp-3 was chosen for the processing of α -TCP/FAp dental composite cements and will be referred to hereinafter only as FAp.

The FAp sample was analyzed in more detail with XRDP and Rietveld refinement was performed to determine all structural parameters of the sample. For comparison with FAp, nano HAp (nHAp) obtained by the same synthesis as FAp was used.

XRDP patterns of FAp and nHAp (Figures 31 and 32, respectively) are very similar, but the positions of the peaks in the XRDP pattern of FAp are mildly shifted towards higher values of 2θ angles indicating that unit cell of FAp is smaller.

The structures of FAp and nHAp are presented in Figures 31 and 32, respectively. Both powders crystallize in the hexagonal space group $\text{P6}_3/c$, with two formula units $\text{Ca}_5(\text{PO}_4)_3\text{F}$ per unit cell, for FAp and with two formula units $\text{Ca}_5(\text{PO}_4)_3\text{OH}$ for nHAp. The crystallographic and Rietveld refinement parameters for both structures are presented in Table 13, from which it can be seen that unit cell of FAp is slightly smaller because of the substitution of OH^- group with F atom. Also, the crystallites of FAp and nHAp are more elongated along the c axis (Table 13) which is in accordance with rod-like morphology of particles observed by FESEM (Figure 30).

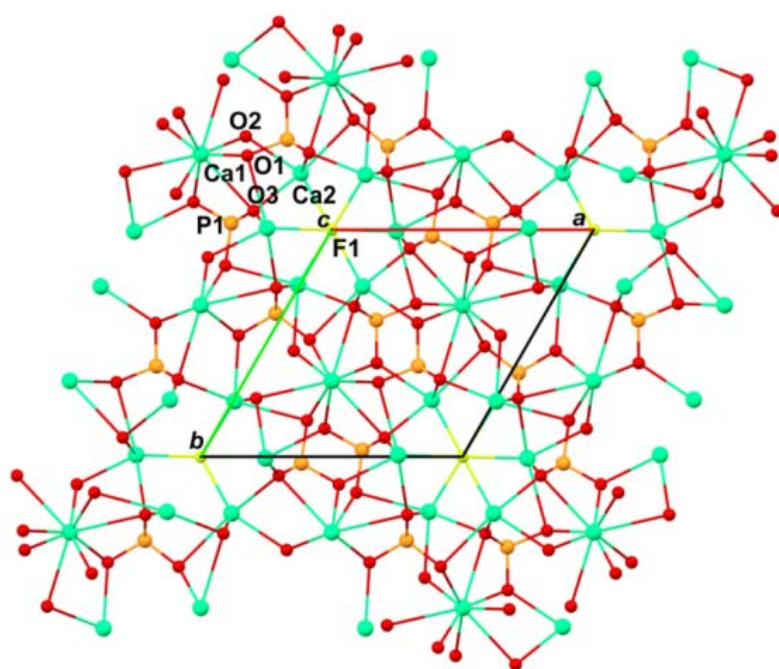
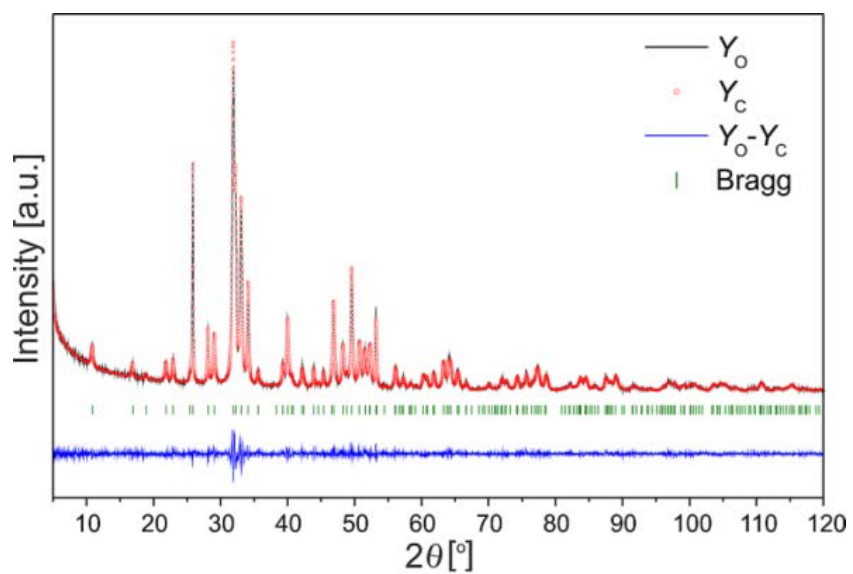


Figure 31. Rietveld refinement (up) and crystal packing diagram in *ab* plane (down) of FAp.

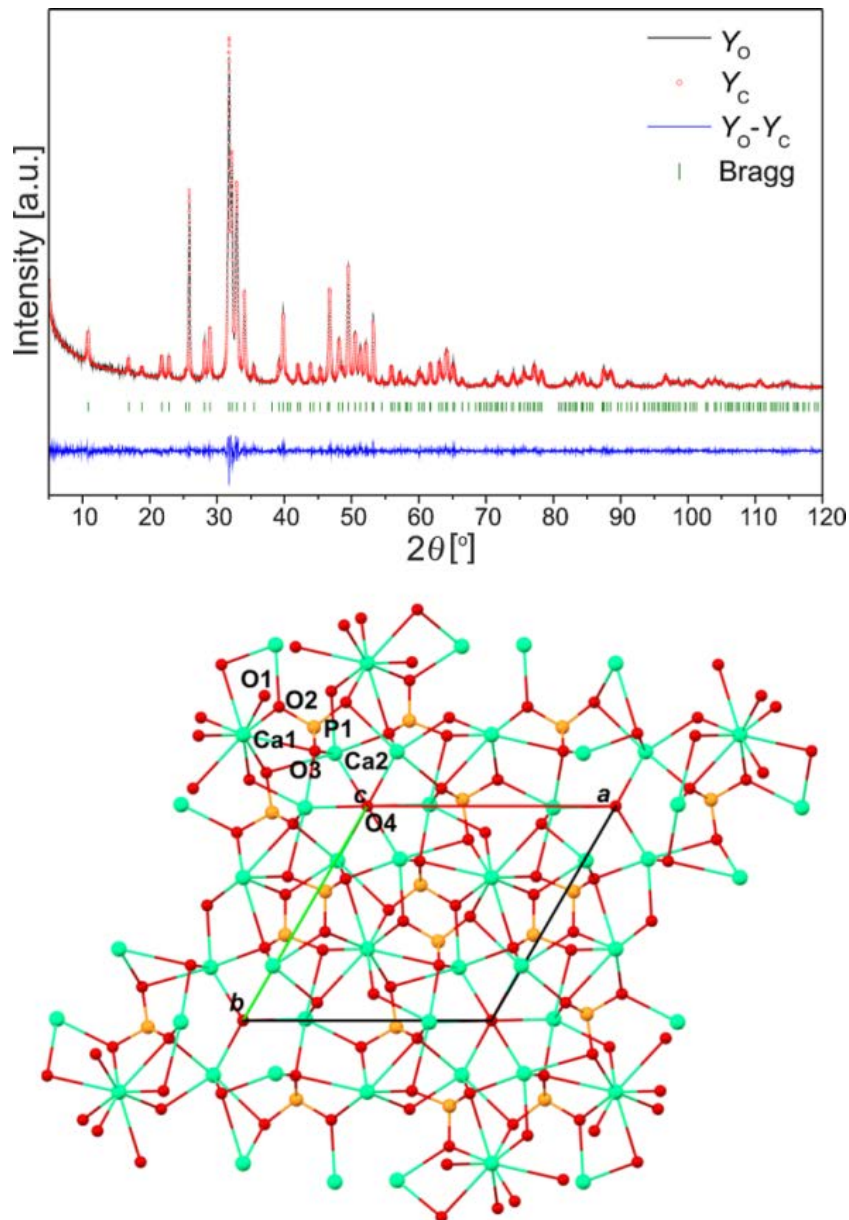


Figure 32. Rietveld refinement (up) and crystal packing diagram in ab plane (down) of nHAp.

Table 13. Crystallographic and Rietveld refinement parameters of nHAp and FAp.

Phase	nHAp	FAp
Crystal system	hexagonal	hexagonal
Space group	$P6_3/c$	$P6_3/c$
a (Å)	9.4205(1)	9.3760(1)
c (Å)	6.88151(9)	6.88276(9)
V (Å ³)	528.9(1)	524.0(1)
Crystallite size (Å)	346(1) [-0.356, 0.935, 0]	330(1) [0.356, -0.935, 0]
Crystallite size (Å)	346(1) [0.935, 0.356, 0]	330(1) [0.935, -0.356, 0]
Crystallite size (Å)	886(9) [0, 0, 1]	983(1) [0, 0, 1]
Strain (%)	0.096(2)	0.105(1)
R_{wp} (%)	4.87	4.92
R_p (%)	3.76	3.82
R_e (%)	3.92	3.92
χ^2	1.5414	1.5744
S	1.2451	1.2548
Maximum shift/e.s.d.	0.081	0.022

Rietveld refinement showed that there is no deficiency of Ca atoms in the structures of nHAp and FAp, so the ratio $\text{Ca/P} < 1.67$ obtained by EDS analysis can be attributed to the errors of this method.

The selected bond lengths for nHAp and FAp are listed in Table 14. The length of Ca2–F1 bond in FAp is shorter than length of Ca2–O4 bond in nHAp (O4 is from the OH⁻ group), which can possibly be the reason for smaller unit cell of FAp.

Table 14. Selected bond lengths (Å) for nHAp and FAp.

nHAp		FAp	
Bond	Bond length, Å	Bond	Bond length, Å
Ca1–O1	2.401	Ca1–O1	2.392
Ca1–O2	2.452	Ca1–O2	2.449
Ca1–O3	2.836	Ca1–O3	2.820
Ca2–O1	2.703	Ca2–O1	2.689
Ca2–O2	2.365	Ca2–O2	2.367
Ca2–O3	2.329	Ca2–O3	2.338
Ca2– O4	2.396	Ca2– F1	2.312
P1–O2	1.536	P1–O1	1.537
P1–O1	1.535	P1–O2	1.542
P1–O3	1.537	P1–O3	1.542

9.1.4. Bioactivity of composite cement specimens

Representative FESEM images presented in Figure 33 show the gradual formation of a new HAp layer on the surface of composite material with 5% of FAp during the exposure to SBF [228]. At day 10, the specimen surface was covered with the newly formed HAp layer to a greater extent compared to day 3, while the surface was nearly completely covered at day 30 in SBF. The similar formation was observed on fractured surfaces of specimens 5-3, 5-10, and 5-30 (Figures 34 and 35). Also, from the images of 0-30 and 10-30 specimens, the newly formed HAp crystallites could be observed, both on the sample surface and in the interior (Figures 36 and 37).

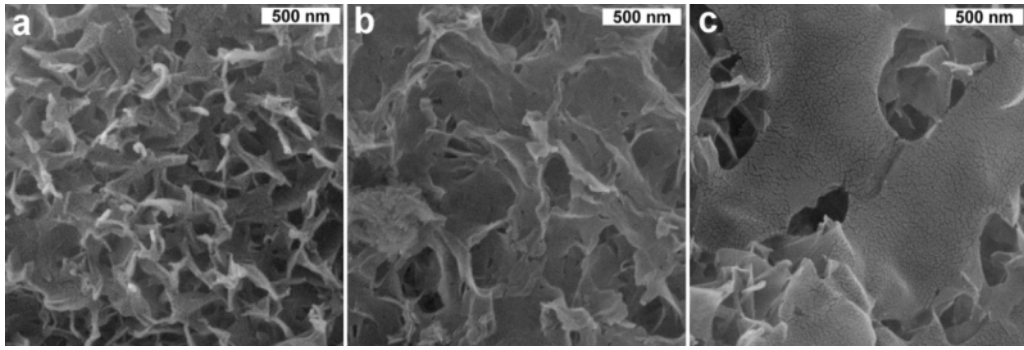


Figure 33. FESEM images of specimen surface: 5-3 (a), 5-10 (b), and 5-30 (c).

These images revealed a high ability of apatite formation in SBF, proving bioactivity of the processed α -TCP/FAp composite cements.

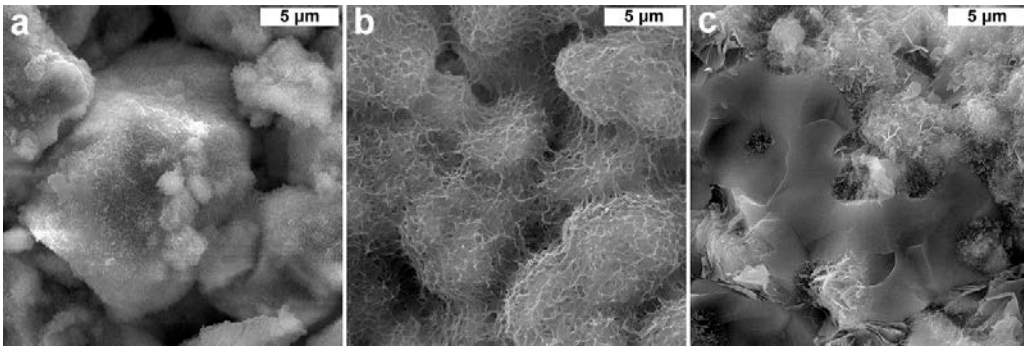


Figure 34. FESEM images of fractured surfaces: 5-3 (a), 5-10 (b), and 5-30 (c).

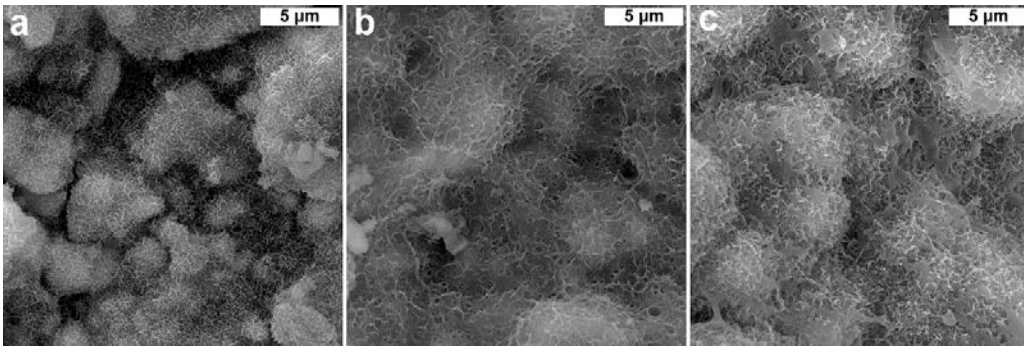


Figure 35. FESEM images of surfaces at magnification of 10kx: 5-3 (a), 5-10 (b), and 5-30 (c).

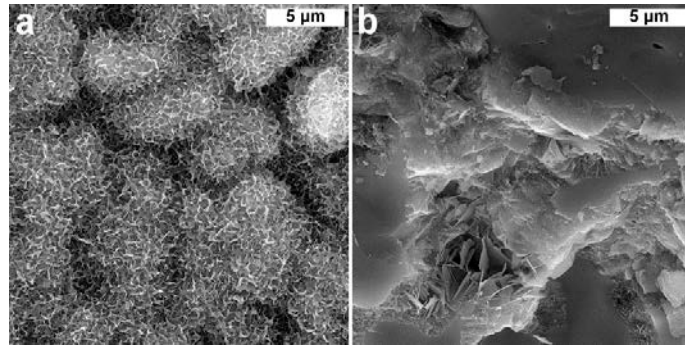


Figure 36. FESEM images: 0-30 surface (a) and 0-30 fracture surface (b).

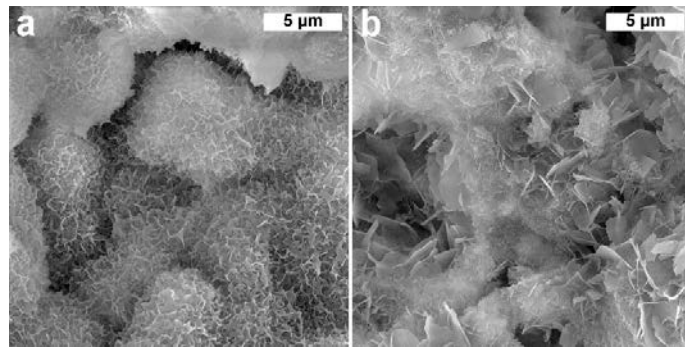


Figure 37. FESEM images: 10-30 surface (a) and 10-30 fracture surface (b).

9.1.5. Mechanical properties of composite cements

Compressive test for composite cements immersed in SBF was performed to establish which composition enables the highest mechanical performance during the transformation of α -TCP to HAp, as well as the influence of the FAp amount on the mechanical strength. The largest increase in strength occurred in the first 10 days (Table 15), indicating that the highest transformation into HAp happened during this time period.

Table 15. Compressive test results for composite cements after immersing in SBF.

	Series			
	0	2.5	5	10
Sample Compressive strength (MPa)	0-0	2.5-0	5-0	10-0
	0.3±0.2	0.2±0.2	0.4±0.1	0.3±0.1
	0-3	2.5-3	5-3	10-3
	4.3±0.9	2.4±0.1	4.4±0.5	4.9±3.5
	0-10	2.5-10	5-10	10-10
	30.2±5.0	21.3±2.8	33.8±3.2	28.2±6.3
	0-30	2.5-30	5-30	10-30
	38.3±5.3	26.1±5.0	29.8±8.1	25.6±8.3

Thereafter, up to day 30, strength partially increased for specimens with more α -TCP or remained at approximately the same level (series 5 and 10). This indicates that specimens 0 and 2.5 have greater potential for remineralization.

The transformation of α -TCP and the formation of a new layer gave, as a result, reduced porosity of the specimens (Figure 33), which further led to increase in compressive strength, which is in good agreement with the literature data [268]. Furthermore, for specimens with 2.5, 5, and 10 % of FAp, compressive strength after 10 days increased over 106, 84, and 94 times, respectively. This indicates that compressive strength was changing with the exposure to SBF from the values corresponding to α -TCP to the literature values measured for HAp [269–272]. The influence of F^- ions on mechanical properties has already been reported, indicating that high concentrations of F^- ions could lead to deterioration of composite mechanical properties [273]. The incorporation of FAp in α -TCP could be used to modify the mechanical characteristics of the composite using the proper control of the composition and porosity. In this study, the highest values of compressive strength were observed in composite cements containing 5% of FAp, indicating that this was the optimal composite concentration that offered high compressive strength value, probably due to low porosity.

9.1.6. Ion release

Composite cement α -TCP/FAp, as a dental material, could serve as a source of F^- ions that have an antimicrobial role as well as the role of reinforcement surrounding natural tooth material. Therefore, we examined the release of F^- ions from the composite. These specimens exhibited a similar F^- ions release pattern (Table 16). F^- ion release reached its maximum after 3 days, then started to decrease or remained constant. Significantly smaller release of F^- ions in composite specimens compared to FAp could be explained by notably lower concentration and suppressed diffusion of F^- ions through the cement.

Table 16. F^- ion release (in ppm) for control (FAp) and composite specimens.

Time	FAp	2.5	5	10
5 min	9.80±0.2	0.07±0.08	0.04±0.02	0.04±0.02
1 h	10.80±0.1	0.04±0.03	0.03±0.01	0.04±0.02
3 h	11.50±0.2	0.05±0.01	0.03±0.01	0.04±0.03
1 day	14.80±0.5	0.07±0.01	0.07±0.05	0.07±0.05
3 days	13.30±0.4	0.12±0.02	0.08±0.02	0.09±0.02
7 days	12.00±0.2	0.10±0.01	0.07±0.02	0.09±0.04

9.1.7. MTT and DET assay for composites α -TCP/FAp

MTT and DET tests were performed for the starting powders and composite cements from series 5, as well as for specimens 0-0, 0-30, 10-0 and 10-30, which have been chosen according to the compressive test. The cell viability chart for the MTT test obtained after 48 h is presented in Figure 38. Comparing powders, it could also be observed the influence of the SBF exposure time on the biocompatibility of composites. While there was no difference in viability between composite cements and powders, specimens of series 5 showed an increase in cell viability when samples immersed in SBF for 10 and 30 days were tested. According to some authors, α -TCP powder was expected to have the lowest biocompatibility [226]. However, the cell viability for composite cements compared to the cell viability of powders was higher or at the same level, which indicated that these specimens were not cytotoxic [22,274]. In addition, FAp showed viability close to 100%. The increased biocompatibility of composites exposed to SBF for prolonged time could also be ascribed to the transformation of α -TCP to HAp. A recent study on FAp/bioactive glass and HAp/bioactive glass revealed some contribution of FAp to cytotoxicity but within acceptable limits [25]. However, the influence of HAp and FAp nanoparticles on fibroblast cells published in earlier research is in accordance with our results, showing no cytotoxicity [35].

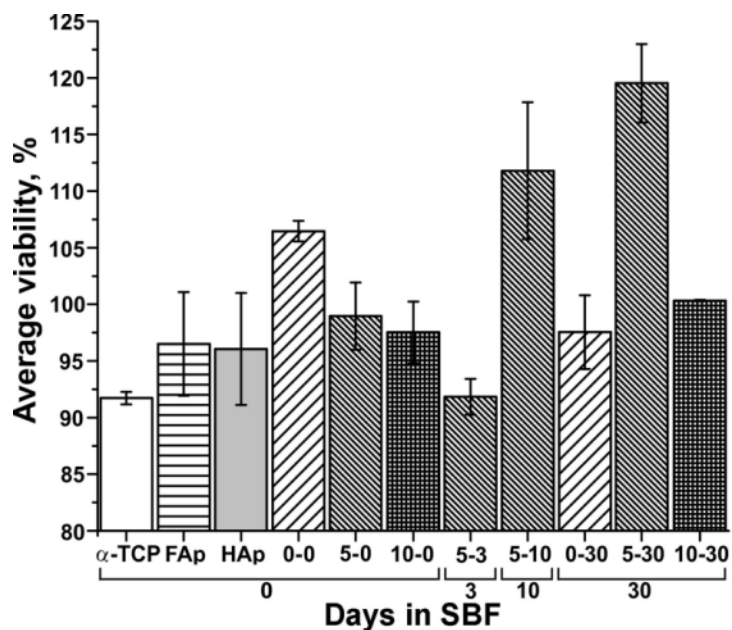


Figure 38. MTT assay of cytotoxic effects of α -TCP/FAp composites on MRC-5 cells.

DET results are presented in Figure 39 and they were in accordance with the MTT assay. All composites induced an insignificant decrease in cell viability. Both MTT and DET tests showed that all of the composite specimens enabled higher cell viability (compared to α -TCP, FAp, and HAp), as well as no cytotoxicity. In addition, these results were better than the MTT and DET results of

samples HAp/ α -TCP doped with Zn^{2+} , Ag^+ , and Cu^{2+} ions after 48 h [22,245]. Based on aforesaid, these composite cements are safe for future dental applications.

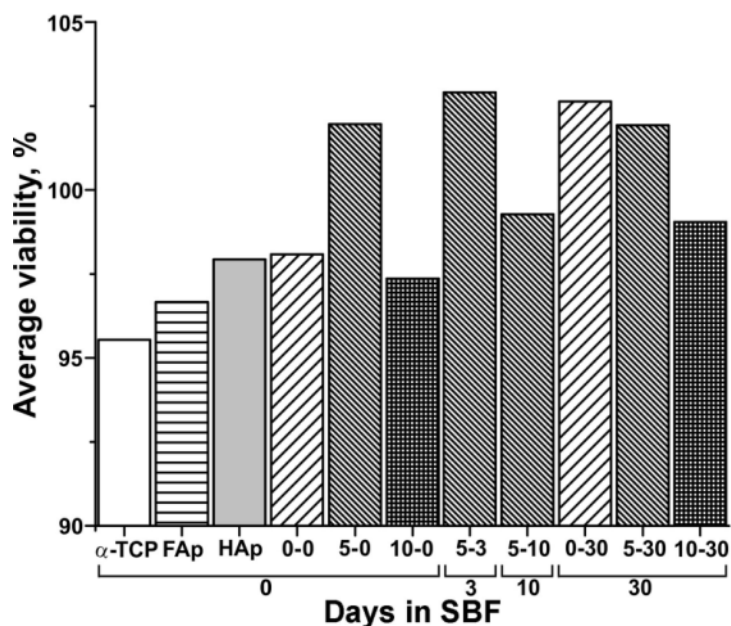


Figure 39. DET assay of cytotoxic effects of α -TCP/FAp composites on MRC-5 cells.

9.2. Characterization of cement pastes

9.2.1. Physical properties of cement samples: setting and working time, flow and solubility

Table 9 presents liquids used for cement pastes preparation and the best values of LPR. CA is often added to the liquids for pastes because it has been reported as a setting accelerator and a calcium ion chelating agent that improves mechanical properties [66,216]. PEG is used for phase stability, i.e. to prevent segregation [221]. Another ingredient added to the solution for rheology modification is HPMC, because it reduces washability, which prolongs the lifetime of cements [214,224]. All of the ingredients added to the starting solution should ensure better cement paste handling and good mechanical properties. Also, desired paste properties could be achieved by controlling the LPR value. Due to the high concentration of CA, the setting of the F1 series was too fast and was disregarded for further study. F2 series, containing Na_2HPO_4 that increases the setting rate, was also deemed unsuitable for dental cement, as well as the F3 series, in which PEG was used for the enhanced phase stability. The viscosity of the F4 series was too low for further use. F5 series that contained HPMC, CA and PEG, and with LPR of 0.45 ml/g exhibited the best setting time and was chosen for further analysis with α -TCP/FAp mixed powders.

Table 17 presents flow, solubility, working and setting time for samples of F5 series: pure α -TCP and α -TCP/FAp with 5 and 10 wt. % of FAp that were labeled as α -TCP/FAp(0), α -TCP/FAp(5) and α -TCP/FAp(10), respectively [275]. The flow of all samples was slightly short of the minimum of 17 mm, required by ISO 6876, probably due to a strong cohesion induced by the addition of PEG [246,247]. Solubility was in agreement with the requirements of ISO 6876 (< 3 % mass fraction) and similar to other tooth filling materials found in the literature [248,276]. Working time is below the upper limit determined by ISO 6876 (30 min). Setting time is lower compared to pastes with HPMC and the LPR value of 0.45 mL/g is comparable, presumably as a result of a high concentration of CA [216,222]. Both α -TCP/FAp based pastes have potential as new filling materials, but α -TCP/FAp(5) could be more appropriate due to the shorter setting time

Table 17. Physical properties of α -TCP and α -TCP/FAp composite cement [275].

Samples	Flow, mm	Solubility, %	Working time, s	Final setting time, min
α -TCP/FAp(0)	16.3	1.9	270	24
α -TCP/FAp(5)	15.6	1.8	270	22
α -TCP/FAp(10)	16.0	2.2	270	27

9.2.2. FESEM analysis of composite cements bioactivity

The most commonly used *in vitro* method for the evaluation of bioactivity of obtained materials is the FESEM observation of the formation of a new HAp layer onto the surface of the tested material in SBF solution. HAp is a dominant dentine and bone constituent, and its formation on the surface of the material that was laid in SBF solution indicates high biocompatibility of the material [228]. Also, the formation of HAp by the transformation of α -TCP on the surface of α -TCP/FAp composite cements in SBF ensures interaction between the host hard tissue and ceramic biomaterial. Therefore, soaking of the samples in SBF and the monitoring of crystal formation gives valuable information about dental material's behavior in the human body. FESEM images (Figure 40, a–c) present morphological changes of the sample surfaces after 10 days in SBF in comparison with the surface of the sample that did not reside in the SBF (Figure 40d). HAp layer formation was observed in all samples (a–c) and the new phase becomes dominant over the entire surface [19,228] that could confirm the expected bioactivity of composite cement [85].

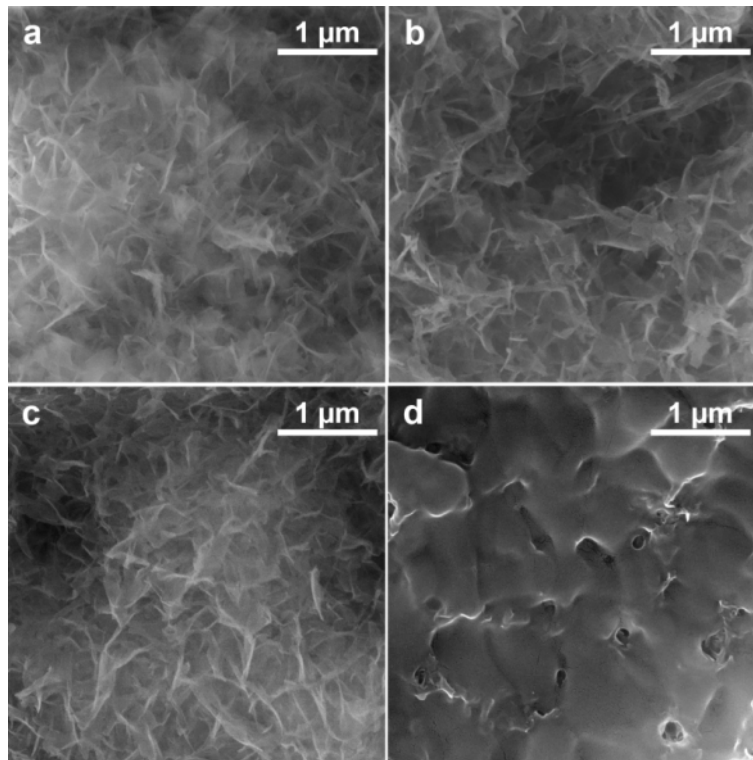


Figure 40. FESEM images of the surface of samples after 10 days in SBF: α -TCP/FAp(0) (a), α -TCP/FAp(5) (b), and α -TCP/FAp(10) (c) and α -TCP/FAp(0) without staying in SBF (d).

9.2.3. XRPD analysis of composite cements bioactivity

The XRPD analyses confirm observation by FESEM and further show that in all samples α -TCP was completely transformed to HAp during soaking in SBF (Figure 41, 1–3). Also, the positions of 2θ angles in the pattern of the samples α -TCP/FAp(5) (labeled as 2) and α -TCP/FAp(10) (labeled as 3) are slightly shifted to the higher values in comparison to pure α -TCP indicating the presence of FAp with a smaller unit cell. In addition, XRPD patterns of the cement samples that have not been immersed in SBF (a–c) show the partial transformation of α -TCP into HAp after 2 days.

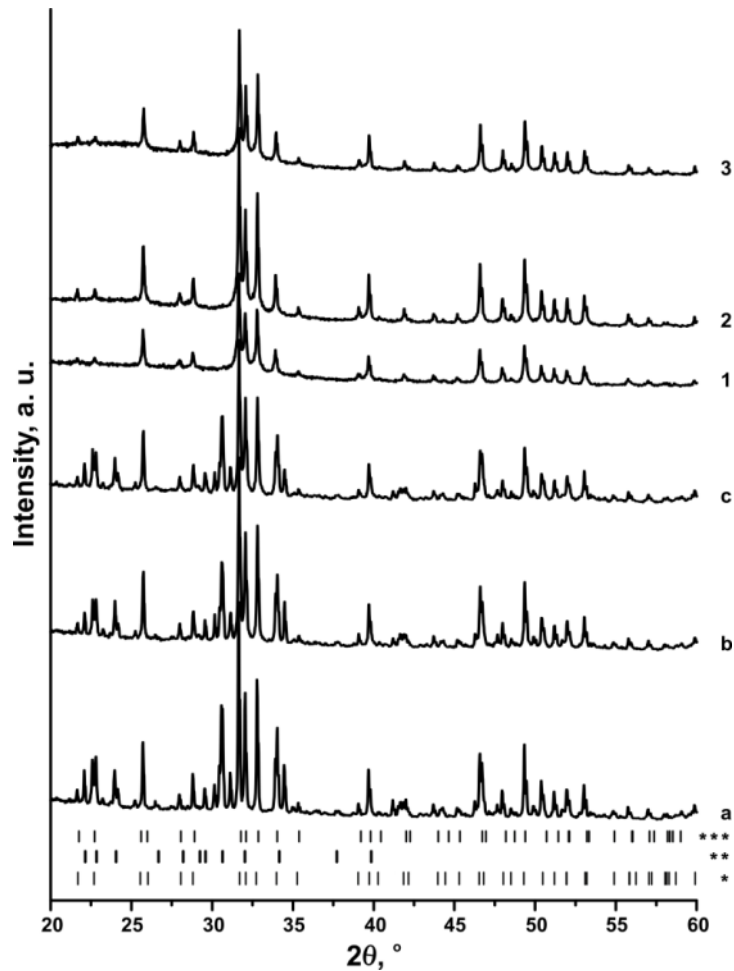


Figure 41. XRPD patterns of samples: α -TCP/FAp(0) (a), α -TCP/FAp(5) (b) and α -TCP/FAp(10) (c), and the same samples (1, 2 and 3, respectively) after 10 days in SBF. * HAp-PDF#74-0556, ** α -TCP-PDF#29-0359 and *** FAp-PDF#83-0556.

9.2.4. FESEM analysis of composite cements biocompatibility

Visual investigation of biocompatibility and cytotoxicity of the samples α -TCP/FAp(0), α -TCP/FAp(5), and α -TCP/FAp(10), after 10 days in SBF, and their influence on L929 and MRC-5 fibroblast cells are presented in Figures 40 and 41. The cell growth on each sample was prominent, indicating no cytotoxicity of α -TCP/FAp cement samples on L929 fibroblast cell culture (Figure 42) [23].

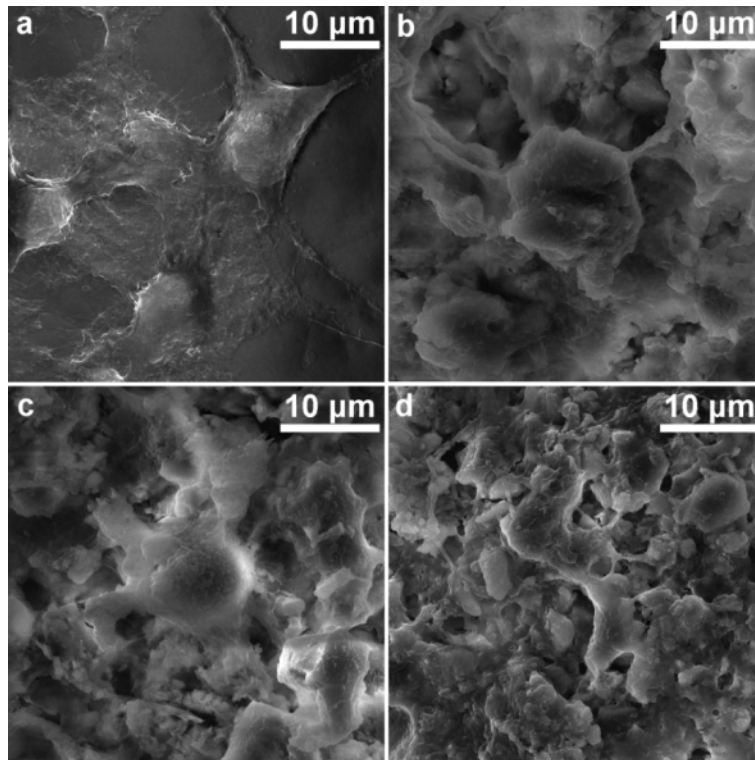


Figure 42. FESEM images of L929 (a) on: α -TCP/FAp(0) (b), α -TCP/FAp(5) (c), and α -TCP/FAp(10) (d).

MRC-5 retained the shape on α -TCP/FAp(0), but it can be also observed on each composite (Figure 43). In all samples, cytoplasmic extensions were observed, indicating that composite cements are not toxic for fibroblast MRC-5 cells [22].

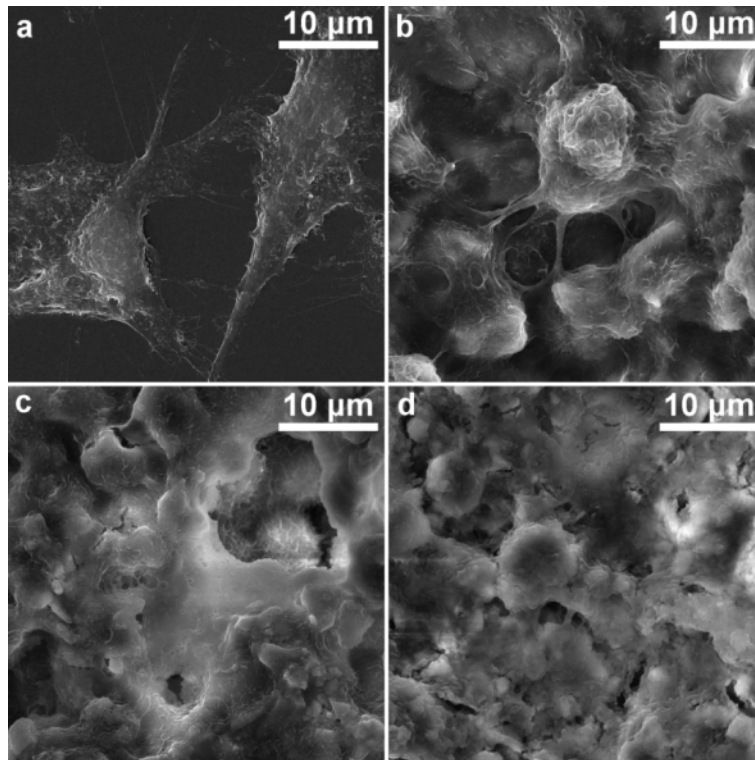


Figure 43. FESEM images of MRC-5 (a) on: α -TCP/FAp(0) (b), α -TCP/FAp(5) (c), and α -TCP/FAp(10) (d).

9.2.5. *In vitro* MTT and DET assay of composite cements biocompatibility

Along with FESEM, *in vitro* MTT and DET methods were employed for the investigation of the influence of FAp on the biocompatibility of samples. Human fibroblast MRC-5 cells and animal fibroblast L929 cells were used as test cultures for viability measurement in the presence of samples α -TCP/FAp(0), α -TCP/FAp(5), and α -TCP/FAp(10), after 10 days in SBF. What the cells looked like after 48 h in the medium and before MTT and DET counting, could be seen in Figures 44 and 45.

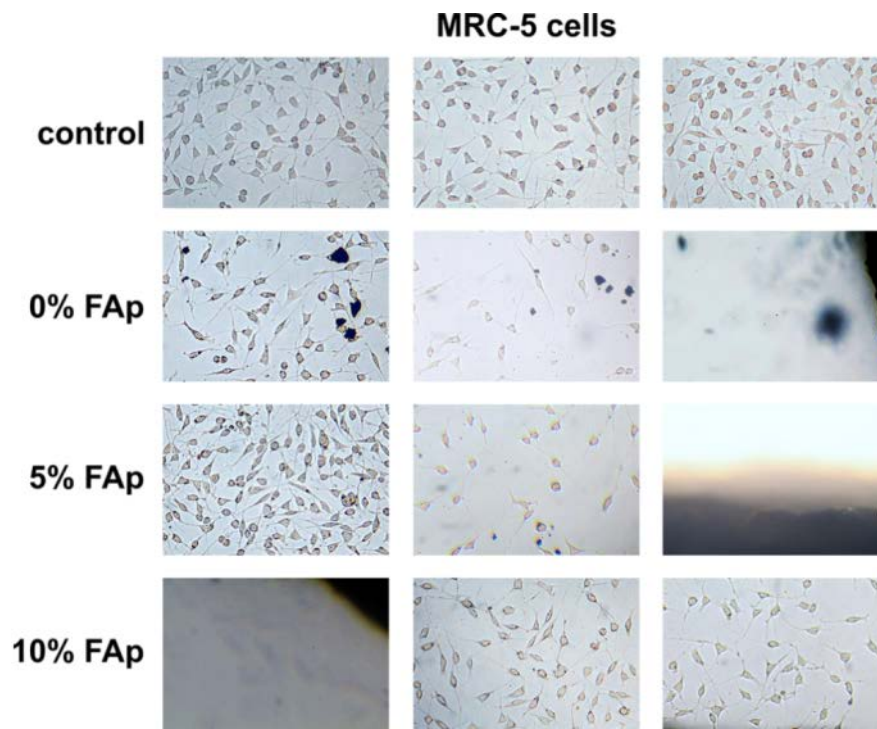


Figure 44. Appearance of MRC-5 cells before MTT and DET tests.

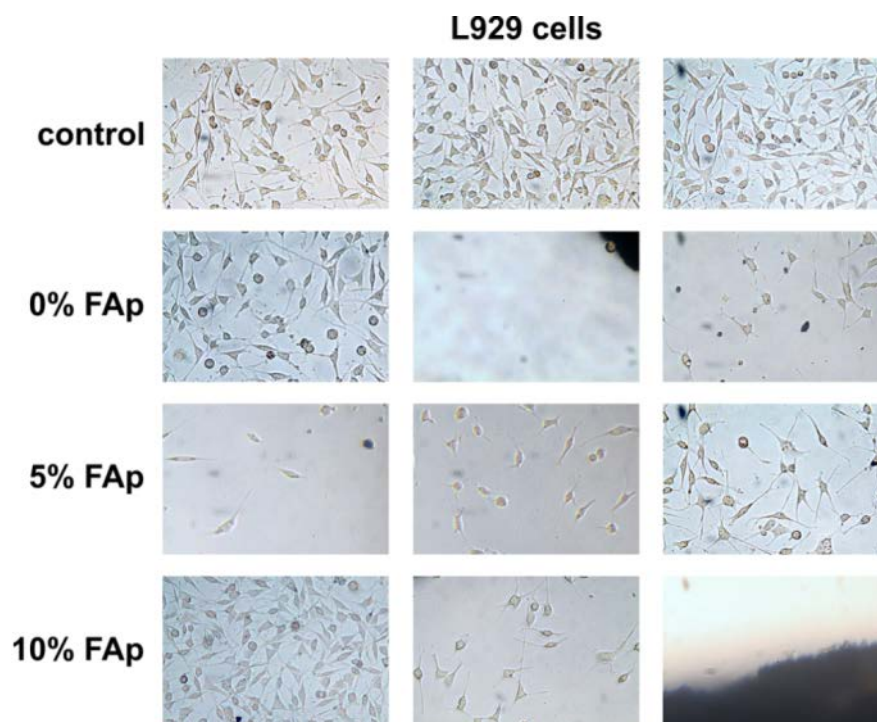


Figure 45. Appearance of L929 cells before MTT and DET tests.

Cell viability obtained with MTT after 48 h is presented in Figure 46. Compared with control samples (100 %K), α -TCP/FAp(5) and α -TCP/FAp(10) showed an increase in cell viability on MRC-5 and an insignificant drop of cell viability on L929, proving non-cytotoxicity of the prepared composites with FAp. Synthetic HAp was already confirmed as non-cytotoxic [25,277,278], although L929 cell viability in the presence of our composites α -TCP/FAp(5) is higher. Sample α -

TCP/FAp(0) induced lower viability of MRC-5 compared to composites α -TCP/FAp(5) and α -TCP/FAp(10), which was in accordance with the literature data [35]. As it can be seen from Figure 46, the cell viability is higher for sample α -TCP/FAp(5) that has been chosen for the dental root canal filling.

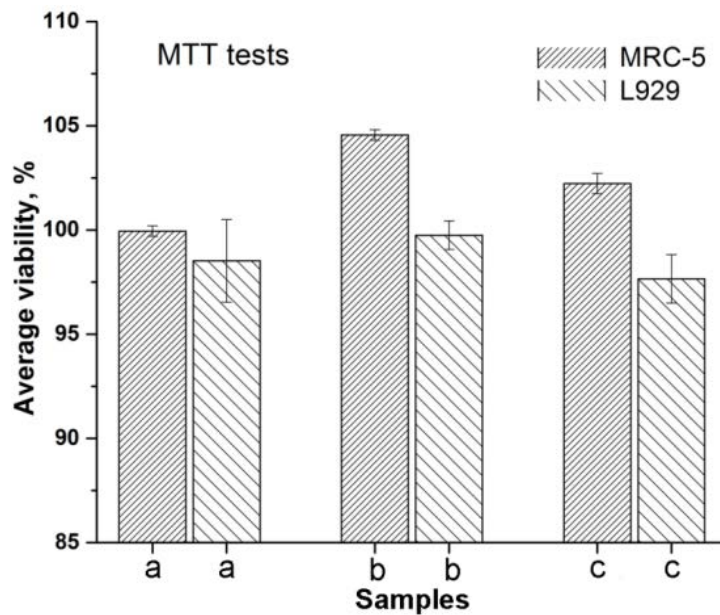


Figure 46. The results of *in vitro* MTT assay on samples: α -TCP/FAp(0) (a), α -TCP/FAp(5) (b), and α -TCP/FAp(10) (c).

The *in vitro* DET results presented in Figure 47 are in agreement with the MTT assay – both composites cause a negligible decrease in cell viability of MRC-5 in comparison to α -TCP/FAp(0). The same trend was observed in the case of L929 cells, for which sample α -TCP/FAp(10) showed the lowest biocompatibility, probably due to a formation of segregates.

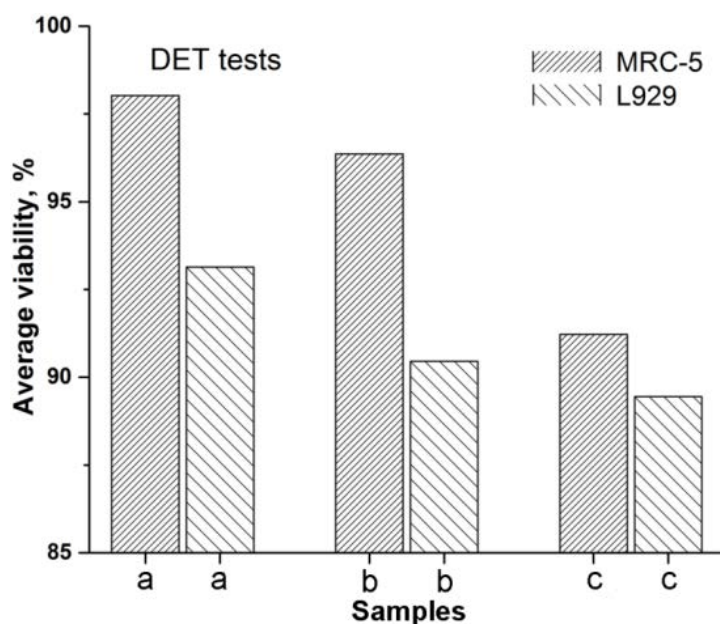


Figure 47. The results of *in vitro* DET assay on samples: α -TCP/FAp(0) (a), α -TCP/FAp(5) (b), and α -TCP/FAp(10) (c).

9.2.6. Analysis of dental cement adhesion to the tooth

Based on investigated biocompatibility, bioactivity and mechanical properties of two α -TCP/FAp composites in [275] study and our previous research [19], sample α -TCP/FAp(5) was chosen as the most appropriate of the tested formulations for the tooth canal filling. Figure 48 presents representative cross-sections of teeth whose canals were filled with either α -TCP/FAp(5) cement (a-c) or with a combination of α -TCP/FAp(5) cement and gutta-percha (d-f). FESEM analysis showed that after 48 h in SBF, areas of microgap formation appear in both cases between α -TCP/FAp(5) and dentin, as similarly shown in previous work [279]. However, the formation of the HAp layer can be observed at the interface, indicating the potential for improved material-dentin adhesion over time. It is still very early to draw a conclusion on the bonding potential of the tested experimental cement. Further bond strength studies are required over short- and long-term periods on a larger sample size. Yet, the viscosity, working and setting time tested in this study appear suitable for the application of this experimental formulation as a root canal sealer. Potential for α -TCP/FAp cement remains to be experimentally confirmed, but strong bioactive behavior seen in the presented study points in this direction.

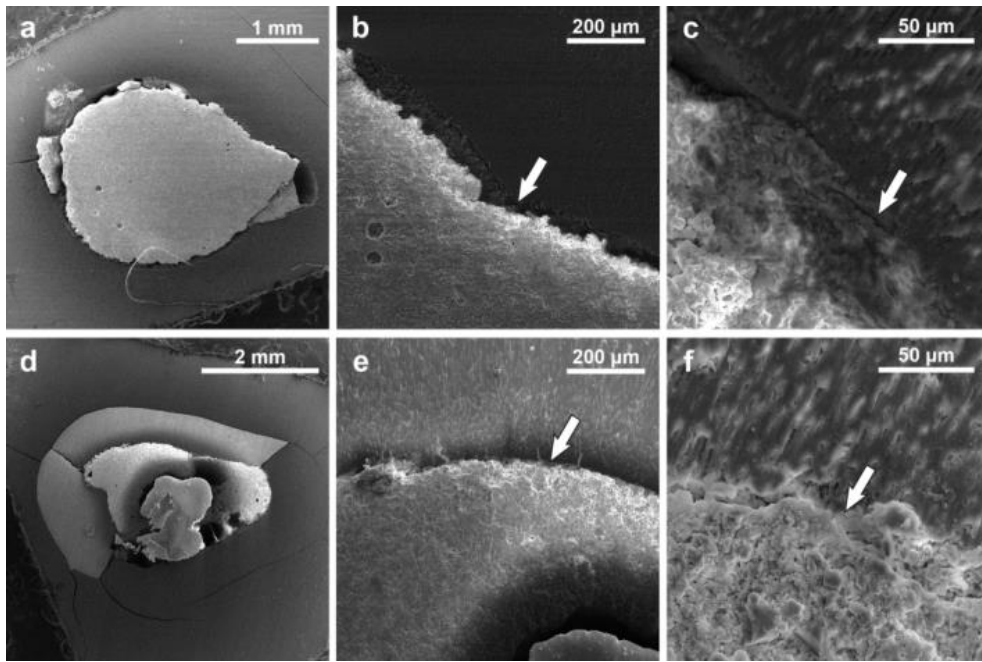


Figure 48. FESEM images of tooth canal filling with α -TCP/FAp(5) without (a–c) and with gutta-percha (d–f).

10. CONCLUSION

With the aim of investigating the influence of different concentrations of fluorapatite (FAp) on compressive strength and biocompatibility of α -TCP/FAp composite cement before and after the soaking of composite cement specimens in the simulated body fluid (SBF), new nanosized FAp, as well as HAp powders were prepared by the hydrothermal method. Calcination of the obtained HAp with the Ca/P molar ratio 1.50 was used for the synthesis of α -TCP. Composite cements were investigated as a potential material for tooth filling and the following conclusions were reached:

- Different reaction mixtures and conditions resulted in the hydrothermal synthesis of nanoparticle FAp powder that consisted of uniform rod-like nanoparticles with an average size of about 90 nm, which was used for the processing of the composites.

- Bioactivity of α -TCP/FAp composite cement was proved by the formation of HAp layer after the soaking of composites in SBF for 3, 5, 10 and 30 days.

- Mechanical testing of α -TCP/FAp showed an increase in compressive strength more than 100 times after 10 days in SBF, due to the transformation of α -TCP into HAp. The highest compressive strength value was observed for the sample with 5% of FAp.

- Composite cement α -TCP/FAp, as a dental material, could serve as a source of F^- ions that have an antimicrobial role as well as the role of reinforcement surrounding natural tooth material. The release of F^- ions from the composite was found to be satisfactory after 3 days.

- *In vitro* α -TCP/FAp powder MTT and DET biocompatibility tests with MRC-5 human fibroblast cells in liquid medium showed that these powders are not cytotoxic. After 96 h, cell viability in contact with composite powders was higher than cell viability in contact with reference samples.

- Novel liquid part of the cement paste was made with 0.5 % hydroxypropyl methylcellulose, 15 % citric acid, 10 % polyethylene glycol and the optimal LPR of 0.45 mL g^{-1}

- The best paste with appropriate physical properties (setting and working time, flow, solubility) and LPR was made with α -TCP/FAp(5) that contained 5 wt.% of FAp.

- Cement sample surfaces after 10 days in SBF compared to the surface of the sample that did not reside in the SBF showed bioactivity through the formation of HAp layer.

- Visual investigation of composite cements after 10 days in SBF, and their influence on L929 and MRC-5 fibroblast cells showed cell growth on each sample and cytoplasmic extensions, indicating that composite cements are not toxic for fibroblast L929 and MRC-5 cells.

- Cell viability obtained with MTT and DET tests on composite cements after 48 h showed approximately the same or increased cell viability in MRC-5 and L929 fibroblast cells, compared to the control sample.

- It was shown that α -TCP/FAp(5) cement is simple for manipulation and suitable for the filling of the root canals of teeth, which makes this material a promising candidate for further development towards dental application.

11. References

- [1] A. Nanci, Ten Cate's Oral Histology: Development, Structure, and Function, 8th edition, Elsevier Mosby, St. Louis, MO 2017.
- [2] P.S. Hart, T.C. Hart, Disorders of human dentin, *Cells Tissues Organs.*, 186 [1] (2007)70–77.
- [3] T. Biswal, S.K. BadJena, D. Pradhan, Sustainable biomaterials and their applications: A short review, *Mater. Today Proc.*, 30 [2] (2020) 274–282.
- [4] H. Naderi, M.M. Matin, A.R. Bahrami, Critical issues in tissue engineering:biomaterials, cell sources, angiogenesis, and drug delivery systems, *J. Biomater. Appl.*, 26 (2011) 383–417.
- [5] Z. Sheikh, S. Najeeb, Z. Khurshid, V. Verma, H. Rashid, M. Glogauer, Biodegradable materials for bone repair and tissue engineering applications, *Materials (Basel).*, 8 (2015) 5744–5794.
- [6] K. Pajor, L. Pajchel, J. Kolmas, Hydroxyapatite and fluorapatite in conservative dentistry and oral implantology - a review, *Materials (Basel)*, 12 [17] (2019) 2683.
- [7] A. Przekora, A Concise Review on Tissue Engineered Artificial Skin Grafts for Chronic Wound Treatment: Can We Reconstruct Functional Skin Tissue In Vitro?, *Cells*, 9 [7] (2020) 1–29.
- [8] A.S. Khan, S. Aamer, A.A. Chaudhry, F.S.L. Wong, I.U. Rehman, Synthesis and characterizations of a fluoride-releasing dental restorative material, *Mater. Sci. Eng. C.*, 33 [6] (2013) 3458–3464.
- [9] S. Koutsopoulos, Synthesis and characterization of hydroxyapatite crystals: A review study on the analytical methods, *J. Biomed. Mater. Res.*, 62 [4] (2002) 600–612.
- [10] L.L. Hench, Sol-gel materials for bioceramic applications, *Curr Opin.*, 2 [5] (1997) 604–610.
- [11] J. Huang, S.M. Best, Ceramic biomaterials, pp 3-30 in *Tissue Engineering Using Ceramics and Polymers – Woodhead 2007*, eds. by A.R. Boccaccini, J.E. Gough, Woodhead Publishing, 2007.
- [12] G. Ayoub, Dj. Veljovic, M.L. Zebic, V. Miletic, E. Palcevskis, R. Petrovic, D. Janackovic, Composite nanostructured hydroxyapatite/yttrium stabilized zirconia dental inserts – The processing and application as dentin substitutes, *Ceram. Int.*, 44 [15] (2018) 18200–18208.
- [13] J.A. Cury, L.M.A. Tenuta, Enamel remineralization: controlling the caries disease or treating early caries lesions?, *Braz. Oral Res.*, 23 [1] (2009) 23–30.
- [14] E.A.A. Neel, A. Aljabo, A. Strange, S. Ibrahim, M. Coathup, A.M. Young, L. Bozec, V. Mudera, Demineralization–remineralization dynamics in teeth and bone, *Int. J. Nanomedicine.*, 11 (2016) 4743–4763.

- [15] A. Altaie, N. Bubb, P. Franklin, M.J. German, A. Marie, D.J. Wood, Development and characterisation of dental composites containing anisotropic fluorapatite bundles and rods, *Dent. Mater.* 36 [8] (2020) 1071–1085.
- [16] A. Elghazel, R. Taktak, K. Elleuch, J. Bouaziz, Mechanical and tribological properties of tricalcium phosphate reinforced with fluorapatite as coating for orthopedic implant, *Mater. Lett.*, 215 (2018) 53–57.
- [17] F. Barandehfard, M. Kianpour Rad, A. Hosseinnia, K. Khoshroo, M. Tahriri, H.E. Jazayeri, K. Moharamzadeh, L. Tayebi, The addition of synthesized hydroxyapatite and fluorapatite nanoparticles to a glass-ionomer cement for dental restoration and its effects on mechanical properties, *Ceram. Int.*, 42 [15] (2016) 17866–17875.
- [18] N. Jmal, J. Bouaziz, Fluorapatite-glass-ceramics obtained by heat treatment of a gel synthesized by the sol-gel processing method, *Mater. Lett.*, 215 (2018) 280–283.
- [19] A. Kazuz, Radovanović, Dj. Veljović, V. Kojić, V. Miletić, R. Petrović, D. Janačković, α -Tricalcium phosphate/fluorapatite based composite cements: Synthesis, mechanical properties, and biocompatibility, *Ceram. Int.*, 46 [16] (2020) 25149–25154.
- [20] J. Jeong, J.H. Kim, J.H. Shim, N.S. Hwang, C.Y. Heo, Bioactive calcium phosphate materials and applications in bone regeneration, *Biomater. Res.*, 23 (2019) 1–11.
- [21] J.S. Al-Sanabani, A.A. Madfa, F.A. Al-Sanabani, Application of Calcium Phosphate Materials in Dentistry, *Int. J. Biomater.*, 2013 (2013) 876132.
- [22] Ž. Radovanović, B. Jokić, D. Veljović, S. Dimitrijević, V. Kojić, R. Petrović, D. Janačković, Antimicrobial activity and biocompatibility of Ag^+ - and Cu^{2+} -doped biphasic hydroxyapatite/ α -tricalcium phosphate obtained from hydrothermally synthesized Ag^+ - and Cu^{2+} -doped hydroxyapatite, *Appl. Surf. Sci.*, 307 (2014) 513–519.
- [23] M. Memarpour, F. Shafiei, A. Rafiee, M. Soltani, M.H. Dashti, Effect of hydroxyapatite nanoparticles on enamel remineralization and estimation of fissure sealant bond strength to remineralized tooth surfaces: An in vitro study, *BMC Oral Health.*, 19 [1] (2019) 1–14.
- [24] R. Taktak, A. Elghazel, J. Bouaziz, S. Charfi, H. Keskes, Tricalcium phosphate-Fluorapatite as bone tissue engineering: Evaluation of bioactivity and biocompatibility, *Mater. Sci. Eng. C.*, 86 (2018) 121–128.
- [25] S. Seyedmajidi, M. Seyedmajidi, E. Zabihi, K. Hajian-Tilaki, A comparative study on cytotoxicity and genotoxicity of the hydroxyapatite-bioactive glass and fluorapatite-bioactive glass nanocomposite foams as tissue scaffold for bone repair, *J. Biomed. Mater. Res. - Part A.*, 106 [10] (2018) 2605–2612.
- [26] <https://www.britannica.com/science/tooth-anatomy> (date of the last access to the site - April 15, 2022.).

- [27] R. Wang, Q. Wang, X. Wang, L. Tian, H. Liu, M. Zhao, C. Peng, Q. Cai, Y. Shi, Enhancement of nano-hydroxyapatite bonding to dentin through a collagen/calcium dual-affinitive peptide for dentinal tubule occlusion, *J Biomater Appl.*, 29 [2] (2014) 268–277.
- [28] C. Robinson, S. Connell, J. Kirkham, S.J. Brookes, R.C. Shore, A.M. Smith, The effect of fluoride on the developing tooth, *Caries. Res.*, 38 [3] (2004) 268–276.
- [29] G.H. Bowden, Microbiology of root surface caries in humans, *J. Dent. Res.*, 69 [5] (1990) 1205–1210.
- [30] K. Papadimitriou, A. Alegria, P.A. Bron, M. de Angelis, M. Gobbetti, M. Kleerebezem, J.A. Lemos, D.M. Linares, P. Ross, C. Stanton, F. Turrioni, D. van Sinderen, P. Varmanen, M. Ventura, M. Zúñiga, E. Tsakalidou, J. Kok, Stress physiology of lactic acid bacteria, *Microbiol. Mol. Biol. Rev.*, 80 [3] (2016) 837–890.
- [31] G. Caggianiello, M. Kleerebezem, G. Spano, Exopolysaccharides produced by lactic acid bacteria: from health-promoting benefits to stress tolerance mechanisms, *Appl. Microbiol. Biotechnol.*, 100 [9] (2016) 3877–3886.
- [32] A. Besinis, T. De Peralta, C.J. Tredwin, R.D. Handy, Review of nanomaterials in dentistry: interactions with the oral microenvironment, clinical applications, hazards, and benefits, *ACS Nano.*, 9 [3] (2015) 2255–2289.
- [33] A.A. Balhaddad, A.A. Kansara, D. Hidan, M.D. Weir, H.H.K. Xu, M.A.S. Melo, Toward dental caries: Exploring nanoparticle-based platforms and calcium phosphate compounds for dental restorative materials, *Bioact. Mater.*, 4 (2019) 43–55.
- [34] S. Kannan, A. Rebelo, J.M.F. Ferreira, Novel synthesis and structural characterization of fluorine and chlorine co-substituted hydroxyapatites, *J. Inorg. Biochem.*, 100 [10] (2006) 1692–1697.
- [35] N. Montazeri, R. Jahandideh, E. Biazar, Synthesis of fluorapatite-hydroxyapatite nanoparticles and toxicity investigations, *Int. J. Nanomedicine.*, 6 (2011) 197–201.
- [36] O.M. Böstman, O.M. Laitinen, O. Tynnenen, S.T. Salminen, H.K. Pihlajamäki, Tissue restoration after resorption of polyglycolide and poly-laevo-lactic acid screws, *J. Bone Joint Surg. Br.*, 87 [11] (2005) 1575–1580.
- [37] W. D. Callister, Jr., *Materials Science and Engineering: An Introduction*, 5th Edition, John Wiley & Sons, New York 1999.
- [38] V. Hasirci, N. Hasirci, *Fundamentals of Biomaterials*, Springer Nature, New York 2018.
- [39] I.E Ruyter, H. Oeysaed, Composites for use in posterior teeth: composition and conversion, *J. Biomed. Mater. Res.*, 21 [1] (1987) 11–23.
- [40] M. Arora, E.K. Chan, S. Gupta, A.D. Diwan, Polymethylmethacrylate bone cements and additives: A review of the literature, *World J. Orthop.*, 4 [2] (2013) 67–74.

- [41] K.A. Athanasiou, C.M. Agrawal, F.A. Barber, S.S. Burkhart, Orthopaedic Applications for PLA–PGA Biodegradable Polymers, *Arthroscopy*, 14 [7] (1998) 726–737.
- [42] S. Desai, B. Bidanda, P. Ba´rtolo, *Metallic and Ceramic Biomaterials: Current and Future Developments*, In: *Bio-Materials and Prototyping Applications in Medicine*, P. Ba´rtolo, B. Bidanda (eds.), Springer, Berlin 2008.
- [43] D.F. Williams, Orthopedic implants: Fundamental principles and the significance of biocompatibility, pp. 1-50 in: *Biocompatibility of Orthopedic Implants*, vol. 1, D.F. Williams (ed.), CRC Press, Boca Raton, Fla 1982.
- [44] K. Prasad, O. Bazaka, M. Chua, M. Rochford, L. Fedrick, J. Spoor, R. Symes, M. Tieppo, C. Collins, A. Cao, D. Markwell, K. Ostrikov, K. Bazaka, *Metallic Biomaterials: Current Challenges and Opportunities*, *Materials*, 10 (2017) 884.
- [45] D. Lin, A. Li, W. Li, S. Zhou, M.V. Swain, Design optimization of functionally graded dental implant for bone remodeling, *Compos. Part B Eng.*, 40 [7] (2009) 668–675.
- [46] R.P. Verma, Titanium based biomaterial for bone implants: A mini review, *Mater. Today Proc.*, 26 [2] (2020) 3148–3151.
- [47] L. Le Guéhenec, A. Soueidan, P. Layrolle, Y. Amouriq, Surface treatments of titanium dental implants for rapid osseointegration, *Dent. Mater.*, 23 [7] (2007) 844–854.
- [48] R.L. Bowen, Properties of a silica-reinforced polymer for dental restorations, *J. Am. Dent. Assoc.*, 66 (1963) 57–64.
- [49] X.Q. Cao, R. Vassen, D. Stoeber, Ceramic materials for thermal barrier coatings, *J. Eur. Ceram.*, 24 [1] (2004) 1–10.
- [50] T. Rouxel, *Mechanical Properties of Ceramics*, pp. 261-324 in *Ceramic Materials: Processes, Properties and Applications*, P. Boch, J.-C. Niepce (eds.), ISTE USA, Newport Beach, CA 2007.
- [51] L.L. Hench, Sol-gel materials for bioceramic application, *Curr. Opin. Solid. State Mater. Sci.*, 2 (1997) 604–610.
- [52] V. dos Santos, R.N. Brandalise, M. Savaris, *Engineering of Biomaterials (Topics in Mining, Metallurgy and Materials Engineering)*, Springer International Publishing AG, Cham 2017.
- [53] S. Mondal, U. Pal, 3D hydroxyapatite scaffold for bone regeneration and local drug delivery applications, *J. Drug Deliv. Sci. Technol.*, 53 (2019) 101131.
- [54] A. Khaskhoussi, L. Calabrese, M. Currò, R. Ientile, J. Bouaziz, E. Proverbio, Effect of the Compositions on the Biocompatibility of New Alumina–Zirconia–Titania Dental Ceramic Composites, *Materials*, 13 [6] (2020) 1374.
- [55] K. Sivaraman, A. Chopra, A. I. Narayan, D. Balakrishnan, Is zirconia a viable alternative to titanium for oral implant? A critical review, *J. Prosthodont. Res.*, 62 (2018) 121–133.

- [56] T.V. Thamaraiselvi, S. Rajeswari, Biological evaluation of bioceramic materials—a review, *Trends Biomater. Artif. Organs.* 18 [1] (2004) 9–17.
- [57] S.V. Dorozhkin, Calcium Orthophosphates as Bioceramics: State of the Art, *J. Funct. Biomater.*, 1 (2010) 22–107.
- [58] D. Sidane, H. Rammal, A. Beljebbar, S.C. Gangloff, D.Chicot, F.Velard, H. Khireddine, A. Montagne, H. Kerdjoudj, Biocompatibility of sol-gel hydroxyapatite-titania composite and bilayer coatings, *Mater. Sci. Eng. C*, 72 (2017) 650–658.
- [59] Y. Josset, Z. Oum'hamed, A. Zarrinpour, M. Lorenzato, J.J. Adnet, D. Laurent-Maquin, *In vitro* reactions of human osteoblasts in culture with zirconia and alumina ceramics, *J. Biomed. Mater. Res.*, 47 (1999) 481–493.
- [60] S.M. Carvalho, A.A.R. Oliveira, E.M.F. Lemos, M.M. Pereira, Bioactive Glass Nanoparticles for Periodontal Regeneration and Applications in Dentistry, pp. 351-383 in *In Micro and Nano Technologies, Nanobiomaterials in Clinical Dentistry (Second Edition)*, K. Subramani, W. Ahmed (Eds.), Elsevier Inc, Amsterdam 2019.
- [61] A. El-Ghannam, P. Ducheyne, Bioactive Ceramics, pp. 204-234 in *Comprehensive Biomaterials II, Volume 1*, P. Ducheyne (Ed.) Elsevier Ltd., Amsterdam 2017.
- [62] L. Hench, Bioceramics: From Concept to Clinic, *J. Am. Ceram. Soc.*, 74 [7] (1991) 1487–1510.
- [63] G. Kaur, V. Kumar, F. Baino, J. C. Mauro, G. Pickrell, I. Evans, O. Bretcanu, Mechanical properties of bioactive glasses, ceramics, glass-ceramics and composites: State-of-the-art review and future challenges, *Mater. Sci. Eng. C*, 104 (2019) 109895.
- [64] S.V. Dorozhkin, Calcium orthophosphates (CaPO₄): occurrence and properties, *Prog. Biomater.*, 5 (2016) 9–70.
- [65] V. Uskokovic, T.A. Desai, Phase composition control of calcium phosphate nanoparticles for tunable drug delivery kinetics and treatment of osteomyelitis. I. Preparation and drug release, *J. Biomed. Mater. Res. Part A*, 101 (2013) 1416–1426.
- [66] K. Kiminami, T. Konishi, M. Mizumoto, K. Nagata, M. Honda, H. Arimura, M. Aizawa, Effects of adding polysaccharides and citric acid into sodium dihydrogen phosphate mixing solution on the material properties of gelatin-hybridized calcium-phosphate cement, *Materials*, 10 (2017) 1–14.
- [67] R.A. Perez, H.W. Kim, M.P. Ginebra, Polymeric additives to enhance the functional properties of calcium phosphate cements, *J. Tissue Eng.*, 3 (2012) 1–20.
- [68] Y.A. Al-Dulaijan, L. Cheng, M.D. Weir, M.A.S. Melo, H. Liu, T.W. Oates, et al., Novel rechargeable calcium phosphate nanocomposite with antibacterial activity to suppress biofilm acids and dental caries, *J. Dent.*, 72 (2018) 44–52.

- [69] J.F. Nguyen, V. Migonney, N.D. Ruse, M. Sadoun, Resin composite blocks via high-pressure high-temperature polymerization, *Dent. Mater.*, 28 (2012) 529–534.
- [70] A. Attia, K.M. Abdelaziz, S. Freitag, M. Kern, Fracture load of composite resin and feldspathic all-ceramic CAD/CAM crowns, *J. Prosthet. Dent.*, 95 (2006) 117–123.
- [71] D.Y. Papadogiannis, R.S. Lakes, Y. Papadogiannis, G. Palaghias, M. Helvatjoglu-Antoniades, The effect of temperature on the viscoelastic properties of nano-hybrid composites, *Dent. Mater.*, 24 (2008) 257–266.
- [72] L.P. Corrales, M.L. Esteves, J. aime E. Vick, Scaffold design for bone regeneration. *Journal of nanoscience and nanotechnology*, *J Nanosci Nanotechnol.*, 14 (2014) 15–56.
- [73] L. Roseti, V. Parisi, M. Petretta, C. Cavallo, G. Desando, I. Bartolotti, B. Grigolo, Scaffolds for Bone Tissue Engineering: State of the art and new perspectives, *Mater. Sci. Eng. C*, 78 (2017) 1246–1262.
- [74] R. Agarwal, A.J. García, Biomaterial strategies for engineering implants for enhanced osseointegration and bone repair, *Adv. Drug Deliv. Rev.*, 94 (2015) 53–62.
- [75] S.H. Dickens, G.M. Flaim, S. Takagi, Mechanical properties and biochemical activity of remineralizing resin-based Ca-PO₄ cements, *Dent. Mater.*, 19 (2003) 558–566.
- [76] S. Gallinetti, C. Canal, M.P. Ginebra, Development and characterization of biphasic hydroxyapatite/ β -TCP cements, *J. Am. Ceram. Soc.*, 97 (2014) 1065–1073.
- [77] S. V. Dorozhkin, Multiphasic calcium orthophosphate (CaPO₄) bioceramics and their biomedical applications, *Ceram. Int.*, 42 (2016) 6529–6554.
- [78] V. V. Silva, F. S. Lameiras, and R. Z. Domingues, Microstructural and mechanical study of zirconia-hydroxyapatite (ZH) composite ceramics for biomedical applications, *Compos. Sci. Technol.*, 61 [2] (2001) 301–310.
- [79] H.H. Xu, L. Sun, M.D. Weir, J.M. Antonucci, S. Takagi, L.C. Chow, et al., Nano DCPA-whisker composites with high strength and Ca and PO(4) release, *J. Dent. Res.*, 85 (2006) 722–727.
- [80] G. Hannink, J.J. Chris Arts, Bioresorbability, porosity and mechanical strength of bone substitutes: What is optimal for bone regeneration?, *Injury*, 42 [S2] (2011) S22–S25.
- [81] M. Prokopowicz, A. Szewczyk, A. Skwira, R. Sądej, G. Walker, Biphasic composite of calcium phosphate-based mesoporous silica as a novel bone drug delivery system, *Drug Deliv. Transl. Res.*, 10 (2020) 455–470.
- [82] A. Haider, K.C. Gupta, I.K. Kang, PLGA/nHA hybrid nanofiber scaffold as a nanocargo carrier of insulin for accelerating bone tissue regeneration, *Nanoscale Res. Lett.*, 9 (2014) 1–12.
- [83] M.P. Ginebra, T. Traykova, J.A. Planell, Calcium phosphate cements as bone drug delivery systems: A review, *J. Control. Release*, 113 (2006) 102–110.

- [84] A. Haider, S. Haider, S.S. Han, I.K. Kang, Recent advances in the synthesis, functionalization and biomedical applications of hydroxyapatite: a review, *RSC Adv.*, 7 (2017) 7442–7458.
- [85] M. Sadat-Shojai, M.T. Khorasani, A. Jamshidi, Hydrothermal processing of hydroxyapatite nanoparticles - A Taguchi experimental design approach, *J. Cryst. Growth.*, 361 (2012) 73–84.
- [86] T.W. Clyne, D. Hull *An Introduction to Composite Materials*, 3rd Edition, Cambridge University Press, New York 2019.
- [87] S. W. Tsai, H. Thomas Hahn, *Introduction to Composite Materials*, Technomic Publishing Company, Inc, Lancaster, Penn 1980.
- [88] I.D. Sideridou, M.M. Karabela, E.C. Vouvoudi, Physical properties of current dental nanohybrid and nanofill light-cured resin composites. *Dent. Mater.*, 27 (2011) 598–607.
- [89] S. Beun, T. Glorieux, J. Devaux, J. Vreven, G. Leloup, Characterization of nanofilled compared to universal and microfilled composites, *Dent. Mater.*, 23 [1] (2006) 51–59.
- [90] C.T.W. Meereis, E.A. Münchow, W.L. de Oliveira da Rosa, A.F. da Silva, E. Piva, Polymerization shrinkage stress of resin-based dental materials: A systematic review and meta-analyses of composition strategies, *J. Mech. Behav. Biomed. Mater.*, 82 (2018) 268–281.
- [91] A. Bacchi, M. Nelson, C.S. Pfeifer, Characterization of methacrylate-based composites containing thio-urethane oligomers, *Dent. Mater.*, 32 (2016) 233–239.
- [92] X. Zhou, X. Huang, M. Li, X. Peng, S. Wang, X. Zhou, L. Cheng, Development and status of resin composite as dental restorative materials, *J. Appl. Polym. Sci.*, 36 [44] (2019) 48180.
- [93] A. Aminoroaya, R. E. Neisiany, S. N. Khorasani, P. Panahi, O. Das, H. Madry, M. Cucchiarini, S. Ramakrishna, A review of dental composites: Challenges, chemistry aspects, filler influences, and future insights, *Compos. B. Eng.*, 216 (2021) 108852.
- [94] M.F. Vassal, J. Nunes-Pereira, S.P. Miguel, I.J. Correia, A.P. Silva, Microstructural, mechanical and biological properties of hydroxyapatite - CaZrO₃ biocomposites, *Ceram. Int.*, 45 (2019) 8195–8203.
- [95] R.J.B. Sackers, R.A.J. Dalmeyer, R. Brand, P.M. Rozing, C.A. van Blitterswijk, Assessment of bioactivity for orthopedic coatings in a gap-healing model, *J. Biomed. Mater. Res.*, 36 (1997) 265–273.
- [96] C.Y. Ooi, M. Hamdi, S. Ramesh, Properties of hydroxyapatite produced by annealing of bovine bone, *Ceram. Inter.*, 33 (2007) 1171–1177.
- [97] V.P. Orlovskii, V.S. Komlev, S.M. Barinov, Hydroxyapatite and hydroxyapatite-based ceramics, *Inorg. Mater.*, 38 [10] (2002) 973–984.

[98] <https://pubchem.ncbi.nlm.nih.gov/compound/Hydroxyapatite#section=2D-Structure> (date of the last access to the site - April 15, 2022.).

[99] K. Lin, J. Chang. Structure and properties of hydroxyapatite for biomedical applications, pp. 3-19 in *Hydroxyapatite (HAp) for Biomedical Applications*, M. Mucalo (Ed.) Elsevier Ltd., Oxford, 2015.

[100] T.G.P. Galindo, Y. Chai, M. Tagaya, Hydroxyapatite Nanoparticle Coating on Polymer for Constructing Effective Biointeractive Interfaces, *J. Nanomater.*, 2019 (2019) 6495239.

[101] W.L. Suchanek, M. Yoshimura, Processing and properties of hydroxyapatite-based biomaterials for use as hard tissue replacement implants, *J. Mater. Res.*, 13 (1998) 94–117.

[102] S. Sprio, M. Dapporto, L. Preti, E. Mazzoni, M.R. Iaquinta, F. Martini, M. Tognon, N.M. Pugno, E. Restivo, L. Visai, A. Tampieri, Enhancement of the Biological and Mechanical Performances of Sintered Hydroxyapatite by Multiple Ions Doping, *Front. Mater. Sci.*, 7 (2020) 224.

[103] D.O. Obada, E.T. Dauda, J.K. Abifarin, D. Dodoo-Arhin, N.D. Bansod, Mechanical properties of natural hydroxyapatite using low cold compaction pressure: Effect of sintering temperature, *Mater. Chem. Phys.*, 239 (2020) 122099.

[104] I. Uysal, F. Severcan, A. Tezcaner, Z. Evis, Co-doping of hydroxyapatite with zinc and fluoride improves mechanical and biological properties of hydroxyapatite, *Prog. Nat. Sci.*, 24 [4] (2014) 340–349.

[105] N.A.S. Mohd Pu'ad, R.H. Abdul Haq, H. Mohd Noh, H.Z. Abdullah, M.I. Idris, T.C. Lee, Synthesis method of hydroxyapatite: A review, *Mater. Today: Proc.*, 29 [1] (2020) 233–239.

[106] M. Sadat-Shojai, M.-T. Khorasani, E. Dinpanah-Khoshdargi, A. Jamshidi, Synthesis methods for nanosized hydroxyapatite with diverse structures, *Acta Biomater.*, 9 [8] (2013) 7591–7621.

[107] M. Vallet-Regí, M.T. Gutiérrez-Ríos, M.P. Alonso, M.I. de Frutos, S. Nicolopoulos, Hydroxyapatite Particles Synthesized by Pyrolysis of an Aerosol, *J. Solid State Chem.*, 112 [1] (1994) 58–64.

[108] H.K. Varma, S. Suresh Babu, Synthesis of calcium phosphate bioceramics by citrate gel pyrolysis method, *Ceram. Int.*, 31 [1] (2005) 109–114.

[109] A. Szcześ, L. Hołysz, E. Chibowski, Synthesis of hydroxyapatite for biomedical applications, *Adv. Colloid Interfac.*, 249 (2017) 321–330.

[110] B. Yeong, X. Junmin, J. Wang, Mechanochemical Synthesis of Hydroxyapatite from Calcium Oxide and Brushite, *J. Am. Ceram. Soc.*, 84 (2001) 465–467.

[111] A. Fahami, R. Ebrahimi-Kahrizsangi, B. Nasiri-Tabrizi, Mechanochemical synthesis of hydroxyapatite/titanium nanocomposite, *Solid State Sci.*, 13 [1] (2011) 135–141.

- [112] A.C. Ferro, M. Guedes, Mechanochemical synthesis of hydroxyapatite using cuttlefish bone and chicken eggshell as calcium precursors, *Mater. Sci. Eng. C*, 97 (2019) 124–140.
- [113] A. Yelten-Yilmaz, S. Yilmaz, Wet chemical precipitation synthesis of hydroxyapatite (HA) powders, *Ceram. Int.*, 44 [8] (2018) 9703–9710.
- [114] P. Wang, C. Li, H. Gong, X. Jiang, H. Wang, K. Li, Effects of synthesis conditions on the morphology of hydroxyapatite nanoparticles produced by wet chemical process, *Powder Technol.*, 203 [2] (2010) 315–321.
- [115] E. Kramer, J. Podurgiel, M. Wei, Control of hydroxyapatite nanoparticle morphology using wet synthesis techniques: Reactant addition rate effects, *Mater. Lett.*, 131 (2014) 145–147.
- [116] M. Wang, H. Chen, W. Shih, H. Chang, M.-H. Hon, I.-M. Hung, Crystalline size, microstructure and biocompatibility of hydroxyapatite nanopowders by hydrolysis of calcium hydrogen phosphate dehydrate (DCPD), *Ceram. Int.*, 41 [2] (2015) 2999–3008.
- [117] K. Sakamoto, S. Yamaguchi, A. Nakahira, M. Kaneno, M. Okazaki, J. Ichihara, et al. Shape-controlled synthesis of hydroxyapatite from α -tricalcium bis(orthophosphate) in organic-aqueous binary systems, *J. Mater. Sci.*, 37 (2002) 1033–1041.
- [118] Y. Yang, Q. Wu, M. Wang, J. Long, Z. Mao, X. Chen, Hydrothermal Synthesis of Hydroxyapatite with Different Morphologies: Influence of Supersaturation of the Reaction System, *Cryst. Growth Des.*, 14 [9] (2014) 4864–4871.
- [119] W. Chen, T. Long, Y.-J. Guo, Z.-A. Zhu, Y.-P. Guo, Hydrothermal synthesis of hydroxyapatite coatings with oriented nanorod arrays, *RSC Adv.*, 4 (2014) 185–191.
- [120] I.S. Neira, F. Guitián, T. Taniguchi, T. Watanabe, M. Yoshimura, Hydrothermal synthesis of hydroxyapatite whiskers with sharp faceted hexagonal morphology, *J Mater Sci.*, 43 (2008) 2171–2178.
- [121] T.T. Hoai, N.K. Nga, L.T. Giang, T.Q. Huy, P.N.M. Tuan, B.T.T. Binh, Hydrothermal Synthesis of Hydroxyapatite Nanorods for Rapid Formation of Bone-Like Mineralization, *J. Elec Mater.*, 46 (2017) 5064–5072.
- [122] C. Xue, Y. Chen, Y. Huang, P. Zhu, Hydrothermal Synthesis and Biocompatibility Study of Highly Crystalline Carbonated Hydroxyapatite Nanorods, *Nanoscale Res. Lett.*, 10 (2015) 316.
- [123] L. Yan, Y. Li, Z.-X. Deng, J. Zhuang, X. Sun, Surfactant-assisted hydrothermal synthesis of hydroxyapatite nanorods, *Int. J. Inorg.*, 3 [7] (2001) 633–637.
- [124] X. Jin, J. Zhuang, Z. Zhang, H. Guo, J. Tan, Hydrothermal synthesis of hydroxyapatite nanorods in the presence of sodium citrate and its aqueous colloidal stability evaluation in neutral pH, *J. Colloid Interface Sci.*, 443 (2015) 125–130.

- [125] Y. Wang, S. Zhang, K. Wei, N. Zhao, J. Chen, X. Wang, Hydrothermal synthesis of hydroxyapatite nanopowders using cationic surfactant as a template, *Mater. Lett.*, 60 [12] (2006) 1484–1487.
- [126] H. Zhang, M. Zhang, Phase and thermal stability of hydroxyapatite whiskers precipitated using amine additives, *Ceram. Int.*, 37 (2011) 279–286.
- [127] M. Salarian, M. Solati-Hashjin, S.S. Shafiei, R. Salarian, Z.A. Nemati, Template-directed hydrothermal synthesis of dandelion-like hydroxyapatite in the presence of cetyltrimethylammonium bromide and polyethylene glycol, *Ceram. Int.*, 35 (2009) 2563–2569.
- [128] I.M.H. Ortiz, R. Parra, M.A. Fanovich, Comparative hydrothermal synthesis of hydroxyapatite by using cetyltrimethylammonium bromide and hexamethylenetetramine as additives, *Ceram. Int.*, 44 [4] (2018) 3658–3663.
- [129] S.H. Li, J.R. de Wijn, P. Layrolle, K. de Groot, Synthesis of macroporous hydroxyapatite scaffolds for bone tissue engineering, *J. Biomed. Mater. Res.*, 61 (2002) 109–120.
- [130] C. Hwang, J. Yun, Flash sintering of hydroxyapatite ceramics, *J. Asian Ceram. Soc.*, 9 [1] (2021) 304–311.
- [131] S. Ramesh, K.L. Aw, R. Tolouei, M. Amiriyan, C.Y. Tan, M. Hamdi, J. Purbolaksono, M.A. Hassan, W.D. Teng, Sintering properties of hydroxyapatite powders prepared using different methods, *Ceram. Int.*, 39 [1] (2013) 111–119.
- [132] A.J. Ruys, M. Wei, C.C. Sorrell, M.R. Dickson, A. Brandwood, B.K. Milthorpe, Sintering effects on the strength of hydroxyapatite, *Biomaterials*, 16 [5] (1995) 409–415.
- [133] K. deGroot, *Ceramics of calcium phosphates: preparation and properties*, pp. 100–114 in *Bioceramics of Calcium Phosphate*. K. deGroot (Ed). CRC Press, Boca Raton, Fla 1983.
- [134] R. Ghosh, R. Sarkar, Synthesis and characterization of sintered hydroxyapatite: a comparative study on the effect of preparation route, *J. Aust. Ceram. Soc.*, 54 (2018) 71–80.
- [135] G. Muralithran, S. Ramesh, Effects of sintering temperature on the properties of hydroxyapatite, *Ceram. Int.*, 26 (2000) 221–230.
- [136] A. Bianco, I. Cacciotti, M. Lombardi, L. Montanaro, E. Bemporad, M. Sebastiani, F-substituted hydroxyapatite nanopowders: Thermal stability, sintering behaviour and mechanical properties, *Ceram. Int.*, 36 (2010) 313–322.
- [137] Z. Evis, M. Usta, and I. Kutbay, Improvement in sinterability and phase stability of hydroxyapatite and partially stabilized zirconia composites, *J. Eur. Ceram. Soc.*, 29 [4] (2009) 621–628.
- [138] C. Garbo, J. Locs, M. D'este, G. Demazeau, A. Mocanu, C. Roman, O. Horovitz, M. Tomoaia-Cotisel, Advanced Mg, Zn, Sr, Si multi-substituted hydroxyapatites for bone regeneration, *Int. J. Nanomedicine*, 15 (2020) 1037–1058.

- [139] E.A. Ofudje, A.I. Adeogun, M.A. Idowu, S.O. Kareem, Synthesis and characterization of Zn-Doped hydroxyapatite: scaffold application, antibacterial and bioactivity studies, *Heliyon*, 5 (2019) e01716.
- [140] Y. Li, J. Widodo, S. Lim, C.P. Ooi, Synthesis and cytocompatibility of manganese (II) and iron (III) substituted hydroxyapatite nanoparticles, *J. Mater. Sci.*, 47 (2012) 754–763.
- [141] A. Mocanu, O. Cadar, P.T. Frangopol, I. Petean, G. Tomoaia, G.A. Paltinean, C.P. Racz, O. Horovitz, M. Tomoaia-Cotisel, Ion release from hydroxyapatite and substituted hydroxyapatites in different immersion liquids: In vitro experiments and theoretical modelling study, *R. Soc. Open Sci.*, 8 [1] (2021) 201785.
- [142] I. Denry, O.M. Goudouri, D.C. Fredericks, A. Akkouch, M.R. Acevedo, J.A. Holloway, Strontium-releasing fluorapatite glass-ceramic scaffolds: Structural characterization and in vivo performance, *Acta Biomater.*, 75 (2018) 463–471.
- [143] V. Aina, G. Lusvardi, B. Annaz, I.R. Gibson, F.E. Imrie, G. Malavasi, L. Menabue, G. Cerrato, G. Martra, Magnesium- and strontium-co-substituted hydroxyapatite: the effects of dopings on the structure and chemico-physical properties, *J. Mater. Sci. Mater. Med.*, 23 [12] (2012) 2867–2879.
- [144] N. Zhang, D. Zhai, L. Chen, Z. Zou, K. Lin, J. Chang, Hydrothermal synthesis and characterization of Si and Sr co-substituted hydroxyapatite nanowires using strontium containing calcium silicate as precursors, *Mater. Sci. Eng. C*, 37 (2014) 286–291.
- [145] C. Ergun, T.J. Webster, R., R.H. Doremus, Hydroxylapatite with substituted magnesium, zinc, cadmium, and yttrium. I. Structure and microstructure, *J. Biomed. Mater. Res.*, 59 (2002) 305–311.
- [146] A. Al-Noaman, N. Karpukhina, S.C.F. Rawlinson, R.G. Hill, Effect of FA on bioactivity of bioactive glass coating for titanium dental implant. Part I: Composite powder, *J. Non Cryst. Solids*, 364 (2013) 92–98.
- [147] C. Rey, C. le Combes, C. Drouet, H. Sfihi, Fluoride-Based Bioceramics, pp. 279-333 in *Fluorine and Health*, A. Tressaud, G. Haufe (Eds), Elsevier B.V., Amsterdam 2008.
- [148] N. Leroy, E. Bres, Structure and substitutions in fluorapatite, *Eur. Cells Mater.*, 2 (2001) 36–48.
- [149] X. Chatzistavrou, S. Papagerakis, P.X. Ma, P. Papagerakis, Innovative approaches to regenerate enamel and dentin, *Int. J. Dent.*, 2012 (2012) 856470.
- [150] S.S. Ghosh, S.S. Ghosh, A.K. Atta, N Pramanik. A succinct overview of hydroxyapatite based nanocomposite biomaterials: Fabrications, physicochemical properties and some relevant biomedical applications, *J. Bionanosci.*, 12 (2018) 143–158.

- [151] Y. Fukase, E. D. Eanes, S. Takagi, I. C. Chow, W. E. Brown, Setting reactions and compressive strengths of calcium phosphate cements, *J. Dent. Res.*, 69 [12] (1990) 1852–1855.
- [152] M. Kamitakahara, C. Ohtsuki, T. Miyazaki, Review paper: Behavior of ceramic biomaterials derived from tricalcium phosphate in physiological condition, *J. Biomater. Appl.*, 23 (2008) 197–212.
- [153] S. Afewerki, N. Bassous, S. Harb, C. Palo-Nieto, G.U. Ruiz-Esparza, F.R. Marciano, T.J. Webster, A.S.A. Furtado, A.O. Lobo, Advances in dual functional antimicrobial and osteoinductive biomaterials for orthopaedic applications, *Nanomed.: Nanotechnol. Biol. Med.*, 24 (2020) 102143.
- [154] E. Fiume, G. Magnaterra, A. Rahdar, E. Verné, F. Baino, Hydroxyapatite for Biomedical Applications: A Short Overview, *Ceramics*, 4 [4] 2021 542–563.
- [155] F. Ridi, I. Meazzini, B. Castroflorio, M. Bonini, D. Berti, P. Baglioni, Functional calcium phosphate composites in nanomedicine, *Adv. Colloid Interface Sci.*, 244 (2017) 281–295.
- [156] K.T. Hunter, T. Ma, In vitro evaluation of hydroxyapatite-chitosan-gelatin composite membrane in guided tissue regeneration, *J. Biomed. Mater. Res. A.*, 101 [4] (2013) 1016–1025.
- [157] K. Lin, M. Zhang, W. Zhai, H. Qu, J. Chang, Fabrication and characterization of hydroxyapatite/wollastonite composite bioceramics with controllable properties for hard tissue repair, *J. Am. Ceram. Soc.*, 94 [1] (2011) 99–105.
- [158] C.C. Coelho, L. Grenho, P.S. Gomes, P.A. Quadros, M.H. Fernandes, Nano-hydroxyapatite in oral care cosmetics: characterization and cytotoxicity assessment, *Sci. Rep.*, 9 (2019) 11050.
- [159] B.T. Amaechi, P.A. AbdulAzees, D.O. Alshareif, M. A. Shehata, P. P. de Carvalho Sampaio Lima, A. Abdollahi, P. S. Kalkhorani, V. Evans, Comparative efficacy of a hydroxyapatite and a fluoride toothpaste for prevention and remineralization of dental caries in children, *BDJ Open*, 5 (2019) 18.
- [160] P. Tschoppe, D.L. Zandim, P. Martus, A.M. Kielbassa, Enamel and dentine remineralization by nano-hydroxyapatite toothpastes, *J. Dent.*, 39 [6] (2011) 430–437.
- [161] R.D. Trushkowsky, A. Oquendo, Treatment of Dentin Hypersensitivity, *Dent. Clin. N. Am.*, 55 [3] (2011) 599–608.
- [162] N. Roveri, E. Battistella, C.L. Bianchi, I. Foltran, E. Foresti, M. Iafisco, M. Lelli, A. Naldoni, B. Palazzo, L. Rimondini, Surface Enamel Remineralization: Biomimetic Apatite Nanocrystals and Fluoride Ions Different Effects, *J. Nanomater.*, 2009 (2009) 746383.
- [163] M. Vano, G. Derchi, A. Barone, R. Pinna, P. Usai, U. Covani, Reducing dentine hypersensitivity with nano-hydroxyapatite toothpaste: A double-blind randomized controlled trial, *Clin. Oral Investig.*, 22 [1] (2018) 313–320.

- [164] E. Pepla, L.K. Besharat, G. Palaia, G. Tenore, G. Migliau, Nano-hydroxyapatite and its applications in preventive, restorative and regenerative dentistry: a review of literature, *Annali di stomatologia*, 5 [3] (2014) 108–114.
- [165] A. Scribante, M.R.D. Farahani, G. Marino, C. Matera, R.R. Baena, V. Lanteri, A. Butera, Biomimetic Effect of Nano-Hydroxyapatite in Demineralized Enamel before Orthodontic Bonding of Brackets and Attachments: Visual, Adhesion Strength, and Hardness in In Vitro Tests, *Biomed Res Int.*, 2020 (2020) 6747498.
- [166] H.W. Kim, H.E. Kim, J.C. Knowles, Fluor-hydroxyapatite sol-gel coating on titanium substrate for hard tissue implants, *Biomaterials* 25 [17] (2004) 3351–3358.
- [167] S. Bose, S. Tarafder, A. Bandyopadhyay, Hydroxyapatite coatings for metallic implants in Hydroxyapatite (HAp) for Biomedical Applications, pp. 143-157 in *Hydroxyapatite (Hap) for Biomedical Applications – WPS 2015*, eds. by M. Mucalo, Elsevier Ltd, 2015.
- [168] T.T. Li, L. Ling, M.C. Lin, Q. Jiang, Q. Lin, J.H. Lin, C.W. Lou, Properties and Mechanism of Hydroxyapatite Coating Prepared by Electrodeposition on a Braid for Biodegradable Bone Scaffolds, *Nanomaterials (Basel)*, 9 [5] (2019) 679.
- [169] K. Kuroda, M. Okido, Hydroxyapatite coating of titanium implants using hydroprocessing and evaluation of their osteoconductivity, *Bioinorg Chem Appl.*, 2012 (2012) 730693.
- [170] M. Eriksson, M. Andersson, E. Adolfsson, E. Carlström, Titanium–hydroxyapatite composite biomaterial for dental implants, *Powder Metall.*, 49 [1] 2006 70–77.
- [171] S. Awasthi, S.K. Pandey, E. Arunan, C. Srivastava, A review on hydroxyapatite coatings for the biomedical applications: experimental and theoretical perspectives, *J. Mater. Chem. B*, 9 [2] (2021) 228–249.
- [172] TT.Li, L. Ling, MC. Lin, H.K. Peng, H.T. Ren, C.W. Lou, J.H. Lin, Recent advances in multifunctional hydroxyapatite coating by electrochemical deposition, *J Mater Sci*, 55 (2020) 6352–6374.
- [173] M. Roy, A. Bandyopadhyay, S. Bose, Induction plasma sprayed Sr and Mg doped nano hydroxyapatite coatings on Ti for bone implant, *J. Biomed. Mater. Res. B Appl. Biomater.*, 99 [2] (2011) 258–265.
- [174] T.J. Levingstone, M. Ardhaoui, K. Benyounis, L. Looney, J.T. Stokes, Plasma sprayed hydroxyapatite coatings: Understanding process relationships using design of experiment analysis, *Surf. Coat.*, 283 (2015) 29–36.
- [175] M.T. Islam, R.M. Felfel, E.A. Abou Neel, D.M. Grant, I. Ahmed, K.M.Z. Hossain, Bioactive calcium phosphate–based glasses and ceramics and their biomedical applications: A review, *J. Tissue Eng.*, 8 (2017) 1–16.

- [176] J. Michel, M. Penna, J. Kochen, H. Cheung, Recent Advances in Hydroxyapatite Scaffolds Containing Mesenchymal Stem Cells, *Stem Cells Int.*, 2015 (2015) 1–13.
- [177] G. Tripathi, B. Basu, A porous hydroxyapatite scaffold for bone tissue engineering: Physico-mechanical and biological evaluations, *Ceram. Int.*, 38 [1] (2012) 341–349.
- [178] B. Leukers, H. Gülkan, S.H. Irsen, S. Milz, C. Tille, M. Schieker, H. Seitz, Hydroxyapatite scaffolds for bone tissue engineering made by 3D printing, *J Mater Sci Mater Med.*, 16 [12] (2005)1121–1124.
- [179] C.M. Curtin, Innovative collagen nano-hydroxyapatite scaffolds offer a highly efficient non-viral gene delivery platform for stem cell-mediated bone formation, *Adv. Mater.*, 24 [6] (2012) 749–754.
- [180] S. Itoh, M. Kikuchi, Y. Koyama, K. Takakuda, K. Shinomiya, J. Tanaka, Development of an artificial vertebral body using a novel biomaterial, hydroxyapatite/collagen composite, *Biomaterials*, 23 [19] (2002) 3919–3926.
- [181] Y. Dan, O. Liu, Y. Liu, Development of Novel Biocomposite Scaffold of Chitosan-Gelatin/Nanohydroxyapatite for Potential Bone Tissue Engineering Applications, *Nanoscale Res Lett*, 11 (2016) 487.
- [182] S. Sathiyavimal, S. Vasantharaj, F.L. Oscar, A. Pugazhendhi, R. Subashkumar, Biosynthesis and characterization of hydroxyapatite and its composite (hydroxyapatite-gelatin-chitosan-fibrin-bone ash) for bone tissue engineering applications, *Int. J. Biol. Macromol.*, 129 (2019) 844–852.
- [183] A. Dubnika, D. Loca, V. Rudovica, M.B. Parekh, L. Berzina-Cimdina, Functionalized silver doped hydroxyapatite scaffolds for controlled simultaneous silver ion and drug delivery, *Ceram. Int.*, 43 [4] (2017) 3698–3705.
- [184] Y.-G. Zhang, Y.-J. Zhu, F. Chen, T.-W. Sun, A novel composite scaffold comprising ultralong hydroxyapatite microtubes and chitosan: preparation and application in drug delivery, *J. Mater. Chem. B*, 5 (2017) 3898–3906.
- [185] R. Sang, M. Chen, Y. Yang, Y. Li, J. Shi, Y. Deng, X. Chen, W. Yang, HAp@GO drug delivery vehicle with dual-stimuli-triggered drug release property and efficient synergistic therapy function against cancer, *J. Biomed. Mater. Res.*, 107A (2019) 2296–2309.
- [186] I.P. Caldas, G.G. Alves, I.B. Barbosa, P. Scelza, F. de Noronha, M.Z. Scelza, In vitro cytotoxicity of dental adhesives: A systematic review, *Dent. Mater.* 35 (2019) 195–205.
- [187] S.-H. Kwon, Y.-K. Jun, S.-H. Hong, I.-S. Lee, H.-E. Kim, Y.Y. Won, Calcium Phosphate Bioceramics with Various Porosities and Dissolution Rates. *J. Am. Ceram. Soc.*, 85 (2002) 3129–3131.

- [188] N. Eliaz, N. Metoki, Calcium Phosphate Bioceramics: A Review of Their History, Structure, Properties, Coating Technologies and Biomedical Applications, *Materials (Basel)*, 10 [4] (2017) 334.
- [189] E. Champion, Sintering of calcium phosphate bioceramics, *Acta Biomater.*, 9 [4] (2013) 5855–5875.
- [190] S. Gomes, C. Vichery, S. Descamps, H. Martinez, A. Kaur, A. Jacobs, J.M. Nedelec, G. Renaudin, Cu-doping of calcium phosphate bioceramics: From mechanism to the control of cytotoxicity, *Acta Biomater.*, 65 (2018) 462–474.
- [191] Y. Chen, J. Wang, X.D. Zhu, Z.R. Tang, X. Yang, Y.F. Tan, Y.J. Fan, X.D. Zhang, Enhanced effect of β -tricalcium phosphate phase on neovascularization of porous calcium phosphate ceramics: in vitro and in vivo evidence, *Acta Biomater.*, 11 (2015) 435–448.
- [192] S.V. Dorozhkin, Biphasic, triphasic and multiphasic calcium orthophosphates, *Acta Biomater.*, 8 (2012) 963–977.
- [193] H. Tebyanian, M.H. Norahan, H. Eyni, M. Movahedin, S.M. Javad-Mortazavi, A. Karami, M.R. Nourani, N. Baheiraei, Effects of collagen/ β -tricalcium phosphate bone graft to regenerate bone in critically sized rabbit calvarial defects, *J. Appl. Biomater. Funct.*, 2019.
- [194] S. Petronis, J. Locs, V. Zalite, M. Pilmane, A. Skagers, I. Salma, G. Salms, Impact of Biphasic Calcium Phosphate Bioceramics on Osteoporotic Hip Bone Mineralization In Vivo Six Months after Implantation, *KEM*, 721 (2016) 229–233.
- [195] O. Suzuki, Y. Shiwaku, R. Hamai, Octacalcium phosphate bone substitute materials: Comparison between properties of biomaterials and other calcium phosphate materials, *Dent. Mater. J.*, 39 [2] (2020) 87–199.
- [196] X. Yin, M.J. Stott, A. Rubio, α - and β -tricalcium phosphate: A density functional study, *Phys. Rev. B Condens. Matter*, 68 [20] (2003) 205205.
- [197] R.G. Carrodegua, S. De Aza, α -Tricalcium phosphate: Synthesis, properties and biomedical applications, *Acta Biomater.*, 7 [10] (2011) 3536–3546.
- [198] G. Cicek, E.A. Aksoy, C. Durucan, N. Hasirci, Alpha-tricalcium phosphate (α -TCP): solid state synthesis from different calcium precursors and the hydraulic reactivity, *J Mater Sci: Mater Med*, 22 (2011) 809–817.
- [199] R.A. Perez, H.-W. Kim, Core-shell designed scaffolds of alginate/alpha-tricalcium phosphate for the loading and delivery of biological proteins, *J. Biomed. Mater. Res. A*, 101 [4] (2013) 1103–1112.
- [200] M. Casas-Luna, H. Tan, S. Tkachenko, D. Salamon, E.B. Montufar, Enhancement of mechanical properties of 3D-plotted tricalcium phosphate scaffolds by rapid sintering, *J. Eur. Ceram*, 39 [14] (2019) 4366–4374.

- [201] R. O'Neill, H.O. McCarthy, E.B. Montufar, M.-P. Ginebra, D.I. Wilson, A. Lennon, N. Dunne, Critical review: Injectability of calcium phosphate pastes and cements, *Acta Biomater.*, 50 (2017) 1–19.
- [202] D. Moreno, F. Vargas, J. Ruiz, M.E López, Solid-state synthesis of alpha tricalcium phosphate for cements used in biomedical applications, *Bol Soc Esp Ceram V.*, 59 [5] (2020) 193–200.
- [203] K. Sawada, K. Nakahara, M. Haga-Tsujimura, T. Iizuka, M. Fujioka-Kobayashi, K. Igarashi, N. Saulacic, Comparison of three block bone substitutes for bone regeneration: long-term observation in the beagle dog, *Odontology*, 106 [4] (2018) 398–407.
- [204] R. Comesaña, F. Lusquiños, J. del Val, T. Malot, M. López-Álvarez, A. Riveiro, F. Quintero, M. Boutinguiza, P. Aubry, A. De Carlos, J. Pou, Calcium phosphate grafts produced by rapid prototyping based on laser cladding, *J. Eur. Ceram*, 31 [1–2] (2011) 29–41.
- [205] A.M. Yousefi, A review of calcium phosphate cements and acrylic bone cements as injectable materials for bone repair and implant fixation, *J Appl Biomater Funct Mater.*, 17 [4] (2019) 1–21.
- [206] F.T. Mariño, J. Torres, M. Hamdan, C.R. Rodríguez, E.L. Cabarcos, Advantages of using glycolic acid as a retardant in a brushite forming cement. *J. Biomed. Mater. Res. B Appl. Biomater.*, 83 [2] (2007) 571–579.
- [207] S.M. Rabiee, F. Moztafzadeh, M. Solati-Hashjin, Synthesis and characterization of hydroxyapatite cement, *J. Mol. Struct.*, 969 [1–3] (2010) 172–175.
- [208] D.J. Verret, Y. Ducic, L. Oxford, J. Smith, Hydroxyapatite cement in craniofacial reconstruction, *Otolaryngol Head Neck Surg.*, 133 [6] (2005) 897–899.
- [209] L. Sun, T. Li, S. Yu, M. Mao, D. Guo, A Novel Fast-Setting Strontium-Containing Hydroxyapatite Bone Cement With a Simple Binary Powder System, *Front Bioeng Biotechnol.*, 9 (2021) 643557.
- [210] J. Engstrand, E. Unosson, H. Engqvist, Hydroxyapatite Formation on a Novel Dental Cement in Human Saliva, *ISRN Dent.*, 2012 (2012) 624056.
- [211] S. Tanodekaew, S. Channasanon, P. Kaewkong, Physico-chemical properties and biocompatibility of *in situ*-hardening polylactide/nano hydroxyapatite composite for bone substitute, *Int. J. Polym.*, (2021).
- [212] A.H. Phakatkar, M.R. Shirdar, M.-L. Qi, M.M. Taheri, S. Narayanan, T. Foroozan, S. Sharifi-Asl, Z. Huang, M. Agrawal, Y.-P. Lu, R. Shahbazian-Yassar, T. Shokuhfar, Novel PMMA bone cement nanocomposites containing magnesium phosphate nanosheets and hydroxyapatite nanofibers, *Mater. Sci. Eng. C*, 109 (2020) 110497.

[213] L.C. Chow, S. Takagi, Premixed calcium phosphate cement pastes. US patent 6793725, (September, 2004).

[214] N. Jeong, J. Park, K. Yoo, W. Kim, D.H. Kim, S.Y. Yoon, Preparation, characterization, and in-vitro performance of novel injectable silanized-hydroxypropyl methylcellulose/ phase transformed calcium phosphate composite bone cements, *Curr Appl Phys.*, 16 [11] (2016) 1523–1532.

[215] J. Zhang, W. Liu, V. Schnitzler, F. Tancret, J.M. Bouler, Calcium phosphate cements for bone substitution: Chemistry, handling and mechanical properties, *Acta Biomater.*, 10 [3] (2014) 1035–1049.

[216] S. Wang, C. Xu, S. Yu, X. Wu, Z. Jie, H. Dai, Citric acid enhances the physical properties, cytocompatibility and osteogenesis of magnesium calcium phosphate cement, *J. Mech. Behav. Biomed. Mater.*, 94 (2019) 42–50.

[217] S. Sarda, E. Fernández, M. Nilsson, M. Balcells, J.A. Planell, Kinetic study of citric acid influence on calcium phosphate bone cements as water-reducing agent, *J. Biomed. Mater. Res.* 61 [4] (2002) 653–659.

[218] A. Yokoyama, S. Yamamoto, T. Kawasaki, T. Kohgo, M. Nakasu, Development of calcium phosphate cement using chitosan and citric acid for bone substitute materials, *Biomaterials*, 23 [4] (2002) 1091–1101.

[219] D. Pastorino, C. Canal, M.P. Ginebra, Drug delivery from injectable calcium phosphate foams by tailoring the macroporosity–drug interaction, *Acta Biomater.*, 12 (2015) 250–259.

[220] J. An, J.G.C. Wolke, J.A. Jansen, S.C.G. Leeuwenburgh, Influence of polymeric additives on the cohesion and mechanical properties of calcium phosphate cements, *J Mater Sci: Mater Med*, 27 (2016) 58.

[221] F. Chen, C. Liu, J. Wei, X. Chen, Z. Zhao, Y. Gao, Preparation and characterization of injectable calcium phosphate cement paste modified by polyethylene glycol-6000, *Mater. Chem. Phys.*, 125 [3] (2011) 818–824.

[222] W. Liu, J. Zhang, P. Weiss, F. Tancret, J.M. Bouler, The influence of different cellulose ethers on both the handling and mechanical properties of calcium phosphate cements for bone substitution, *Acta Biomater.*, 9 [3] (2013) 5740–5750.

[223] R.M. Seyedlar, A. Nodehi, M. Atai, M. Imani, Gelation behavior of in situ forming gels based on HPMC and biphasic calcium phosphate nanoparticles, *Carbohydr Polym.*, 99 (2014) 257–263.

[224] Z. Ding, X. Wang, J. Sanjayan, P.X.W. Zou, Z.K. Ding, A feasibility study on HPMC-improved sulphoaluminate cement for 3D printing, *Materials (Basel)*, 11 [12] (2018) 1–18.

- [225] L.E. Carey, H.H. Xu, C.G. Simon Jr, S. Takagi, L.C. Chow, Premixed rapid-setting calcium phosphate composites for bone repair, *Biomaterials*, 26 [24] (2005) 5002–5014.
- [226] D. Mukhtar-Fayyad, Cytocompatibility of new bioceramic-based materials on human fibroblast cells (MRC-5), *Oral Surgery, Oral Med. Oral Pathol. Oral Radiol. Endod.*, 112 [6] (2011) e137–e142.
- [227] S. Heinemann, S. Rössler, M. Lemm, M. Ruhnnow, B. Nies, Properties of injectable ready-to-use calcium phosphate cement based on water-immiscible liquid, *Acta Biomater.*, 9 [4] (2013) 6199–6207.
- [228] A.A. Zadpoor, Relationship between in vitro apatite-forming ability measured using simulated body fluid and in vivo bioactivity of biomaterials, *Mater Sci Eng C Mater Biol Appl.*, 35 (2014) 134–143.
- [229] H.H.K. Xu, P. Wang, L. Wang, C. Bao, Q. Chen, M.D. Weir, L.C. Chow, L. Zhao, X. Zhou, M.A. Reynolds, Calcium phosphate cements for bone engineering and their biological properties, *Bone Res.*, 5 (2017) 17056.
- [230] L. Borkowski, A. Przekora, A. Belcarz, K. Palka, G. Jozefaciuk, T. Lübek, M. Jojczuk, A. Nogalski, G. Ginalska, Fluorapatite ceramics for bone tissue regeneration: Synthesis, characterization and assessment of biomedical potential, *Mater Sci Eng C Mater Biol Appl.*, 116 (2020) 111211.
- [231] M. Mansoorianfar, M. Mansourianfar, M. Fathi, S. Bonakdar, M. Ebrahimi, E.M. Zahrani, A. Hojjati-Najafabadi, D. Li, Surface modification of orthopedic implants by optimized fluorine-substituted hydroxyapatite coating: Enhancing corrosion behavior and cell function, *Ceram. Int.*, 46 [2] (2020) 2139–2146.
- [232] C. Xie, H. Lu, W. Li, F.M. Chen, Y.M. Zhao, The use of calcium phosphate-based biomaterials in implant dentistry, *J. Mater. Sci. Mater. Med.*, 23 (2012) 853–862.
- [233] J.A. Lett, M. Sundareswari, K. Ravichandran, Porous hydroxyapatite scaffolds for orthopedic and dental applications-the role of binders, *Mater. Today Proc.*, 3 [6] (2016) 1672–1677.
- [234] S.M. Hsu, F. Ren, C. Batich, A.E. Clark, V. Craciun, J.F. Esquivel-Upshaw, Dissolution activation energy of a fluorapatite glass-ceramic veneer for dental applications, *Mater. Sci. Eng. C*, 111 (2020) 110802.
- [235] J. Wei, J. Wang, W. Shan, X. Liu, J. Ma, C. Liu, J. Fang, S. Wei, Development of fluorapatite cement for dental enamel defects repair, *J. Mater. Sci. Mater. Med.*, 22 [6] (2011) 1607–1614.
- [236] M. Azami, S. Jalilifiroozinezhad, M. Mozafari, M. Rabiee, Synthesis and solubility of calcium fluoride/hydroxy-fluorapatite nanocrystals for dental applications, *Ceram. Int.*, 37 [6] (2011) 2007–2014.

- [237] A.D. Anastasiou, M. Nerantzaki, E. Gounari, M.S. Duggal, P.V. Giannoudis, A. Jha, D. Bikiaris, Antibacterial properties and regenerative potential of Sr²⁺ and Ce³⁺ doped fluorapatites; a potential solution for peri-implantitis, *Sci. Rep.*, 9 [11] (2019) 14469.
- [238] D. Stojanovic, Dj. T. Janackovic, D. Markovic., G.M. Tasic, B.V. Aleksandric, Z.Z. Kojic, A Tissue-Implant Reaction Associated With Subcutan Implantation Of Alpha-Tricalcium Phosphate, Dental Ceramic And Hydroxyapatite Bioceramics In Rats, *Acta Vet.*, 54 [4] (2008) 381–393.
- [239] R.G. Hill, X. Chen, D.G. Gillam, In vitro ability of a novel nanohydroxyapatite oral rinse to occlude dentine tubules, *Int. J. Dent.*, 2015 (2015) 1–7.
- [240] M. Vano, G. Derchi, A. Barone, U. Covani, Effectiveness of nano-hydroxyapatite toothpaste in reducing dentin hypersensitivity: A double-blind randomized controlled trial, *Quintessence Int.*, 45 (2014) 703–711.
- [241] K. Hornby, M. Evans, M. Long, A. Joiner, M. Laucello, A. Salvaderi, Enamel benefits of a new hydroxyapatite containing fluoride toothpaste, *Int. Dent. J.*, 59 [6S1] (2009) 325–331.
- [242] M. Esteves-Oliveira, N. Santos, H. Meyer-Lückel, R. Wierichs, J. Rodrigues Caries-preventive effect of anti-erosive and nano-hydroxyapatite-containing toothpastes in vitro, *Clin. Oral Investig.*, 21 (2017) 291–300.
- [243] S.T. Taha, H. Han, S.R. Chang, I. Sovadinova, K. Kuroda, R.M. Langford, B.H. Clarkson, Nano/micro fluorhydroxyapatite crystal pastes in the treatment of dentin hypersensitivity: An in vitro study, *Clin. Oral Investig.*, 19 (2015) 1921–1930.
- [244] C.J. Tredwin, A.M. Young, E.A.A. Neel, G. Georgiou, J.C. Knowles, Hydroxyapatite, fluor-hydroxyapatite and fluorapatite produced via the sol-gel method: Dissolution behaviour and biological properties after crystallisation, *J. Mater. Sci. Mater. Med.* 25 (2014) 47–53.
- [245] Ž. Radovanović, D. Veljović, B. Jokić, S. Dimitrijević, G. Bogdanović, V. Kojić, R. Petrović, D. Janačković, Biocompatibility and antimicrobial activity of zinc(II)-doped hydroxyapatite, synthesized by a hydrothermal method, *J. Serbian Chem. Soc.*, 77 (2012) 1787–1798.
- [246] A. Katakidis, K. Sidiropoulos, E. Koulaouzidou, C. Gogos, N. Economides, Flow characteristics and alkalinity of novel bioceramic root canal sealers, *Restor. Dent. Endod.*, 45 (2020) e42.
- [247] F.F.E. Torres, R. Bosso-Martelo, C.G. Espir, J.A. Cirelli, J.M. Guerreiro-Tanomaru, M. Tanomaru-Filho, Evaluation of physicochemical properties of root-end filling materials using conventional and micro-CT tests, *J. Appl. Oral Sci.*, 25 [4] (2017) 374–380.

- [248] F.F.E. Torres, J.M. Guerreiro-Tanomaru, R. Bosso-Martelo, G.M. Chavez-Andrade, M. Tanomaru Filho, Solubility, porosity and fluid uptake of calcium silicate-based cements, *J. Appl. Oral Sci.*, 26 (2018) e20170465.
- [249] M. Toledano, E. Muñoz-Soto, F.S. Aguilera, E. Osorio, M.P. González-Rodríguez, M.C. Pérez-Álvarez, M. Toledano-Osorio, A zinc oxide-modified hydroxyapatite-based cement favored sealing ability in endodontically treated teeth, *J. Dent.*, 88 (2019) 103162.
- [250] Q. Lin, X. Zhang, D. Liang, J. Li, W. Wang, Z. Wang, C.-P. Wong, The in vivo dissolution of tricalcium silicate bone cement, *J Biomed Mater Res A.*, 109 [12] (2021) 2527–2535.
- [251] M. Toledano-Osorio, F.S. Aguilera, R. Osorio, E. Muñoz-Soto, M.C. Pérez-Álvarez, M.T. López-López, C.D. Lynch, M. Toledano, Hydroxyapatite-based cements induce different apatite formation in radicular dentin, *Dent Mater.*, 36 [1] (2020) 167–178.
- [252] R. Tamilselvi, M. Dakshinamoorthy, K. Arumugam, B. Sathyapriya, P. Lakshmanan, Effect of CPP ACP and nano hydroxyapatite incorporated GIC on remineralization of dentin, *Indian J. Public Health Res. Dev.*, 10 [12] (2019) 936–941.
- [253] S. Davaie, S. Shahabi, M. Behroozibakhsh, S. Vali, F. Najafi, Bioactive glass modified calcium phosphate cement with improved bioactive properties: A potential material for dental pulp-capping approaches, *J. Biomim. Biomater. Biomed. Eng.*, 51 (2021) 1–14.
- [254] S. Ebrahimi, C.S. Sipaut, The effect of liquid phase concentration on the setting time and compressive strength of hydroxyapatite/bioglass composite cement, *Nanomaterials*, 11 [10] (2021) 2576.
- [255] M. Fathi, A. Massit, A. El Yacoubi, B.C. El Idrissi, Development of an apatitic calcium phosphate cements: Effect of liquid/powder ratio on the setting time, *Mor. J. Chem.*, 8 [1] (2020) 176–183.
- [256] R. Imataki, Y. Shinonaga, T. Nishimura, Y. Abe, K. Arita, Mechanical and functional properties of a novel apatite-ionomer cement for prevention and remineralization of dental caries, *Materials*, 12 [23] (2019) 3998.
- [257] F.M. Saltareli, G.B. Leoni, N. de Lima Ferraz Aguiar, N.S. de Faria, I.R. Oliveira, L. Bachmann, W. Raucci-Neto, Apatite-like forming ability, porosity, and bond strength of calcium aluminate cement with chitosan, zirconium oxide, and hydroxyapatite additives, *Microsc. Res. Tech.*, 84 [6] (2021) 1192–1204.
- [258] K. Sharma, S. Sharma, S. Thapa, M. Bhagat, V. Kumar, V. Sharma, Nanohydroxyapatite-, gelatin-, and acrylic acid-based novel dental restorative material, *ACS Omega*, 5 [43] (2020) 27886–27895.

- [259] M. Moraveji, N. Nezafati, M. Pazouki, S. Hesarak, Bioorthogonal surface modified α -TCP-based bone filler for enhancement of apatite formation and bioactivity, *Ceram. Int.*, 45 [5] (2019) 5981–5986.
- [260] International Standard ISO 6876, Dentistry – Root canal sealing materials, 3rd edition, 2012.
- [261] D. Stojanović, D. Janačković, M. Danica, G. Tasić, B. Aleksandrić, K. Zvezdana, A tissue-implant reaction associated with subcutan implantation of alpha-tricalcium phosphate, dental ceramic and hydroxyapatite bioceramics in rats, *Acta Vet. Brno*, 58 (2008) 381–393.
- [262] T. Kokubo, H. Kushitani, C. Ohtsuki, S. Sakka, T. Yamamuro, Chemical reaction of bioactive glass and glass-ceramics with a simulated body fluid, *J. Mater. Sci.: Mater. Med.*, 3 [2] (1992) 79–83.
- [263] Ž.M. Radovanović, The influence of silver, copper and zinc ions on the properties of bioceramic materials based on calcium hydroxyapatite and calcium phosphate, Doctoral Dissertation, University of Belgrade, Faculty of Technology and Metallurgy, Belgrade, 2016.
- [264] T. Mosmann, Rapid colorimetric assay for cellular growth and survival: Application to proliferation and cytotoxicity assays, *J. Immunol. Methods*, 65 [1] (1983) 55–63.
- [265] Bogdanović G., Raletid-Savić J., Marković N., In vitro assays for antitumor-drug screening on human tumor cell lines: dye exclusion test and colorimetric cytotoxicity assay, *Onkološki arhiv*, 2 (1994) 181–184.
- [266] M. Šupová, Substituted hydroxyapatites for biomedical applications: A review, *Ceram. Int.*, 41 (2015) 9203–9231.
- [267] J. Zheo, X. Dong, M. Bian, J. Zhao, Y. Zhang, Y. Sun, J. Chen, X. Wang, Solution combustion method for synthesis of nanostructured hydroxyapatite, fluorapatite and chlorapatite, *Appl. Surf. Sci.*, 314 (2014) 1026–1033.
- [268] F.H. ElBatal, M.A. Azooz, Y.M. Hamdy, Preparation and characterization of some multicomponent silicate glasses and their glass-ceramics derivatives for dental applications, *Ceram. Int.*, 35 (2009) 1211–1218.
- [269] H. Kurita, M. Hirano, J.M.A. de Blicck, C.P.A.T. Klein, K. de Groot, Calcium phosphate cement: in vitro and in vivo studies of the α -tricalcium phosphate-dicalcium phosphate dibasic-tetracalcium phosphate monoxide system, *J. Mat. Sci: Mater Med.*, 6 (1995) 340–347.
- [270] E. Cichoń, A. Ślósarczyk, A. Zima, Influence of Selected Surfactants on Physicochemical Properties of Calcium Phosphate Bone Cements, *Langmuir*, 35(42) (2019) 13656–13662.
- [271] S. Pramanik, A. Kumar Agarwal, K.N. Rai, A. Garg, Development of high strength hydroxyapatite by solid-state-sintering process, *Ceram. Int.*, 33 (2007) 419–426.

- [272] E. Charrière, S. Terrazzoni, C. Pittet, Ph. Mordasini, M. Dutoit, J. Lemaître, Ph. Zysset, Mechanical characterization of brushite and hydroxyapatite cements, *Biomaterials*, 22 (2001) 2937–2945.
- [273] K.A. Gross, L.M. Rodríguez-Lorenzo, Sintered hydroxyfluorapatites. Part II: Mechanical properties of solid solutions determined by microindentation, *Biomaterials*, 25 (2004) 1385–1394.
- [274] M. Tamai, R. Nakaoka, T. Tsuchiya, Cytotoxicity of various calcium phosphate ceramics, *Key Eng. Mater.*, 309–311 (2006) 263–266.
- [275] A. Kazuz, Ž. Radovanović, Dj. Veljović, V. Kojić, D. Jakimov, T. Vlajić-Tovilović, V. Miletić, R. Petrović, Dj. Janačković, α -Tricalcium phosphate/fluorapatite-based cement – Promising dental root canal filling material, *Process. Appl. Ceram.*, 16 (2022) 22–29.
- [276] F.F.E. Torres, J.M. Guerreiro-Tanomaru, J.C. Pinto, I. Bonetti-Filho, M. Tanomaru-Filho, Evaluation of flow and filling of root canal sealers using different methodologies, *Rev. Odontol. Da UNESP*. 48 (2019) 1–7.
- [277] N.F. Rajab, T.A. Yaakob, B.Y. Ong, M. Hamid, A.M. Ali, B.O. Annuar, S.H. Inayat-Hussain, DNA damage evaluation of hydroxyapatite on fibroblast cell L929 using the single cell gel electrophoresis assay, *Med. J. Malaysia*, 59 [Suppl B] (2004) 170–171.
- [278] M. Szymonowicz, M. Korczynski, M. Dobrzynski, K. Zawisza, M. Mikulewicz, E. Karuga-Kuzniewska, B. Zywicka, Z. Rybak, R.J. Wiglusz, Cytotoxicity evaluation of high-temperature annealed nanohydroxyapatite in contact with fibroblast cells, *Materials (Basel)*, 10 (2017) 590.
- [279] S.Y. Kim, K.J. Kim, Y.A. Yi, D.G. Seo, “Quantitative microleakage analysis of root canal filling materials in single-rooted canals”, *Scanning*, 37 [4] (2015) 237–245.

Biography

Abdulmoneim Mohamed Kazuz

Birthdate: March 27th, 1979 in Tripoli, Libya.

Postgraduate and undergraduate degrees:

- Abdulmoneim M. Kazuz is a doctoral candidate in Materials Engineering at the University of Belgrade, studying under supervision of Professor Dr Djordje Janačković. The working title of his thesis is “The Processing of Different Calcium Phosphate Bioceramic Materials and application in Dental Practice”.

- Before coming to Belgrade he completed two postgraduate programs: a High Diploma in Interceptive Orthodontic for short stage in 2010 and a Master degree in Dental Science in 2011, from Danube-University Krems, Austria.

- In 2008, Abdulmoneim M. Kazuz received his Bachelor degree in Dentistry from University of Al-Thadi.

- In 2002 Abdulmoneim M. Kazuz obtained his Bachelor degree in Dental Technology at Tripoli University.

Career:

- During 2003–2011, Abdulmoneim M. Kazuz worked as a dental researcher in forensic laboratories at Medical Tripoli center (Tripoli. Libya).

- Before and in between working as a dental researcher, he worked as dental technician and an orthodontic specialist in many dental clinics during 2003–2008.

- Currently, Abdulmoneim M. Kazuz works as a Teaching Assistant in the Department of Dental Technology at Tripoli College, since 2012.

Прилог 1.

Изјава о ауторству

Потписани-а _____ **Abdul Moneim Mohamed Saed Kazuz** _____

број индекса или пријаве докторске дисертације - 4045/2014 _____

Изјављујем

да је докторска дисертација под насловом

Bioaktivni materijali na bazi α -trikalcijum-fosfatnih cemenata i fluoroapatita: sinteza, svojstva i primena u stomatologiji (Bioactive materials based on α -tricalcium phosphate cements and fluoroapatite: synthesis, properties and applications in dentistry).

- резултат сопственог истраживачког рада,
- да предложена дисертација у целини ни у деловима није била предложена за добијање било које дипломе према студијским програмима других високошколских установа,
- да су резултати коректно наведени и
- да нисам кршио/ла ауторска права и користио интелектуалну својину других лица.

У Београду, 20.4.2022.

Потпис докторанда



Прилог 2.

Изјава о истоветности штампане и електронске верзије докторског рада

Име и презиме аутора __ **Abdul Moneim Mohamed Saed Kazuz** _____

Број број индекса или пријаве докторске дисертације 4045/2014 _____

Студијски програм __ Инжењерство материјала _____

Наслов рада _ Bioaktivni materijali na bazi α -trikalcijum-fosfatnih cemenata i fluoroapatita: sinteza, svojstva i primena u stomatologiji (Bioactive materials based on α -tricalcium phosphate cements and fluoroapatite: synthesis, properties and applications in dentistry)

Ментор _Проф.Др Ђорђе Јанаћковић _____

Потписани _ **Abdul Moneim Mohamed Saed Kazuz**

изјављујем да је штампана верзија мог докторског рада истоветна електронској верзији коју сам предао/ла за објављивање на порталу **Дигиталног репозиторијума Универзитета у Београду**.

Дозвољавам да се објаве моји лични подаци везани за добијање академског звања доктора наука, као што су име и презиме, година и место рођења и датум одбране рада.

Ови лични подаци могу се објавити на мрежним страницама дигиталне библиотеке, у електронском каталогу и у публикацијама Универзитета у Београду.

Потпис докторанда

У Београду, 20. 4. 2022.



Прилог 3.

Изјава о коришћењу

Овлашћујем Универзитетску библиотеку „Светозар Марковић“ да у Дигитални репозиторијум Универзитета у Београду унесе моју докторску дисертацију под насловом:

Bioaktivni materijali na bazi α -trikalcijum-fosfatnih cemenata i fluoroapatita: sinteza, svojstva i primena u stomatologiji (Bioactive materials based on α -tricalcium phosphate cements and fluoroapatite: synthesis, properties and applications in dentistry)

која је моје ауторско дело.

Дисертацију са свим прилозима предао/ла сам у електронском формату погодном за трајно архивирање.

Моју докторску дисертацију похрањену у Дигитални репозиторијум Универзитета у Београду могу да користе сви који поштују одредбе садржане у одабраном типу лиценце Креативне заједнице (Creative Commons) за коју сам се одлучио/ла.

1. Ауторство
2. Ауторство - некомерцијално
3. Ауторство – некомерцијално – без прераде
4. Ауторство – некомерцијално – делити под истим условима
5. Ауторство – без прераде
6. Ауторство – делити под истим условима

(Молимо да заокружите само једну од шест понуђених лиценци, кратак опис лиценци дат је на полеђини листа).

Потпис докторанда

У Београду, 20.4.2022.

